The Astron Astrophys Rev (1992) 4:267–361

THE
ASTRONOMY
AND
ASTROPHYSICS
REVIEW

Solar oscillations and the equation of state

Jørgen Christensen-Dalsgaard[1,2] and Werner Däppen[3,4,5,2]

[1,*] Institut for Fysik og Astronomi, Aarhus Universitet, DK-8000 Aarhus C, Denmark
[2] Institute for Theoretical Physics, University of California, Santa Barbara, CA 93106, USA
[3,*] Department of Physics and Astronomy, USC, Los Angeles, CA 90089-1342, USA
[4] Space Science Department, ESA-ESTEC, NL-2200 AG Noordwijk, The Netherlands
[5] Institut für Astronomie, Universität Wien, A-1180 Wien, Austria

Received June 23, 1992

Summary. Accurate measurements of observed frequencies of solar oscillations are providing a wealth of data on the properties of the solar interior. The frequencies depend on solar structure, and on the properties of the plasma in the Sun. Here we consider in particular the dependence on the thermodynamic state. From an analysis of the equations of stellar structure, and the relevant aspects of the properties of the oscillations, we argue that in the convection zone one can isolate information about the equation of state which is relatively unaffected by other uncertainties in the physics of the solar interior. We review the different treatments that have been used to describe the thermodynamics of stellar plasmas. Through application of several of these to the computation of models of the solar envelope we demonstrate that the sensitivity of the observed frequencies is in fact sufficient to distinguish even quite subtle features of the physics of solar matter. This opens up the possibility of using the Sun as a laboratory for statistical mechanics, under conditions that are out of reach in a terrestrial laboratory.

Key words: Solar structure – Solar oscillations – Thermodynamics of stellar interiors – Helioseismology

1. Introduction

Solar acoustic oscillations have opened a new window into the Sun. By their nature they link the local sound speed in the interior with the observed oscillation frequencies. The spatial resolution of the solar disk allows the identification of a large number of individual oscillation modes, which are classified in terms of spherical harmonics. Modes in a large range of angular degrees, between $l = 0$ and a few thousand, are observed. The frequencies of these modes are centered around 3 mHz, which corre-

* Permanent address

Correspondence to: J. Christensen-Dalsgaard

sponds to periods around 5 minutes. They have been determined with high precision: typical relative errors are of the order of 10^{-4}. The modes are confined to a cavity, which extends, broadly speaking, from the surface of the Sun, where the waves lose their material support, to the inner turning point which lies deeper the lower the angular degree l is. Radial modes, with $l = 0$, have no inner turning point and penetrate directly to the centre.

The observed modes of solar oscillation are standing acoustic waves; hence the quantity most obviously probed is the sound speed. Since the oscillations are largely adiabatic (except very near the surface), the frequencies are determined predominantly by the local adiabatic sound speed, which is a thermodynamic quantity. In addition, the frequencies depend on the density distribution in the Sun. Powerful techniques have been developed to use these frequencies for various purposes. Helioseismology, as this still relatively young field is called, has successfully addressed a whole range of interesting topics of solar physics. Here, we merely mention a few of them: the solar helium abundance, the structure of the convection zone and the position of its base, the possible physical processes in the solar core that might take place in addition to those assumed in the "standard" model (with applications to the solar neutrino problem), and the profile of internal rotation of the Sun. Thus, helioseismology provides observational constraints for the theory of stellar evolution and the underlying physical processes. Conversely, progress in observational stellar physics will increase our knowledge about the Sun. This is true in particular of analyses of multi-mode stellar oscillations, including solar-like oscillations of other stars; this field of study is now generally known as *asteroseismology*.

As is well known, the three basic material properties required in stellar models are the equation of state, opacity, and the nuclear-energy generation rate. Here, we concentrate on the equation of state, which relates density to pressure and temperature. In the following, we shall use the term equation of state in a slightly broader sense, so that it encompasses as well all thermodynamic quantities. These quantities must be consistent with each other, that is, their appropriate Maxwell relations have to be satisfied. Such *formal* consistency is always achieved if the equation of state and the thermodynamic quantities stem from a single thermodynamic potential. In trivial models (e.g. in a plasma assumed to be fully ionized everywhere) it is possible to write down a consistent equation of state and thermodynamic quantities independently. However, in more realistic cases, modelling a thermodynamic potential is the only practical way to obtain the equation of state and thermodynamic quantities.

In a solar-like star the physical conditions are far from extreme, and hence a description of the plasma in terms of a mixture of partially ionized ideal gases is often adequate; however, the extraordinary high accuracy of observed oscillation frequencies puts higher demands on the equation of state. This has been recognized early and models with improved equations of state were used in helioseismic studies (Berthomieu et al. 1980; Lubow et al. 1980; Ulrich 1982; Ulrich and Rhodes 1983; Shibahashi et al. 1983, 1984; Noels et al. 1984). These early studies not only showed the importance of an accurate equation of state in helioseismology, but they also suggested the exciting prospect of a helioseismic diagnostic of the equation of state. This makes possible studies of properties of matter in the solar interior, under conditions that cannot be achieved on Earth.

Improvements in the equation of state beyond the model of a mixture of ideal gases are difficult. This has both technical and conceptual reasons. As a fundamental conceptual reason we mention the fact that in a plasma environment already the

idea of isolated atoms (and compound ions) has to be abandoned: the early studies mentioned above clearly showed that the interactions between atoms and environment could not be neglected, so that, strictly speaking, one has always to deal with complicated many-body states. Of course, many formalisms for strongly-coupled plasmas have been developed. However, since their motivation is different, they mostly aim at understanding qualitative phenomena, and they are normally not suited for the purposes of stellar models. That is, their results are not sufficiently precise, nor do they allow a description of realistic astrophysical mixtures. These two reasons illustrate some of the technical difficulties that one encounters when one goes away from the extremely comfortable hypothesis of the ideal gas.

The weakly non-ideal plasma of the solar interior can thus become very complicated if high accuracy is demanded. Given the virtual impossibility of rigorous formalisms, it is no wonder that a large number of more-or-less phenomenological treatments have been developed, mainly built around perturbational treatments of ideal gases. The three principal non-ideal effects are related to: (i) the internal partition functions of bound systems, (ii) pressure ionization, and (iii) collective interactions of the charged particles. The internal partition functions contain the difficult problem of excited states, where and how they are to be cut off, and their magnitude is an important element in determining the ionization balances. Pressure ionization has to be provided by non-ideal interaction terms, because the ideal gases would spuriously recombine toward the central regions of the Sun.

The collective interactions between the charged particles lead to the third non-ideal correction. In the Sun, the interactions are often treated in the Debye-Hückel approximation. They lead to the usual (negative) Coulomb-pressure correction, as well as to corresponding changes in other thermodynamic quantities. The nature of this Coulomb effect depends on the location in the Sun. Beneath the hydrogen and helium ionization zones, where most of the atoms are ionized, the Debye-Hückel term is straightforward. Quantitatively, it provides a correction to the pressure which is typically of the order of a few per cent relative to the total pressure. In the regions of partial ionization of hydrogen and helium, the Coulomb effect is more complicated. Here, the net change of pressure and thermodynamic quantities involves two components: a direct change, and an "induced" one due to the fact that the Coulomb interaction also changes the ionization equilibrium. This induced part plays a very important role in the thermodynamic derivatives (such as adiabatic sound speed), where it can cause relative changes of a few per cent despite the significantly smaller pressure changes. This is easily understood from the strong dependence of thermodynamic quantities on ionization. Quantitatively, going from the photosphere to the helium ionization zones, the (negative) net Coulomb pressure correction grows from some 10^{-4} to a few per cent of the total pressure. However, as a result of the induced part the thermodynamic quantities are affected at the per cent level already in the upper part of the hydrogen ionization zone where, due to the reduced total charge, the pressure correction is still only of order 10^{-4} to 10^{-3}. We shall show in Sect. 4 that among all non-ideal corrections to the equation of state it is precisely this collective Coulomb interaction and its important induced part that have the most significant helioseismic consequences.

For certain astrophysical applications, it can well be that lower demands on the accuracy of the equation of state are sufficient. Especially the calibration of solar evolutionary models with the present-age radius and luminosity often reduces the influence of given quantities on uncertainties in the equation of state. For instance,

any uncertainty in the pressure in the solar centre is easily compensated with a slight change in the helium abundance. Many aspect of such a recalibrated model remain virtually unchanged and thus independent of the equation of state. However, if the helium abundance is determined by the same calibration, it is affected by the whole uncertainty in the equation of state. Similarly, in other cases, an interesting physical quantity might be the result of a spatially weighting over zones that pose little difficulty to the equation of state. Examining the range of solar models with respect to different, commonly used equations of state, but with all other assumptions being kept unchanged, allows a simple examination of the influence of the uncertainty in the equation of state. As a first purpose of this article, we make a systematic presentation of the influence of the equation of state on various physical quantities of solar models.

As we have just mentioned, there are cases where the net influence of uncertainties in the equation of state is less severe than for local thermodynamic quantities. However, there is one important application, the helioseismic determination of the solar helium abundance which does not profit from favourable cancellations. The key idea of this helium abundance determination is based on the signature of the second ionization zone of helium on the adiabatic exponent Γ_1, and thus on sound speed. In a zone of partial ionization Γ_1 is lowered. This lowering can be qualitatively understood in the following way. First notice that Γ_1 is approximately equal to the ratio of specific heat at constant pressure c_p over specific heat at constant volume c_V. Then consider that in regions of partial ionization, both specific heats become much larger than their ideal gas values (which for c_V and c_p correspond to $3/2k_B$ and $5/2k_B$ per particle, respectively, k_B being Boltzmann's constant), because heat increments are used to ionize, with temperature changing little (the analogy is the latent heat at phase transitions of ordinary matter). However, the difference of the (caloric) specific heats $c_p - c_V$ is, according to the first law of thermodynamics, a thermal quantity. It stays close to its ideal-gas value even when c_p and c_V are very big. Thus the ratio c_p/c_V and also Γ_1 become smaller (for example, in the Sun, Γ_1 attains 1.2 in the ionization zone of hydrogen). The lowering of Γ_1 in the second helium ionization zone can therefore, in principle, be used as a measure of the Sun's helium abundance in the convection zone (see Sects. 2.1.2 and 4.1.2). The technical tools to use the oscillation frequencies to obtain such a localized information are being developed and some tests with artificial data have been successfully carried out (for a recent review of the current situation, see Kosovichev et al. 1992). However, it is clear that any uncertainty in the absolute accuracy of Γ_1 will directly translate into the so determined helium abundance.

From this example we can see two things. First, there is a case where the absolutely accurate theoretical prediction of the equation of state at certain conditions is essential. Second, helioseismology has the potential to localize thermodynamical properties, in principle everywhere in the Sun. This suggests the idea of Gough (1984a) to use the power of helioseismology simultaneously, both to determine the equation of state in regions where the influence of sound speed on the helium abundance is less, and also, equipped with that knowledge of the equation of state, to determine the helium abundance through the sound speed in the second ionization zone of helium.

To probe issues of atomic and plasma physics by helioseismology sounds rather ambitious, but it is feasible because of two fortunate circumstances. The first is the exceptional accuracy of the observations, and the second the fact that the quantity immediately probed by the oscillation frequencies – adiabatic sound speed – is a purely thermodynamic one. To be more precise, helioseismic inference determines sound

speed as a function of depth. However, in the convection zone the thermal structure is sufficiently simple that the depth dependence can essentially be transformed into a dependence of sound speed on the thermodynamic variables.

Without further bias, helioseismic probing can therefore be directly applied to the underlying physics. So far, we have found sufficient evidence to support the claim that solar observations can be used as a laboratory to test material properties under conditions that cannot be achieved on Earth. In this way, we define the second purpose of this article: to put helioseismic constraints on the equation of state.

In the following, we first review the basic tools of helioseismology (Sect. 2). Of course we shall be selective in view of our restricted topic and only discuss that part of the field that has a direct bearing on the tests of the equation of state. Then we shall present an overview of the equation of state, showing currently used models and exposing open issues (Sect. 3). After that we shall bring the two topics together and discuss the connection between the equation of state and helioseismology (Sect. 4). We shall examine both the forward direction, that is the propagation of uncertainties in the equation of state to helioseismic results, and the backward direction, that is a quantitative assessment of present and future helioseismic constraints on the equation of state.

2. Helioseismology

2.1 Properties of the solar interior

The connection between the physical properties of the solar plasma which we wish to probe by means of helioseismology and the observed frequencies goes through computations of solar models. Hence it is useful to review very briefly normal calculations of such models, and their possible shortcomings (see also Bahcall and Ulrich 1988; Turck-Chièze et al. 1988; Bahcall 1989; Turck-Chièze 1990).

2.1.1 Standard models and their limitations

It is assumed that the model is in hydrostatic and thermal equilibrium, and that energy is transported either diffusively by radiation, or according to some simplified description of convection, depending on whether or not the given region of the Sun is stable or unstable towards convection. Thus the model satisfies the following equations (Clayton 1968):

Hydrostatic equilibrium:

$$\frac{dp}{dr} = -\frac{Gm\rho}{r^2} , \tag{2.1}$$

where r is the distance to the solar centre, p is pressure, ρ is density, G is the gravitational constant, and the mass m interior to r is determined by

$$\frac{dm}{dr} = 4\pi\rho r^2 \; ; \tag{2.2}$$

Thermal equilibrium:

$$\frac{dL}{dr} = 4\pi r^2 \rho \left[\epsilon - \frac{d}{dt}\left(\frac{u}{\rho}\right) + \frac{p}{\rho^2}\frac{d\rho}{dt}\right] \; , \tag{2.3}$$

where L is the luminosity at r, ϵ is the rate of energy generation per unit mass, and u is the internal energy per unit volume (the last two terms on the right-hand side come from the change in internal energy and the release of gravitational potential energy due to the changing structure of the star as it evolves; these are small during the main-sequence evolution of the Sun);

Energy transport:

$$\frac{dT}{dr} = -\frac{3\kappa\rho L}{64\pi\sigma r^2 T^3} \qquad \text{(radiative transport)} \; , \tag{2.4a}$$

or

$$\frac{dT}{dr} = \left(\frac{dT}{dr}\right)_c \qquad \text{(convective transport)} \; , \tag{2.4b}$$

where T is temperature, κ is opacity, σ is the Stefan-Boltzmann constant and $(dT/dr)_c$ is obtained from a simplified description of the relation between the temperature gradient and energy transport in the convection zone. Evolution is controlled by the gradual fusion of hydrogen into helium; it is assumed that there is no mixing or diffusion in the solar interior, so that the composition in any given mass-shell is determined solely by the local nuclear burning.

With these assumptions the structure is largely determined by the *microphysics* of the solar interior, i.e.,

- the equation of state
- the opacity
- the nuclear reaction rates.

In addition, the computation requires that the solar mass is known, as well as the initial chemical composition, which is assumed to be uniform. The goal is to compute a model at the age of the present Sun, which is also assumed to be known, with the observed radius and surface luminosity.

In practice, the initial helium abundance Y_0 cannot be determined independently and must be regarded as a free parameter of the calculation, as must the "mixing-length" parameter α_C which measures the efficiency of convective energy transport near the solar surface. Y_0 and α_C are adjusted until the model of the present Sun has the correct radius and luminosity. In this way one obtains what is sometimes called a "standard solar model". It is evidently dependent on the uncertainties in the assumed microphysics, but is otherwise well-defined.

The topic of the present review is precisely the dependence of the models, and hence the oscillation frequencies, on the microphysics, particularly the equation of state. The models are also sensitive to the assumed nuclear reaction rates, but to a lesser extent: because of the high temperature sensitivity of the reaction rates, changes in the parameters describing the nuclear reactions can be compensated for in the model by a modest change in temperature, and hence in general have little effect on the overall structure of the model or its oscillation frequencies [see also Christensen-Dalsgaard (1988a) and Lebreton et al. (1988). Of course, the computed

neutrino flux is quite sensitive to the nuclear reaction parameters; see, for example, Bahcall and Ulrich (1988) and Bahcall (1989)].

It is evident that our ability to investigate the microphysics by means of helioseismology depends on the validity of the other assumptions on which the computations are based. In fact, the computation of standard solar models ignores, or grossly simplifies, a number of processes that might be labelled the *macrophysics* of the Sun. These include

- energy transport
- dynamics of convection
- convective overshoot
- microscopic diffusion
- core mixing
- magnetic fields.

Energy transport by radiation is treated adequately in the solar interior in the diffusion approximation; on the other hand, energy transport by convection is treated in a rather crude way, which furthermore depends on the *a priori* unknown parameter α_C. Near the surface convection is probably sufficiently vigorous to have dynamic effects on the average hydrostatic equilibrium, yet such effects are often ignored. At the lower boundary of the convection zone motion is normally supposed to stop at the point where convective instability ceases; there is no doubt, however, that motion extends into the convectively stable region through convective overshoot, although the extent of the overshoot is uncertain. Microscopic diffusion is likely to have some effect on the composition profile in the convectively stable region, yet with a few exceptions has been ignored. Instabilities in the deep interior could lead to material mixing, affecting the composition profile and hence solar evolution. Finally, magnetic fields dominate the structure of the upper solar atmosphere and may have some effect at the photospheric level. The nature or strength of the subphotospheric field is unknown, but one probably cannot totally exclude a field of sufficient magnitude to have an effect on the overall structure of the Sun.

Despite the complications it introduces, convection in a certain sense simplifies the structure of the outer parts of the Sun. Regardless of the uncertain details of convective energy transport, there is no doubt that except in a thin boundary layer near its top the convection zone is very nearly adiabatically stratified (e.g. Gough and Weiss 1976), so that the gradient of density ρ is given by

$$\frac{1}{\Gamma} \equiv \frac{d\ln\rho}{d\ln p} \simeq \frac{1}{\Gamma_1} , \tag{2.5}$$

where r is distance from the centre, p is pressure, and $\Gamma_1 = (\partial \ln p/\partial \ln \rho)_s$, the derivative being at constant specific entropy s. The structure of the adiabatic part of the convection zone is determined by this relation, together with the equation of hydrostatic support. Hence it only depends on the equation of state, the composition and the constant value of the specific entropy, which in turn is essentially fixed by the value of α_C; in particular, the convection zone structure is insensitive to the opacity.

It should also be noted that much of the uncertain macrophysics is concentrated very near the surface. This is true of the dynamical effects of convection, since convective velocities are likely to be very small elsewhere, of the details of convective energy transport, and of the effects of the visible magnetic field. Apart from convective overshoot and a hypothetical strong internal magnetic field, the remaining difficulties listed are concerned with the composition profile in the radiative interior of the model.

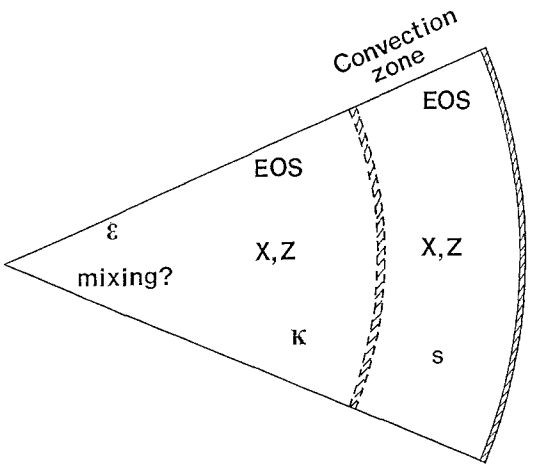

Fig. 1. Schematic representation of solar structure. The thin hashed area near the surface indicates the region where the physics is uncertain, because of effects of convection, nonadiabaticity, etc. At the base of the convection zone, convective overshoot and diffusion introduce additional uncertainty. The structure of the adiabatic part of the convection zone is determined by the equation of state (EOS), and the constant values of specific entropy s, and composition (given by the abundances X and Z of hydrogen and heavy elements). Beneath the convection zone the structure also depends on opacity κ and the energy generation rate ϵ

Although the list of problems is not exhaustive, this argument gives some support to the simplified view of solar structure shown in Fig. 1.

2.1.2 Properties of the convection zone

According to the description of solar structure in Fig. 1, the convection zone is particularly well suited for testing the properties of the equation of state, and determining the composition, because its structure is independent of opacity. The properties of the observed five-minute oscillations, which are predominantly acoustic modes, are largely determined by the adiabatic sound speed c, given by

$$c^2 = \frac{\Gamma_1 p}{\rho} \,. \tag{2.6}$$

It was noted by Gough (1984a) that, assuming adiabatic stratification, c satisfies the following identity

$$W \equiv \frac{r^2}{Gm}\frac{dc^2}{dr} = \frac{1-\Gamma_1-\Gamma_{1,\rho}}{1-\Gamma_{1,c^2}} \equiv \Theta \,, \tag{2.7}$$

where $\Gamma_{1,\rho} \equiv (\partial \ln \Gamma_1/\partial \ln \rho)_{c^2}$ and $\Gamma_{1,c^2} \equiv (\partial \ln \Gamma_1/\partial \ln c^2)_\rho$ (see also Däppen and Gough 1984, 1986; Däppen et al. 1988). It is straightforward to verify Eq. (2.7) from Eq. (2.5), assuming equality, and Eqs. (2.1) and (2.6). The quantity Θ depends on the equation of state and the chemical composition. In W, c can be determined helioseismically, as discussed in Sect. 2.3.2. Furthermore, in the outer parts of the convection zone m can be assumed to be constant and equal to the surface value; in fact, the entire convection zone contains only about 2 per cent of the Sun's mass (cf. Christensen-Dalsgaard et al. 1991). A more complete analysis of observed oscillation

frequencies allows $\rho(r)$ and hence $m(r)$ to be determined (see Sect. 2.3.3). It follows that W can essentially be determined observationally; thus Eq. (2.7) provides a direct relation between a quantity that is, at least in principle, observable, and the properties of the solar plasma.

This relation is illustrated in Fig. 2, which shows W and Θ computed for a standard solar model. Very near the surface, departure from adiabaticity causes the two curves to differ. One should also note the feature at $r/R \simeq 0.98$. This is related to the variation of Γ_1 in the second helium ionization zone; hence the magnitude of this feature depends on the abundance of helium. As pointed out by Däppen and Gough (1984, 1986), and discussed in more detail in Sect. 4.1.2 below, this may provide a measure of the helium abundance in the solar convection zone.

In most of the convection zone hydrogen and helium are essentially completely ionized. Then $\Gamma_1 \simeq 5/3$ and, consequently, $\Theta \simeq -2/3$. If, furthermore, m is assumed to be constant Eq. (2.7) can be integrated to yield the variation of c^2 with r. Assuming the sound speed to vanish at the surface, $r = R$, and neglecting the contribution from the relatively thin region where Γ_1 varies substantially due to ionization, the result is

$$c^2 \simeq (\Gamma_1 - 1)\frac{GM}{R}\left(\frac{R}{r} - 1\right) \tag{2.8}$$

(Christensen-Dalsgaard 1986). Thus, in this approximation, $c(r)$ in the convection zone depends only on the total mass and surface radius of the Sun.

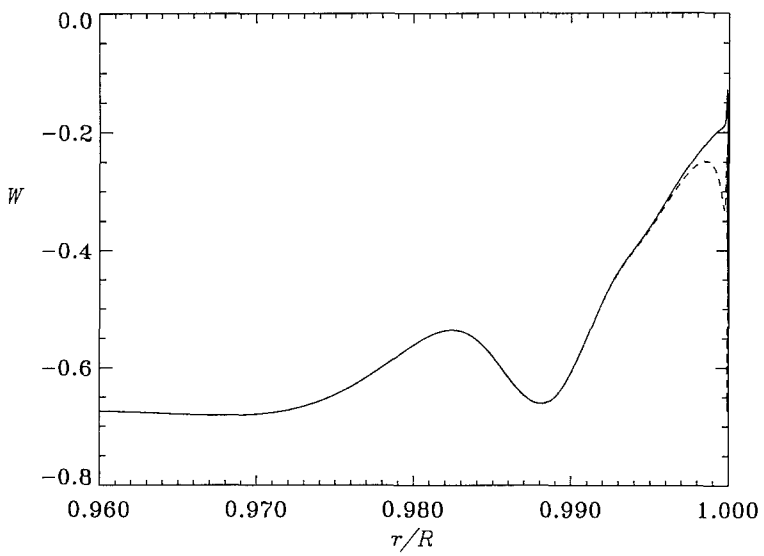

Fig. 2. The quantities W (dashed curve) and Θ (solid curve) defined by Eq. (2.7). They have been computed for Model C1 (cf. Table 1), using the CEFF equation of state (cf. Sect. 3.3.2)

2.1.3 Effects of changes in the convection zone

We are concerned with the sensitivity of the solar models and frequencies to changes in the assumed physics. In general, it is possible to obtain relations between such changes by linearizing Eqs. (2.1) – (2.4) describing solar structure (Däppen 1983). However, to aid the subsequent discussion of the effects of changes in the equation of state in the hydrogen and helium ionization zones, it is useful to derive approximate relations, valid in the convection zone. We assume that the changes are so small that the linear approximation is applicable, and use "δ" to denote differences between two equilibrium models *at fixed radius* r. Of particular interest is the change in the sound speed, since this to a large extent determines the change in the frequencies of the p modes (cf. Eq. [2.37] below). From Eq. (2.6) it follows that

$$\delta \ln c = \frac{1}{2}\left(\delta \ln \Gamma_1 + \delta \ln \frac{p}{\rho}\right) , \tag{2.9}$$

where ln is the natural logarithm. Assuming that the mass is constant in the convection zone, it is straightforward to show from Eq. (2.1) of hydrostatic support, and the definition of Γ in Eq. (2.5) that

$$\delta \ln \frac{p}{\rho} = \left(\frac{r}{R}\right)^2 H_p^{-1}\left[H_{p,s}\left(\delta \ln \frac{p}{\rho}\right)_s + \int_r^R \left(\frac{R'}{r}\right)^2 \frac{\delta \ln \Gamma}{\Gamma} dr'\right] ; \tag{2.10}$$

here

$$H_p = \frac{p}{g\rho} \tag{2.11}$$

is the pressure scale height, g being gravity, and the subscript s indicates values at $r = R$.

The change in Γ can be thought of as consisting of two parts: the change in the superadiabatic gradient $\Gamma - \Gamma_1$, and the change in Γ_1. The former is localized to the very thin region where convection is significantly superadiabatic, and hence in most of the star its contribution can be considered as a constant term in the square brackets in Eq. (2.10). The change in Γ_1 can be written as

$$\begin{aligned}\delta \ln \Gamma_1 =& (\delta \ln \Gamma_1)^{(i)} \\ &+ \left(\frac{\partial \ln \Gamma_1}{\partial \ln p}\right)_{\rho,X} \delta \ln p + \left(\frac{\partial \ln \Gamma_1}{\partial \ln \rho}\right)_{p,X} \delta \ln \rho + \left(\frac{\partial \ln \Gamma_1}{\partial X}\right)_{p,\rho} \delta X .\end{aligned} \tag{2.12}$$

Here $(\delta \ln \Gamma_1)^{(i)}$ is the intrinsic change, at fixed p, ρ and X, brought about by a possible change in the equation of state; the remaining terms arise from the changes in p, ρ and X, and the dependence of Γ_1 on these quantities. Notice that δX is constant in the convection zone.

With the possible exception of intrinsic changes to the equation of state, $\delta \ln \Gamma_1$ is of significant size only in the ionization zones of hydrogen and helium. The same is therefore true of $\delta\Gamma$. Since H_p^{-1} decreases roughly as T^{-1} with increasing depth (cf. Eq. [2.11]) it follows from Eqs. (2.9) and (2.10) that within the convection zone, and outside the ionization zones, $\delta \ln c$ likewise decreases with increasing depth. In particular, if the changes in Γ_1 and the superadiabatic gradient can be neglected, there is no change in the sound speed in the convection zone; this is obviously consistent with the approximation (2.8) for the sound speed.

From the equation of hydrostatic support, again neglecting the variation of mass, it also follows that the change in p is related to the change in p/ρ by

$$\begin{aligned}\delta \ln p =&(\delta \ln p)_s - \int_r^R \delta\left(\ln\frac{p}{\rho}\right)\frac{g\rho}{p}dr' \\ =&(\delta \ln p)_s - \int_{\ln p_s}^{\ln p} \delta\left(\ln\frac{p}{\rho}\right) d\ln p' \ .\end{aligned} \tag{2.13}$$

Since pressure varies very rapidly with depth in the outer part of the convection zone (between depths of $0.001R$ and $0.01R$, p increases by roughly a factor 1000) even a fairly small change in p/ρ, of predominantly the same sign, can lead to a considerable change in p. An example of this is considered in Sect. 4.2.1.

The changes in p/ρ and p are coupled through the change in Γ_1, as is evident from Eq. (2.12). Thus in general the changes to the model satisfy a set of coupled, linear differential equations (see also Däppen 1983). Nevertheless, the integral relations (2.10) and (2.13) provide some indication of the behaviour of the changes. Also, since the derivatives of Γ_1 in Eq. (2.12) are quite small except in the hydrogen ionization zone, there may be circumstances where the intrinsic change in Γ_1 dominates, and where therefore $\delta \ln c$ can be calculated without consideration of the changes in p and ρ.

2.2 Properties of solar oscillations

The present section gives an overview of the theory of stellar oscillations, particularly those aspects that concern the determination of the oscillation frequencies, and a very brief summary of the observations of solar oscillations. More extensive presentations can be found, for example, in the reviews by Deubner and Gough (1984), Christensen-Dalsgaard et al. (1985), Christensen-Dalsgaard (1988a), Libbrecht (1988a), Vorontsov and Zharkov (1989), Gough and Toomre (1991), Libbrecht and Woodard (1991), Christensen-Dalsgaard and Berthomieu (1991), and Gough (1992), as well as in the classical review by Ledoux and Walraven (1958) and the books by Cox (1980) and Unno et al. (1989).

2.2.1 Geometry of the modes

Small-amplitude oscillations of a spherical star can be separated into normal modes, each of which has a harmonic dependence on time, and depends on the spherical coordinates θ and ϕ (co-latitude and longitude) as a spherical harmonic. The displacement for a single mode can be written

$$\boldsymbol{\delta r}(r,\theta,\phi,t) = Re\left\{\left[\xi_r(r)Y_l^m\boldsymbol{a}_r + \xi_h(r)\left(\frac{\partial Y_l^m}{\partial\theta}\boldsymbol{a}_\theta + \frac{1}{\sin\theta}\frac{\partial Y_l^m}{\partial\phi}\boldsymbol{a}_\phi\right)\right]e^{-i\omega t}\right\}\ , \tag{2.14}$$

where $\boldsymbol{a}_r$, $\boldsymbol{a}_\theta$ and $\boldsymbol{a}_\phi$ are unit vectors in the r, θ and ϕ directions. Here $Y_l^m(\theta,\phi) = c_{lm}P_l^m(\cos\theta)e^{im\phi}$ is a spherical harmonic, P_l^m being a Legendre function and c_{lm} a normalization constant defined such that the integral of $|Y_l^m|^2$ over the sphere is unity. In particular, Eq. (2.14) describes the variation of the displacement, and hence

the velocity, over the solar surface, and thus determines the observable properties of the oscillation. The variation of the displacement with the distance r from the centre is determined by the *eigenfunctions* $\xi_r(r)$ and $\xi_h(r)$. The dependence of the perturbation of a scalar quantity, such as pressure, on position and time may similarly be written as

$$p'(r,\theta,\phi,t) = Re\left\{\left[\tilde{p}(r)Y_l^m\right] e^{-i\omega t}\right\} , \tag{2.15}$$

where $\tilde{p}$ is the amplitude function, which describes the radial variation of the perturbation.

The mode is characterized by three wavenumbers: n is the *radial order* whose absolute value, roughly, gives the number of zeros in ξ_r; l is the *degree*, and m the *azimuthal order* of the mode. The degree of the mode is related to its horizontal wavenumber k_h and wavelength λ_h at radius r by

$$k_h = \frac{2\pi}{\lambda_h} = \frac{L}{r} , \tag{2.16}$$

where $L = \sqrt{l(l+1)}$. As is seen from Eq. (2.14), m, which is in the range $-l$ to l, is twice the number of zeros around the equator.

If the processes that damp or excite the oscillations are neglected, ω is real, and the eigenfunctions ξ_r and ξ_h may also be chosen to be real. In addition to the *angular frequency* ω, which is used in Eq. (2.14), the *cyclic frequency* $\nu = \omega/(2\pi) = 1/P$, is commonly used, particularly in discussions of observed frequencies; here P is the oscillation period.

In general, the frequency $\omega = \omega_{nlm}$ depends on all three wavenumbers. However if rotation or other departures from spherical symmetry are ignored, ω_{nlm} does not depend on m. This follows from the fact that in this case there is no preferred axis in the star; since m depends on the choice of coordinate axis, the physics of the oscillations, and hence their frequencies, must be independent of m. For slow rotation a modal description as in Eq. (2.14) is still possible, provided that the rotation axis is chosen as coordinate axis. Rotation introduces a splitting in the oscillation frequencies; this may be used to determine the variation of angular velocity within the Sun [Duvall et al. (1984); Brown et al. (1989); for reviews, see also Harvey (1988) and Christensen-Dalsgaard (1990a)]. Here, however, we neglect effects of rotation and other departures from spherical symmetry, and hence assume that the frequencies are independent of m.

2.2.2 Physics of solar oscillations

The equations governing oscillations with small amplitudes are obtained by linearizing the equations of hydrodynamics. It is common to ignore the processes that damp or excite the oscillations, by assuming them to occur *adiabatically*, i.e., without heat loss or gain. In this case the perturbations of pressure and density are related by

$$\frac{\delta p}{p} = \Gamma_1 \frac{\delta \rho}{\rho} . \tag{2.17}$$

Note that in this section only δ denotes the *Lagrangian* perturbation, i.e., the perturbation following the motion (it should not be confused with its usage elsewhere to

denote differences between different equilibrium models). It is related to the local, or *Eulerian* perturbation, indicated by a prime, by, for example

$$\delta p = p' + \boldsymbol{\delta r} \cdot \nabla p \,. \tag{2.18}$$

We assume that the dependence of the variables on θ, ϕ and time has been separated as in Eqs. (2.14) and (2.15), and we suppress the tildes on the amplitude functions. The equations of adiabatic oscillations may then be written

$$\frac{d\xi_r}{dr} = -\left(\frac{2}{r} + \frac{1}{\Gamma_1 p}\frac{dp}{dr}\right)\xi_r + \frac{1}{\rho c^2}\left(\frac{S_l^2}{\omega^2} - 1\right)p' - \frac{l(l+1)}{\omega^2 r^2}\Phi' \,, \tag{2.19}$$

$$\frac{dp'}{dr} = \rho(\omega^2 - N^2)\xi_r + \frac{1}{\Gamma_1 p}\frac{dp}{dr}p' + \rho\frac{d\Phi'}{dr} \,, \tag{2.20}$$

$$\frac{1}{r^2}\frac{d}{dr}\left(r^2\frac{d\Phi'}{dr}\right) = -4\pi G\left(\frac{p'}{c^2} + \frac{\rho\xi_r}{g}N^2\right) + \frac{l(l+1)}{r^2}\Phi' \,. \tag{2.21}$$

Here Φ' is the perturbation in the gravitational potential, and we introduced the characteristic acoustical frequency

$$S_l = \frac{Lc}{r} = k_h c \,, \tag{2.22}$$

and the buoyancy frequency N, given by

$$N^2 = g\left(\frac{1}{\Gamma_1 p}\frac{dp}{dr} - \frac{1}{\rho}\frac{d\rho}{dr}\right) \,, \tag{2.23}$$

where g is the gravitational acceleration. It may also be shown that the amplitude ξ_h of the horizontal component of the displacement (cf. Eq. [2.14]) is given by

$$\xi_h = \frac{1}{r\omega^2}\left(\frac{p'}{\rho} - \Phi'\right) \,. \tag{2.24}$$

Equations (2.19), (2.20) and (2.21) constitute a fourth-order system of ordinary linear differential equations for the 4 dependent variables ξ_r, p', Φ' and $d\Phi'/dr$. They must be supplemented by four boundary conditions. Two of these are obtained from regularity of the solution at $r = 0$, which is a regular singular point of the equations. One surface condition results from demanding the continuity of Φ' and its first derivative. Finally, a condition can be obtained by considering the behaviour of the oscillations in the solar atmosphere.

Equations (2.19) – (2.21) depend on the structure of the equilibrium model. In fact, the coefficients in these equations are essentially completely determined if the density ρ and the adiabatic exponent Γ_1 are given as functions of r, assuming that the model is in hydrostatic equilibrium. Given ρ, the interior mass $m(r)$ is obtained by integrating Eq. (2.2), with the obvious boundary condition $m(r) = 0$. Then $p(r)$ can be obtained from Eq. (2.1) by integrating from the surface; this requires an assumption about the surface pressure, which, for example, can be obtained from semi-empirical

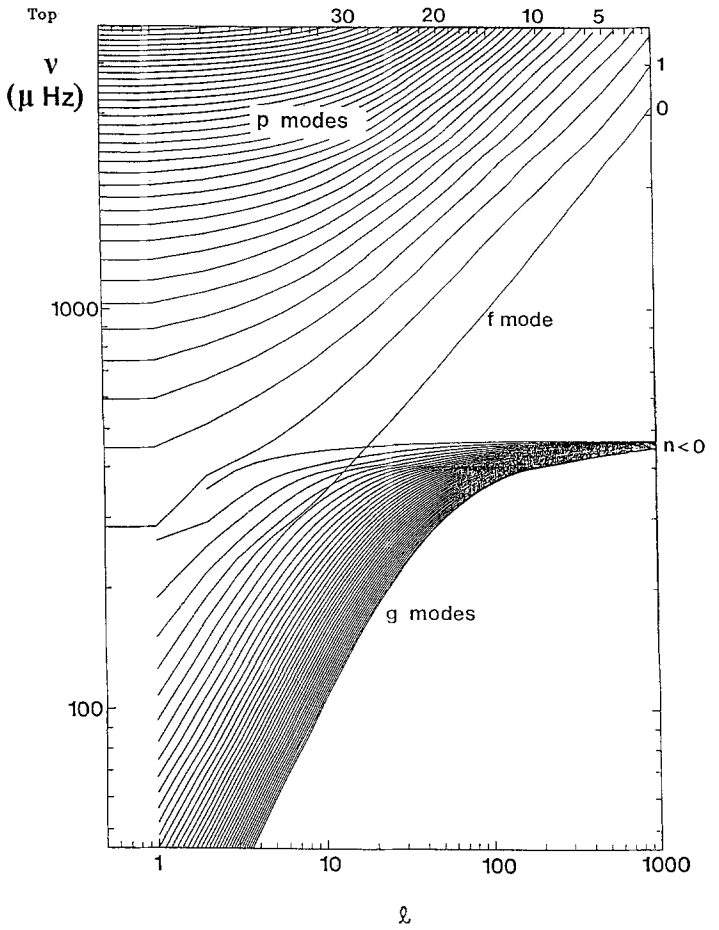

Fig. 3. Adiabatic oscillation frequencies for a standard model of the present Sun, as functions of the degree l. For clarity points corresponding to modes with a given radial order have been connected by straight lines, some of which have been labelled by the radial order. Only g modes with order less than 40 have been included

models of the solar atmosphere (e.g. Vernazza et al. 1981). Given $p(r)$, $\rho(r)$ and $\Gamma_1(r)$, the coefficients may be evaluated.

In the adiabatic approximation the computation of the oscillation frequencies is a straightforward numerical problem. Nevertheless, some care is needed to obtain sufficient precision, particularly in view of the fact that the radial order of some of the observed modes is high. To illustrate the results, Fig. 3 shows computed eigenfrequencies for a standard solar model, as functions of the degree l. The curves are labelled by the radial order of the modes; by convention, the sign of n is used to distinguish different types of oscillations (see below), whereas $|n|$, at least in the limit when it is large, gives the number of zeros in the radial direction in the eigenfunctions. From the figure it is evident that there are two distinct, but slightly overlapping, groups of modes, with very different behaviour of the frequency as a function of l. The upper set of modes has $n > 0$; they are known as *p modes*, since for these modes the dominant restoring force is the pressure perturbation; thus they have the character of

standing sound waves (see also Sect. 2.2.3). The modes with $n = 0$, although similar to the p modes in the behaviour of the frequencies, are in fact physically distinct; for l greater than about 20 they behave approximately as surface gravity waves, with frequency

$$\omega \simeq g_s k_h = \frac{g_s}{R} L \,, \tag{2.25}$$

where g_s is the surface gravity. They are known as *f modes*. Finally, the modes with $n < 0$ are known as *g modes*; here the dominant restoring force is gravity acting on the density perturbations, and the modes have the character of standing gravity waves. Only the g modes with $|n| \leq 40$ have been shown; the g mode spectrum extends to zero frequency at all degrees, although the modes obviously become increasingly crowded with increasing degree. On the other hand, the gap between the g and the f modes is real.

An important global property of a mode of oscillation, beside the frequency, is its integrated kinetic energy or, equivalently, its inertia. Here we consider the dimensionless inertia

$$E_{nl} = \frac{4\pi \int_0^R [\xi_r^2 + l(l+1)\xi_h^2] \rho r^2 dr}{M[\xi_r^2(R_{\text{phot}}) + l(l+1)\xi_h^2(R_{\text{phot}})]} \,, \tag{2.26}$$

where R_{phot} is the photospheric radius. This is related to the modal mass M_{nl} (cf. Goldreich and Keeley 1977) by $M_{nl} = E_{nl} M$, and defined such that the time-averaged kinetic energy in the oscillation is

$$\frac{1}{2} M_{nl} V_{rms}^2 = \frac{1}{2} E_{nl} M V_{rms}^2 \,, \tag{2.27}$$

where V_{rms}^2 is the mean, over the solar surface and time, of the squared total photospheric velocity of the mode. For p modes E_{nl} decreases rapidly with increasing frequency up to about 3000 μHz. This is related to the behaviour of the eigenfunctions: at low frequencies there is a region just beneath the solar surface where the displacement increases roughly exponentially with depth; hence the interior amplitude is substantially larger than the surface value (Libbrecht 1988b; Christensen-Dalsgaard 1988b), and E_{nl} is large. At high frequencies, on the other hand, the mode is oscillatory essentially to the surface, and the surface and interior amplitudes are comparable. Furthermore, E_{nl} decreases substantially with increasing l at fixed frequency; the increase in l causes the mode to be confined closer to the surface, and hence to involve a smaller fraction of the mass of the Sun.

The calculations described so far ignore a number of complicating features that are so far badly understood, such as

- nonadiabaticity
- excitation, more generally
- dynamical effects of convection
- detailed atmospheric behaviour
- magnetic fields.

This approximation is in some sense similar to those underlying the computation of standard solar models. Calculations that do take into account some of the features (Christensen-Dalsgaard and Frandsen 1983; Kidman and Cox 1984; Balmforth and Gough 1988, 1990; Balmforth 1992a–c; see also Sect. 4.3) show that they may change

the frequencies by several μHz. Thus they have a substantial effect on comparisons between observed and computed frequencies. On the other hand, the complications are all (again with the possible exception of a very strong deep-seated magnetic field) located near the solar surface. Thus they add to the uncertainty of the surface region indicated in Fig. 1 but do not directly affect the properties of the oscillations in the deeper solar interior.

2.2.3 Asymptotic properties of p modes

Although the numerical solution of the equations of adiabatic oscillations is relatively simple, it does not immediately provide an understanding of the properties of the oscillations. Such understanding may be obtained by means of asymptotic theory. It was shown by Gough (Deubner and Gough 1984; Gough 1986a) how to write down an approximate form of the oscillation equations, from which it is straightforward to obtain the asymptotic behaviour of the solution. Here we restrict the discussion to p modes and present a description of the asymptotic behaviour which, although extremely simple, nevertheless contains the most important results of the more complete theory.

The p modes can be approximated locally by plane sound waves, with the dispersion relation $k^2 \equiv k_r^2 + k_h^2 = \omega^2/c^2$. Here k, k_r and k_h are the length, and the radial and horizontal components, of the wave vector. For a mode of oscillation, k_h is given by Eq. (2.16), so that

$$k_r^2 = \frac{\omega^2}{c^2} - \frac{L^2}{r^2} \,. \tag{2.28}$$

Close to the surface, c is small and hence k_r is large. Here the modes propagate almost vertically. With increasing depth, c increases and k_r decreases, until the point is reached where $k_r = 0$ and the wave propagates horizontally. The location $r = r_t$ of this *turning point* is determined by

$$\frac{c(r_t)}{r_t} = \frac{\omega}{L} \,. \tag{2.29}$$

It corresponds to a point of total internal reflection; for $r < r_t$, $k_r^2 < 0$, and the mode decays exponentially. The behaviour at the surface requires a more careful analysis, showing that below a critical cut-off frequency (which in the solar atmosphere corresponds to a cyclic frequency of about 5200 μHz) the wave is reflected by the steep density gradient. Thus the wave propagates in a series of "bounces" between the surface and the turning point. A mode of oscillation is a standing wave, formed as an interference pattern between such bouncing waves. It is trapped between the surface and r_t, and hence its frequency depends largely on conditions in this region. Figure 4 illustrates r_t as calculated from Eq. (2.29). Modes at the highest values of l observed are confined to the outermost fraction of a per cent of the solar radius, whereas the lowest-degree modes penetrate essentially to the centre.

Due to the rapid decrease of the sound speed with increasing radius, the first term on the right-hand side of Eq. (2.28) is substantially larger than the second except near or below the turning point. As a result, except near their turning points modes of the same frequency but different degree have essentially the same k_r; thus the properties of the modes, and their response to solar structure, are similar.

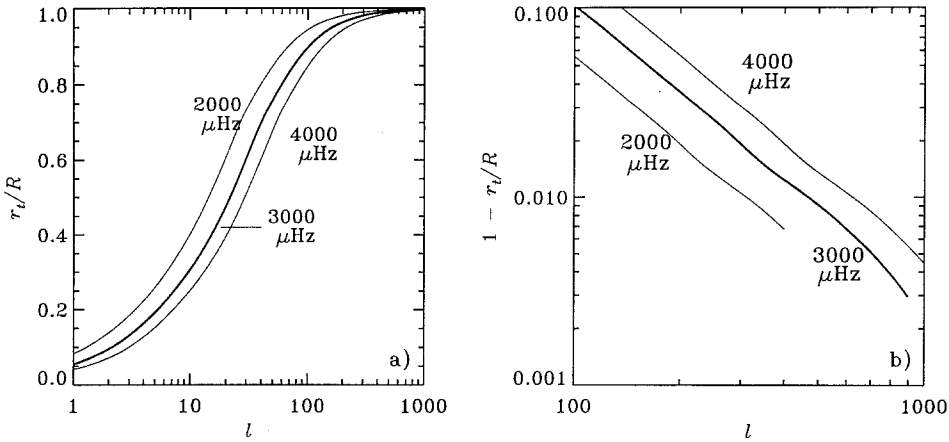

Fig. 4. The turning point radius r_t **a** and the penetration depth $R - r_t$ **b**, in units of the solar radius R, as a function of degree l for three values of the frequency ν. The curves have been calculated from Eq. (2.29) for a standard model of the present Sun. In panel **b** the curves terminate at the degree where the frequency equals the f-mode frequency; for p modes the degree is below this value at a given frequency (see also Fig. 3)

This simple description of the p modes may be extended to give an asymptotic relation for their frequencies (Gough 1984b; Christensen-Dalsgaard et al. 1985): the condition for a standing wave is that the change in phase in the radial direction is an integral multiple of π, apart from a contribution which takes into account the phase change at the inner turning point and at the surface. This condition may be expressed as

$$\int_{r_t}^{R} k_r dr \simeq (n + \alpha)\pi \ ,$$

or

$$\int_{r_t}^{R} \left[1 - \left(\frac{Lc}{\omega r}\right)^2\right]^{1/2} \frac{dr}{c} \simeq \frac{\pi[n + \alpha(\omega)]}{\omega} \ , \tag{2.30}$$

where we used Eq. (2.28). Here α is the quantity which takes into account the phase change at the reflection points; the reflection at the lower turning point introduces a phase change of $\pi/4$, whereas the outer reflection, and hence α, depends on conditions near the surface. As indicated, α is in general a function of the frequency, but not of the degree, of the mode. Indeed, as discussed above, the waves propagate almost vertically near the surface; hence their behaviour here is essentially independent of the horizontal wavenumber and so, therefore, is α.

A more careful analysis of the asymptotic behaviour near the centre of the solution for modes of low degree, including radial modes, shows that L should be replaced by $l + 1/2$ [Brodsky and Vorontsov (1987, 1988a); see also Kemble (1937) for the corresponding result for solutions to the Schrödinger equation]. Except at low l this modification evidently has little effect; hence in the following we take $L = l + 1/2$. We note also that the derivation of Eq. (2.30) assumes the *Cowling approximation*, i.e., that the perturbation Φ' in the gravitational potential can be neglected (Cowling 1941). It is straightforward, however, to extend it to take into account the leading-order effect of Φ', by using Jeans's (1929) dispersion relation for waves in a homogeneous, gravitating medium (Christensen-Dalsgaard 1991a); the resulting expression for the

frequency correction was obtained previously by Vorontsov (1988a, 1989) and Tassoul (1990) through more complete asymptotic analyses.

As r_t is a function of ω/L, Eq. (2.30) may be written as

$$\frac{\pi[n+\alpha(\omega)]}{\omega} = F\left(\frac{\omega}{L}\right) , \tag{2.31}$$

where

$$F(w) = \int_{r_t}^{R} \left(1 - \frac{c^2}{r^2 w^2}\right)^{1/2} \frac{dr}{c} . \tag{2.32}$$

That solar oscillations satisfy a relation of this form was first found by Duvall (1982) from observed frequencies. In fact, since Eq. (2.31) is a relation between observable quantities, the function F can be determined observationally. This is achieved by fitting the observed frequencies to a relation of the form given in this equation to determine, in addition to $F(w)$, the function $\alpha(\omega)$. It should be noted that in this fit $F(w)$ is determined only to within an additive constant, and correspondingly $\alpha(\omega)$ is determined to within a term proportional to ω. This led Brodsky and Vorontsov (1987, 1988a) to consider instead

$$\beta(\omega) \equiv -\omega^2 \frac{d}{d\omega}\left(\frac{\alpha}{\omega}\right) , \tag{2.33}$$

which clearly does not suffer from this indeterminacy.

For small l Eq. (2.30) reduces to

$$\nu_{nl} \sim (n + \frac{l}{2} + \frac{1}{4} + \alpha)\Delta\nu + \epsilon_{nl} \tag{2.34}$$

(Vandakurov 1967; Tassoul 1980), where

$$\Delta\nu = \left(2\int_0^R \frac{dr}{c}\right)^{-1} \tag{2.35}$$

is the inverse of twice the sound travel time between the centre and the surface, and ϵ_{nl} is a small correction term. Thus, neglecting ϵ_{nl}, there is approximately a uniform spacing $\Delta\nu$ between modes of same degree, but different order. Equation (2.34) also predicts the approximate equality $\nu_{nl} \simeq \nu_{n-1,l+2}$. This frequency pattern has been observed for the solar five-minute modes of low degree.

It is of great interest to consider the *deviations* from this simple behaviour, introduced by ϵ_{nl}. This can conveniently be analysed by considering the separation $\delta\nu_{nl} = \nu_{nl} - \nu_{n-1,l+2}$; it is predominantly determined by conditions in the solar core since, as argued above, only here does the behaviour of the modes depend substantially on l. From asymptotic analysis (e.g. Tassoul 1980; Gough 1986a) one finds that

$$\delta\nu_{nl} \simeq -(4l+6)\frac{\Delta\nu}{4\pi^2\nu_{nl}} \int_0^R \frac{dc}{dr}\frac{dr}{r} , \tag{2.36}$$

where we neglected a small term in the surface sound speed. This relation was analysed in more detail by Gabriel (1989), Gough and Novotny (1990) and Christensen-Dalsgaard (1992a); although its precision, when compared with numerically computed frequencies, is somewhat questionable, it nonetheless indicates the sensitivity of $\delta\nu_{nl}$

to the conditions in the solar core. In Sect. 4.4 we consider examples of this sensitivity, and compare the computed separation with values obtained from observed frequencies.

It is of interest to use Eq. (2.30) to estimate the effects on the frequencies of *changes* in the equilibrium model. If δc denotes the difference in c between two solar models, at fixed r, and $\delta\alpha$ denotes the difference in α at fixed frequency, it follows by linearization, assuming δc and $\delta\alpha$ to be small, that (Christensen-Dalsgaard et al. 1988a)

$$S\frac{\delta\omega}{\omega} \simeq \int_{r_t}^{R} \left(1 - \frac{L^2c^2}{r^2\omega^2}\right)^{-1/2} \frac{\delta c}{c}\frac{dr}{c} + \pi\frac{\delta\alpha}{\omega} , \tag{2.37}$$

where

$$S = \int_{r_t}^{R} \left(1 - \frac{L^2c^2}{r^2\omega^2}\right)^{-1/2} \frac{dr}{c} - \pi\frac{d\alpha}{d\omega} . \tag{2.38}$$

Since α is assumed to be a function of ω alone, and r_t is determined by ω/L, the scaled frequency difference $S\delta\omega/\omega$ is predicted to be of the form

$$S\frac{\delta\omega}{\omega} \simeq H_1\left(\frac{\omega}{L}\right) + H_2(\omega) , \tag{2.39}$$

where the two functions H_1 and H_2 are determined by Eq. (2.37). Furthermore, the last term on the right-hand side of Eq. (2.38) is in general relatively small compared with the first, and hence S is approximately a function of ω/L. Equation (2.39) evidently describes a very special dependence of $\delta\omega$ on ω and L.

Since c/r decreases quite rapidly with increasing r, $(Lc/r\omega)^2 \ll 1$ except near the turning point r_t; hence as a rough approximation $1 - L^2c^2/r^2\omega^2$ may be replaced by 1 in the integrals in Eqs. (2.37) and (2.38). If furthermore the term in $\delta\alpha$ can be neglected, the result is the very simple relation between the changes in sound speed and frequency:

$$\frac{\delta\omega}{\omega} \simeq \frac{\displaystyle\int_{r_t}^{R} \frac{\delta c}{c}\frac{dr}{c}}{\displaystyle\int_{r_t}^{R} \frac{dr}{c}} . \tag{2.40}$$

This shows that the change in sound speed in a region of the Sun affects the frequency with a weight determined by the time spent by the mode, regarded as a superposition of traveling waves, in that region. Thus changes near the surface, where the sound speed is low, have relatively large effects on the frequencies. Although this expression is only a rough approximation, it is a useful guide in attempts to interpret frequency differences between models, or between observed and computed frequencies.

The dependence of α on frequency is determined by the structure of the outer few per cent of the radius of the Sun, including the region where hydrogen and helium ionization takes place. Consequently, $\alpha(\omega)$ provides a potentially powerful diagnostics of effects of the equation of state. In Sect. 4 we make extensive use of differences in α, expressed in terms of the function $H_2(\omega)$ introduced in Eq. (2.39), to characterize the frequency differences between pairs of models or between the Sun and a model. It is possible to express $H_2(\omega)$ in terms of integrals of appropriate kernels multiplying differences in the structure of the model (Christensen-Dalsgaard and Pérez Hernández 1988, 1992). This may eventually enable a study of the outer layers of the Sun from

inversion of H_2 as determined from the observed frequencies. In such an analysis it is a substantial problem that α is affected also by the uncertainties in our description of the physics of the very superficial layers of the Sun, including the superadiabatic part of the convection zone; however, as discussed in Sect. 4.1.1 it is possible to achieve some separation of the different effects by considering the variation of H_2 with ω. We note also that Marchenkov and Vorontsov (1990, 1991) presented a method for inverting differences between the observed Vorontsov phase function $\beta(\omega)$ and $\beta(\omega)$ for a reference model, to determine corrections to the structure near the surface of the model.

As discussed in Sect. 2.3.2, the asymptotic relations (2.30) and (2.37) permit an almost direct, and surprisingly precise, inversion for the solar sound speed or the sound-speed difference between the Sun and a model.

2.2.4 Observations of solar oscillations

Solar oscillations have been observed with a variety of techniques, but the most detailed data have so far been obtained by measuring Doppler velocity [for a review of observing techniques, see Brown (1988); a brief overview of techniques for observing and analysing solar oscillations was given by Christensen-Dalsgaard (1992a)]. From spatially resolved observations modes corresponding to individual spherical harmonics may be isolated through a suitable spatial transform; this has led to the detection of modes with degrees as high as 1500, where the observations are restricted by seeing in the Earth's atmosphere. In addition, particularly sensitive measurements of low-degree modes can be obtained from unresolved Doppler observations, in light integrated over the solar disk.

The *five-minute oscillations* have cyclic frequencies between about 1 and 5 mHz, and extend in l from radial modes, with $l = 0$, to the observational cut-off in degree. It follows from the theoretical properties of the oscillations discussed above that they correspond predominantly to p modes but also, at moderate and high degree, include f modes. The five-minute oscillations are the only modes whose degrees and radial orders have been determined. This is a prerequisite for the use of the observed frequencies to study the solar interior, and hence helioseismic investigations of the solar interior have up to now been based on these modes. A characteristic feature is that their distribution of power as a function of frequency and the average amplitude per mode are largely independent of l (Christensen-Dalsgaard and Gough 1982; Libbrecht et al. 1986). The maximum velocity amplitude for single modes is about $15\,\mathrm{cm\,sec^{-1}}$. This corresponds to a relative amplitude in broad-band intensity of order 10^{-6}; such observations were carried out from the SMM satellite (Woodard and Hudson 1983) and more recently from the Soviet Mars probe PHOBOS (Toutain and Fröhlich 1992). The mode *lifetimes* are strongly dependent on frequency (Libbrecht 1988c; Jefferies et al. 1991; Duvall et al. 1991), varying from about a day at high frequency to several months at the lowest frequencies observed.

Libbrecht et al. (1990) published an extensive compilation of frequencies of five-minute oscillations; the most accurately determined of these have relative errors of order 10^{-5}. Furthermore, sets of accurate frequencies of low-degree modes were presented by Elsworth et al. (1991) on the basis of data from a network of whole-disk observing stations, and by Toutain and Fröhlich (1992) based on the space observations of intensity oscillations mentioned above.

In the following we are exclusively concerned with the properties of the five-minute oscillations. Nevertheless, it should be mentioned that there have been claims for the detection of other types of oscillations in the Sun. At intermediate frequencies, between 0.1 and 2 mHz, there have been reports, although not substantiated by other observing techniques, of oscillations observed in the solar limb intensity (Hill and Caudell 1985). At even lower frequencies, corresponding to periods of more than 2 hours, there have been observations of a number of oscillations, both in Doppler velocity (e.g. Severny et al. 1976; Brookes et al. 1976; Scherrer and Wilcox 1983; van der Raay 1988) and, somewhat less directly, in intensity (Fröhlich and Delache 1984a,b; Fröhlich 1988). If the observations are indeed of solar eigenmodes, they would have to be g modes of fairly high order; this would make then extremely valuable as probes of the deep solar interior. It is probably fair to say, however, that the reality or solar origin of these long-period oscillations are still questionable (Fossat et al. 1988; Garcia et al. 1988; Elsworth et al. 1989).

2.3 Inverse analysis

Neglecting again rotation and other departures from spherical symmetry the oscillation frequencies ω_{nl} are functionals

$$\omega_{nl} = \mathcal{F}_{nl}\,[\rho(r),\ p(r), \ldots] \tag{2.41}$$

of the structure of the Sun. So far we have discussed how to obtain the frequencies, given the structure. With the ability to do so, one can compare observed frequencies with computations based on different models, and in this way obtain some information about solar structure. In particular, as discussed in Sect. 4.3, one may be able to choose between different formulations of the physics in the model. However, it is evidently desirable to attempt to invert the process, to obtain more extensive information about the properties of the solar interior from the observed frequencies.

Such *inverse analyses* are, in a certain sense, implicit in any type of scientific measurement, since a raw measurement rarely supplies the quantity that one is interested in. However, in the present case the relation between the desired properties of the Sun, e.g. $\rho(r)$, and the observed quantities is more complex, since each frequency is sensitive to the structure of a substantial part of the Sun; thus the inverse problem is correspondingly more difficult. Similar problems are encountered in other branches of science, such as geophysics and radiation theory, and there is a substantial literature dealing with them (Parker 1977; Deepak 1977; Craig and Brown 1986; Tarantola 1987).

Here we provide a brief description of the principles of helioseismic inversion and discuss their application to the study of the solar internal structure. For more extensive treatments the papers by, for example, Gough (1985), Thompson (1991) and Gough and Thompson (1991) may be consulted.

2.3.1 Principles of helioseismic inversion

As discussed in Sect. 2.2.2 the equations of adiabatic oscillations depend on the structure of the equilibrium model only through the density $\rho(r)$ and adiabatic exponent $\Gamma_1(r)$; given $\rho(r)$, the pressure $p(r)$ can be computed from the equation of hydrostatic

equilibrium, which must be satisfied to a high degree of precision. Thus p, ρ and Γ_1 are the only quantities that are directly constrained by the observed frequencies. Furthermore, in the important case of the solar five-minute oscillations, the frequencies are mainly determined by a combination of p, ρ and Γ_1, *viz.* the adiabatic sound speed given by Eq. (2.6).

To move beyond the determination of these properties of the solar interior, additional constraints must be imposed. As discussed by Gough and Kosovichev (1988) this may be done at two levels. At the level of what they term *secondary inversions* one imposes Eqs. (2.3) and (2.4) of thermal equilibrium and energy transport, together with expressions for the equation of state, opacity and energy generation rate. It is then possible to determine the variation of, for example, temperature T and hydrogen abundance X in the solar interior. At the level of *tertiary* inversion one imposes in addition the constraint that the evolution of the Sun is in accordance with that of standard solar models. Then, as discussed in Sect. 2.1.1, the structure of the present Sun is completely determined by the microphysics, whose properties one may therefore attempt to determine through the inversion.

According to this argument inversion for the microphysics, which is in some sense the subject of this review, might appear essentially impossible, given the assumptions required in computing standard solar models. This argument, however, may be too formalistic, since it ignores the possibility that a sufficiently comprehensive description of the structure of certain regions of the Sun can be made without involving the complete set of assumptions. For our purposes the most important example, already discussed at some length in Sect. 2.1.2, is the convection zone. If one accepts the assumptions that the stratification in the convection zone is essentially adiabatic and that it is chemically homogeneous, its structure is determined by the equation of state, as well as by the constant values of the specific entropy and the composition, the latter being essentially specified by the abundances X and Z of hydrogen and heavy elements. It does not appear unreasonable to expect that sufficiently detailed information will become available to allow the determination of the composition, and at the same time provide information about the equation of state in the regions of partial ionization of hydrogen and helium. We return to this point in Sect. 4 below. As a second example, we may consider the region beneath the convection zone, but outside the region where nuclear burning takes place. Here it might be reasonable to assume the composition to be constant and equal to the composition in the convection zone, and the luminosity is presumably also equal to its surface value. Furthermore, it is likely that the uncertainty in the equation of state, insofar as it affects the structure of the model and the oscillation frequencies, is modest. In that case the dominant uncertainty would be in the opacity, and one would perhaps be justified in attempting to get information from the observations about the opacity in the temperature range corresponding to this region.

It is obvious that some caution is required in these examples, as indeed in any analysis of helioseismic data. In the case of the convection zone, for example, it is conceivable that magnetic fields sufficiently strong to affect the structure might exist, and hence invalidate investigations of the equation of state that neglected them. Similarly, diffusion beneath the convection zone would lead to abundance inhomogeneities which would introduce errors in attempts to probe the opacity. Only by careful consideration of all the available data, and through attempts to construct a consistent picture of the solar interior, can we hope to minimize the effects of such uncertainties; however, it is evident that we can never completely eliminate the pos-

sibility of being misled by the Sun's potentially boundless ingenuity in introducing new, as yet unimagined complications.

The goal of the inverse analysis is to isolate information about localized regions of the solar interior. That this is possible, in principle, from observations of the five-minute oscillations follows from the structure of the eigenfunctions (c.f. the discussion of their asymptotic properties in Sect. 2.2.3). Consider two modes with slightly different degree, and hence slightly different r_t, but almost the same frequency. Since their eigenfunctions are similar away from the turning points, the frequency difference between these two modes is mainly determined by the region in the model between the two turning points. Hence the difference is a measure of conditions in that region. In practice much more elaborate combinations of the frequencies than simple differences are needed to obtain truly localized information about the solar interior; but the principle remains the same. Thus inversions based on the five-minute oscillations are *differential* processes. In particular they involve cancellation of the large contribution to the frequencies coming from near the surface, where the eigenfunctions are large. To obtain accurate results on the deep solar interior therefore requires very precise frequency measurements.

Although inversion of the five-minute oscillations, due to their relatively limited range in frequency, is principally controlled by the variation in turning point position with degree, it should be noticed that inversion is possible also on the basis of low-degree oscillations alone, provided that the data cover a sufficient range in radial order (Cooper 1981; Christensen-Dalsgaard and Gough 1984; Christensen-Dalsgaard et al. 1990). The principle of the inversion in this case is similar to a Fourier analysis in space, since the observed frequencies can be regarded as a set of Fourier coefficients, in a generalized sense, of the underlying solar structure. Given a sufficiently extensive set of Fourier coefficients one may attempt to reconstruct the underlying structure; this corresponds to the inversion.

A general property of the inversions is that we desire an infinite amount of information, e.g. the dependence of structure on position in the Sun, from a finite amount of data. Thus the problem is underdetermined. To obtain a definite solution, we must impose additional constraints. The nature of these constraints vary, but in general they require that the solution be smooth, in a suitable sense, and hence they act to limit the resolution achieved in the inversion. Furthermore, observational errors must be taken into account. In general, there is a trade-off between achieving high resolution and restricting the errors in the result. This trade-off is controlled by one or more parameters in the inversion procedures, which must be determined as part of the analysis. Additional, external constraints may result from other known properties of the Sun; in particular it is obvious that the structure should be such as to be consistent with the observed surface mass and radius of the Sun.

2.3.2 Asymptotic inversion

Simple, yet powerful, inversion techniques are based on the asymptotic relation (2.30). As discussed in Sect. 2.2.3 the function $F(w)$, which is related to the sound speed c through Eq. (2.32), can be determined from observed frequencies. Given F, Eq. (2.32) provides an integral equation for c as a function of r. This can be inverted analytically (Gough 1984b), to yield

$$r = r\left(\frac{c}{r}\right) = R\exp\left[-\frac{2}{\pi}\int_{c_s/R}^{c/r}\left(w^{-2}-\frac{r^2}{c^2}\right)^{-1/2}\frac{dF}{dw}dw\right], \qquad (2.42)$$

where c_s is the surface value of c; hence $c(r)$ can be determined. This procedure was described in more detail by Gough (1986b). It was applied to observed frequencies by Christensen-Dalsgaard et al. (1985) who were able to determine the sound speed in much of the Sun with a precision of considerably better than 1 per cent. It is interesting that an essentially identical inversion technique for inversion of data on free oscillations of the Earth was proposed by Brodsky and Levshin (1979). There are other similar inversion techniques, based on the asymptotic expression (2.31) or extensions of it, which have been developed by several authors (Brodsky and Vorontsov 1987, 1988a; Kosovichev 1988; Shibahashi 1988; Shibahashi and Sekii 1988; Vorontsov 1988a, 1989; Sekii and Shibahashi 1989; Vorontsov and Shibahashi 1990, 1992; also see Vorontsov and Zharkov 1989). They are mainly distinguished by the methods of fitting the data to the asymptotic expression, particularly the separation into parts depending on ω/L and on ω.

A very attractive feature of these inversion methods is that they are *absolute*: the sound speed $c(r)$ is obtained directly from the data, without any use of a solar model. However, they suffer from systematic errors arising from inaccuracies in the asymptotic Eq. (2.42). It was shown by Christensen-Dalsgaard et al. (1989) that these errors to a large extent cancel if one considers instead differences between frequencies of pairs of models. This suggests that a *differential asymptotic inversion* of the solar data may be more accurate; here the solar frequencies are compared with those of a suitable reference model, and the inversion is aimed at estimating the differences between the solar sound speed and the sound speed of the reference. This procedure can be based on Eq. (2.39). As discussed in more detail in Sect. 4.1.1 the function $H_1(w)$ can be estimated by fitting this expression to differences between observed solar frequencies and those of the reference model; then the sound-speed difference between the Sun and the model can be determined from

$$\frac{\delta c}{c} = -\frac{2a}{\pi}\frac{d}{d\ln r}\int_{a_s}^{a}(a^2-w^2)^{-1/2}H_1(w)dw\,, \qquad (2.43)$$

where $a = c/r$ and $a_s = a(R)$. Christensen-Dalsgaard et al. showed that this method could recover even quite considerable sound-speed differences between pairs of models with an accuracy better than 0.5 per cent in most of the model.

2.3.3 Numerical inversions

The asymptotic inversion is based on an approximate relation for the frequencies, and so it suffers from inherent errors. Furthermore, its use is obviously restricted to analysis of p-mode data; it is not possible, for instance, to include data on the high-degree f modes which are observed. To make full use of the data requires inversion techniques based on numerically computed frequencies. As discussed in Sect. 2.3.1 the adiabatic oscillation frequencies are determined as

$$\omega_{nl} = \mathcal{F}_{nl}^{(\mathrm{ad})}[\rho(r), \Gamma_1(r)]\,, \qquad (2.44)$$

where the $\mathcal{F}_{nl}^{(\mathrm{ad})}$ are complicated nonlinear functionals of the equilibrium variables. Assuming for the moment the validity of the adiabatic approximation, we therefore

seek to "solve" the equations

$$\omega_{nl}^{(\mathrm{obs})} = \mathcal{F}_{nl}^{(\mathrm{ad})}[\rho(r), \Gamma_1(r)] \tag{2.45}$$

for a given set of observed frequencies $\omega_{nl}^{(\mathrm{obs})}$, to obtain $\rho(r)$ and $\Gamma_1(r)$. The solution requires iterative techniques, where the equations are linearized around an initial reference model. Let $(\rho_0(r), \Gamma_{1,0}(r))$ correspond to the reference model, which has oscillation frequencies $\omega_{nl}^{(0)}$. We seek to determine the corrections $\delta\rho(r) = \rho(r) - \rho_0(r)$ and $\delta\Gamma_1(r) = \Gamma_1(r) - \Gamma_{1,0}(r)$ to match the differences $\omega_{nl}^{(\mathrm{obs})} - \omega_{nl}^{(0)}$ between the observed frequencies and those of the reference model. By linearizing Eq. (2.45), assuming $\delta\rho$ and $\delta\Gamma_1$ to be small, one obtains

$$\omega_{nl}^{(\mathrm{obs})} - \omega_{nl}^{(0)} = \int_0^R K_{nl}^{(\rho)}(r)\delta\rho(r)dr + \int_0^R K_{nl}^{(\Gamma_1)}(r)\delta\Gamma_1(r)dr \ , \tag{2.46}$$

where the kernels $K_{nl}^{(\rho)}$ and $K_{nl}^{(\Gamma_1)}$ are determined from the eigenfunctions in the reference model. To these equations must be added the constraint that the mass of the Sun and the reference model be the same, i.e.,

$$\delta M = 4\pi \int_0^R \delta\rho(r) r^2 dr = 0 \ . \tag{2.47}$$

In this way the original problem in Eq. (2.45) has been replaced by the linear inversion problem in Eqs. (2.46) and (2.47). Having determined $\delta\rho$ and $\delta\Gamma_1$ we may then obtain the corrected model. In principle the procedure should then be iterated, by repeating it using the corrected model as reference; so far, however, there is little experience with the convergence properties of this iteration (but see Cooper 1981). On the other hand, it seems that in practice the linearization in Eq. (2.46) is quite accurate, so that even the initial correction may be adequate (Gough and Kosovichev 1988, 1990).

In reality, the inversion should take into account the departures from the adiabatic approximation, and other effects near the solar surface. In the absence of a reliable theory for the properties of the oscillations in this region, these effects can be incorporated by including in Eq. (2.45) a suitably parameterized unknown term which is determined, or eliminated, as part of the inversion procedure (see Dziembowski et al. 1990; Däppen et al. 1991; Kosovichev et al. 1992). Note that this is analogous to eliminating the surface uncertainty through the effects of $\alpha(\omega)$ or $H_2(\omega)$ in the asymptotic inversion methods.

The pair (ρ, Γ_1) considered above is only one amongst several pairs involving ρ, p, Γ_1 or, for example, the sound speed c or the buoyancy frequency N. Indeed, given the importance of the sound speed in determining the p-mode frequencies, the most sensible pair for analyzing the five-minute oscillations may be (c, Γ_1). In this case the envelope of the kernel for $\delta c/c$ is approximately given by the asymptotic kernel implicit in Eq. (2.37). The calculation of such kernels is discussed by Gough and Kosovichev (1990) and Gough and Thompson (1991).

If further assumptions about the model are imposed, one may derive kernels relating the frequency differences to differences in other aspects of the model, such as the variables describing the composition. To do so, the kernels for the primary quantities, for example ρ and Γ_1, are combined with relations derived by linearizing

the Eqs. (2.1) – (2.4) of stellar structure. This procedure was discussed in more detail by Gough and Kosovichev (1988, 1990) who also presented examples of such kernels.

A number of techniques exist for solving the linear inversion problem specified by Eq. (2.46). One technique is based on forming linear combinations of the observed data $\omega_{nl}^{(\mathrm{obs})} - \omega_{nl}^{(0)}$ such that the corresponding combinations of the kernels provide a localized average of the unknown functions $\delta\rho$ and $\delta\Gamma_1$. Other techniques involve least squares fits of parameterized version of the unknown functions to the data, with additional constraints included to ensure that the solution is sufficiently smooth. Descriptions of these methods, with further references, can be found in the papers quoted in the introduction to this section. We note also that Christensen-Dalsgaard et al. (1990) made a careful analysis of some of these methods, and of the differential asymptotic technique discussed in Sect. 2.3.2, as applied to the mathematically similar problem of inversion for the solar internal rotation.

3. The equation of state

The equations of stellar structure (2.1) – (2.4) are formulated in a general way, with no specific assumptions about the properties of matter. The density, which for example appears in the equation of hydrostatic equilibrium, is not an independent field but is a function of pressure, temperature and the chemical composition by virtue of the equation of state. The equation of state is therefore crucial for the internal structure of the star. Similarly, another property of matter, opacity, enters the equation of heat transport. It governs the flow of radiation (and thus the temperature gradient) in the radiative interior, but it has virtually no influence in the convection zone with the exception of a small strongly superadiabatic layer just beneath the photosphere.

From a theoretical point of view, it is much easier to compute the equation of state than the opacity. The equation of state can be dealt with within the framework of equilibrium statistical mechanics. An equilibrium system can be characterized by mean values of conserved quantities, such as energy and particle number (for extensive reviews of the more recent literature see, for example, Ebeling et al. 1976; Kraeft et al. 1986; Eliezer et al. 1986; Däppen et al. 1987; Hummer and Mihalas 1988; Däppen et al. 1991; Ebeling et al. 1991).

Opacity, however, is a transport quantity. Computing transport quantities requires considering non-equilibrium states and additional observables, which are, in the context of hydrodynamics, particle-, momentum-, and energy *currents* determined by the respective equations of continuity. Linear response theory often provides the framework for these computations (for an introduction see Kraeft et al. 1986).

As a consequence, the computation of the equation of state is the simpler problem. Besides the general fact that equilibrium quantities are easier to compute than transport quantities, there are two *specific* reasons for this. Firstly, already at lower densities where "atoms" exist (i.e., where many-body effects can be neglected), to determine the equation of state it suffices to know the *energy levels* of atoms (and their occupation); for the opacity, however, transition matrix elements between all sorts of atomic *states* have to be known aś well. Secondly, at higher densities, where many-body effects become important (and where one cannot speak of "atoms"), there are at least roads to a correct treatment of the equation of state (we shall show some of them in this chapter). Extending these techniques to opacity calculations faces the difficulty that

again more detailed information about the quantum-mechanical many-body states is required.

3.1 Statistical mechanical foundation of the equation of state

Two different kinds of information are required in the description of the thermodynamic state of an astrophysical plasma. Firstly, one needs thermodynamical relations. One of these is the equation of state $\rho(p, T)$ itself, which is essential for the solution of the hydrostatic equilibrium Eq. (2.1). In addition, other thermodynamic quantities are needed: principally the adiabatic pressure-density gradient Γ_1, which determines the structure of most of the convection zone, and is crucial for sound speed and thus oscillation frequencies. Secondly, the thermodynamic state has to be known in opacity calculations to provide the occupation of individual levels of atoms and ions and the fractions of ions of any given chemical element. Strictly speaking, there is no fundamental reason for introducing atoms and ions and their level populations in an opacity calculation. As we shall mention below (Sect. 3.4), one can model the thermodynamics without starting out from the concept of atoms, ions, or levels (which at any rate are merely approximations to the complex situation of particles in a plasma). However, even then somewhat heuristic concepts of atoms and ions have to be introduced in the opacity calculation (see Rogers 1986; Däppen et al. 1991). Nevertheless, often the approximate ideas of (modified) atoms and ions are already introduced in the thermodynamic part, which gives then the necessary information about level populations directly, to be used in opacity calculations. Needless to say, in a consistent stellar model the thermodynamic quantities and the opacity should be based on the same equation of state. Although this is an obvious requirement, we would like to mention that it is not satisfied in many models.

The typical task of quantum statistical mechanics consists in the calculation of the (total) partition function (see Huang 1963, Reichl 1980)

$$Z(T, V, \boldsymbol{N}) = \mathrm{Tr}(\mathrm{e}^{-H/k_B T}) \; . \tag{3.1}$$

Here, H is the Hamiltonian operator of the quantum system with N_i particles of species i, $i = 1, \ldots, m$ [i.e., $\boldsymbol{N} = (N_1, N_2, \ldots, N_m)$] confined to a box of volume V, and k_B is the Boltzmann constant. (We note that this is the canonical point of view; the alternative, equivalent grand-canonical approach is another possibility, which is discussed in Sect. 3.4). The partition function directly leads to the thermodynamical potential of the free energy

$$F(T, V, \boldsymbol{N}) = -k_B T \ln Z(T, V, \boldsymbol{N}) \; , \tag{3.2}$$

from which all thermodynamic quantities can be derived. It is evident that various approximations are necessary before Eq. (3.1) can be evaluated. One such approximation consists in treating the motion of the heavy particles (nuclei, atoms, ions) according to classical mechanics, which is certainly appropriate as long as one does not approach the conditions of the interior of neutron stars. Thus, only electrons have to be described by quantum mechanics.

Such a separation of effects leads to a factorization in Eq. (3.1), which is translated into a sum in Eq. (3.2). The free energy thus becomes modular, which is a very useful property of models that are based on the canonical partition function. The classical contribution in Eq. (3.1) is obtained from an integration over the Hamiltonian

coordinates p_i and q_i ($i = 1, \ldots, 3N$). Neglecting velocity-dependent interactions between the particles, the classical integrations over p_i and q_i factorize, resulting in the Maxwell-Boltzmann distribution for the heavy particles multiplied by the so-called configuration integral

$$Q(T, V, \boldsymbol{N}) = \int dp_1 \cdots dp_{3N}\, dq_1 \cdots dq_{3N}\, \mathrm{e}^{-\mathcal{V}/k_B T} , \tag{3.3}$$

where $\mathcal{V} = \mathcal{V}(q_1, \ldots, q_{3N})$ is the interaction potential of the heavy particles. Equation (3.3) is at the base of the (negative) Coulomb-pressure correction for the charged particles and of excluded-volume effects of neutral particles (such as hard-sphere and Van-der-Waals type corrections).

An approximate evaluation of the Coulomb pressure correction is made in the Debye-Hückel theory, where it is assumed that each charge is surrounded by a cloud of opposite charge, screening the Coulomb interaction outside a sphere with radius

$$\lambda_D = \left(\frac{4\pi e^2 < Z^2 >}{k_B T} \right)^{-1/2} , \tag{3.4}$$

called the Debye radius. Here

$$< Z^2 > = \sum_j Z_j^2 n_j , \tag{3.5}$$

where the sum runs over all charged particles with particle densities $n_j = N_j/V$ and charge Z_j. A convenient dimensionless parameter of the Debye-Hückel theory is the ratio ζ of the Coulomb potential energy of unit charges at the distance λ_D to the average kinetic energy $k_B T$, thus $\zeta = (e^2/\lambda_D)/k_B T = l_L/\lambda_D$ (where $l_L = e^2/k_B T$ is the Landau length). The values of these parameters in the solar convection zone were studied in detail by Baturin (1991) and Vorontsov et al. (1992). With these definitions, the free energy of the classical Coulomb interaction in the Debye-Hückel approximation can be written as (see Ebeling et al. 1976)

$$F_{DH} = -\frac{\zeta}{3} < Z^2 > k_B T . \tag{3.6}$$

The specific form of the Debye-Hückel Coulomb free energy used in many astrophysical equations of state is that adopted by Graboske et al. (1969). There, two additional effects are taken into account. First, in the sum of Eq. (3.5), the weight of partially degenerate electrons is reduced (by a factor involving Fermi integrals), and second, a multiplicative correction factor τ is used as a rough approximation for the non-vanishing size of the charged particles (see also Ebeling et al. 1991). The Debye-Hückel approximation is basically valid as long as there are still relatively many particles in the so-called Debye sphere (with the Debye length as its radius).

Once the heavy particles are separated out, electrons remain, and they are, of course, treated according to quantum mechanics. The quantum mechanical electrons interact in two totally different ways. First, being Fermions, electrons obey Pauli's exclusion principle, which results in *de facto* interaction effects (see Sect. 3.4), even if their underlying dynamics (i.e., in their Hamiltonian) were assumed to be non-interacting. Second, the Coulomb repulsion of the electrons couples them in the dynamical equations, making it, formally speaking, impossible to work with the

extremely useful one-electron states. In moderate-density astrophysical applications (such as the Sun), the dynamical interaction has not been taken into account, but it remains to be seen if the high demands of helioseismology will not force us to do so. The dynamically interacting electron gas was treated by Gell-Mann and Brueckner (1957), Gell-Mann (1957) and Sawada (1957); practical approximative formulae can be found in Tanaka et al. (1985), and a general review was given by Ichimaru (1982).

In the treatment of electrons, we find a bifurcation into two distinct classes of approach, the "chemical picture" and the "physical picture" (Krasnikov 1977). While in the more conventional chemical picture bound configurations (atoms, ions and molecules) are introduced and treated as new and independent species, only *fundamental* particles (electrons and nuclei) appear in the physical picture. In the chemical picture, reactions between the various species occur, and thus the thermodynamical equilibrium must be sought among the stoichiometrically allowed set of concentration variables by means of a maximum entropy (or minimum free-energy) principle. In contrast, the physical picture has the aesthetic advantage that there is no need for a minimax principle; the question of bound states is dealt with implicitly through the Hamiltonian describing the interaction between the fundamental particles. The different physical assumptions of the two pictures have been the source of considerable difficulties in recent comparisons and interpretations (see Rouse 1983; Ebeling et al. 1985; Däppen et al. 1987).

There is an intuitive simplicity in the chemical picture: we usually take the existence of atoms in plasmas for granted, at least at densities that are not too high. However, this simplicity has to be paid for by additional minimization procedures in the multidimensional space of abundances of each species, restricted by the appropriate stoichiometrical relations and by mass and charge conservation. The physical idea behind this minimization is simple: the "internal" degrees of freedom, such as ionization degrees, are not adjustable by the experimenter; he can control only "external" parameters, like temperature, density, and mass fractions of each chemical element. The thermodynamic equilibrium is then determined as the one configuration, compared with those having different internal parameters, that minimizes the free energy, or equivalently, maximizes entropy. Once this minimum is found, the model free energy delivers all thermodynamic quantities in a straightforward way by differentiation.

It should be clear that the advantage of the chemical picture lies in the possibility to model complicated plasmas, and to obtain numerically smooth and consistent thermodynamical quantities (see Sect. 3.2). Nevertheless, the heuristic method of the separation of the atomic-physics problem from that of statistical mechanics is not satisfactory, and attempts have been made to avoid the concept of a perturbed atom in a plasma altogether. Thus in the physical picture only fundamental particles (electrons and nuclei) enter. This has the advantage that the constraints appearing in the chemical picture (i.e., mass and charge conservation) are automatically satisfied. In the absence of constraints, it becomes possible to use the powerful apparatus of the grand-canonical partition function. In the chemical picture, however, this road is barred, because the aforementioned constraints are expressed in numbers of particles and not in terms of the chemical potentials, the independent variables of the grand-canonical partition function. In the physical picture, one can try to build a theory of partially ionized plasmas similar to well-known cluster expansions for real gases (Rogers 1981; for an introduction into cluster expansions see Huang 1963). We come back to the physical picture in more detail in 3.4.

3.2 Requirements on an equation of state

For many astrophysical applications crude recipes for the equation of state are quite adequate (e.g. Saha's equation with ground-state partition functions, together with an imposed total ionization above certain temperatures and densities). Such formalisms, however, do not satisfy thermodynamic consistency, which is expressed by the condition that the equation of state and the thermodynamical quantities must be derived from a single thermodynamical potential. It is evident, for example, that imposing total ionization as described above violates thermodynamic consistency. Such inconsistencies can cause problems in finer applications, such as helioseismology. These *formal* problems are independent of those due to inadequacies in the quality of the description of reality. The reason is that in the usual formulation of the stellar pulsation equations thermodynamic identities are used several times during the manipulations of the hydrodynamical equations. Consider, as an example, how the adiabatic temperature gradient enters the derivation of the adiabatic pulsation equations after the substitution of pressure perturbations by density perturbations (which are further transformed using mass conservation). The adiabatic gradient thus inserted must be consistent with the equation of state used in the equation of hydrostatic support. Therefore, the equation of state and the thermodynamical quantities have to be at least formally consistent.

From these considerations it is clear that the degree of *formal* precision required of an equation of state strongly depends on the chosen purpose. Equilibrium models and adiabatic pulsations need second-order thermodynamic quantities (the terminology refers to derivatives of the free energy or any other equivalent thermodynamic potential). Nonadiabatic pulsation calculations have to go one level deeper: third-order quantities such as derivatives of the adiabatic gradient or specific heat are also required. In a complicated equation of state that comprises many nonideal effects it is a highly nontrivial matter to achieve accurate third-order quantities.

Another aspect regarding the formal precision concerns the interpolation in tables. In most concrete stellar models, which are already by themselves quite demanding on computing resources, the inclusion of a realistic equation of state as a subprogramme would exceed current capabilities. As a consequence, the equation of state (like the opacity, for that matter), is precomputed in large tables, from which it is interpolated. Such interpolations, however, introduce errors that have to be kept under control (see Sect. 4.1.3).

Formal precision is of course not enough, and perhaps the most transparent solar physics application that demonstrates the need for *absolute* accuracy of the physical description is the thermodynamic method to determine the helium abundance of the solar convection zone. In the absence of laboratory experiments, comparisons between conceptually and technically different formalisms can give a feeling for their *absolute* accuracy. Under very fortunate circumstances, which are the subject of this article, there is hope to use astrophysical information to assess the absolute quality of a physical model.

3.3 Equations of state in the chemical picture: free-energy-minimization method

Most realistic equations of state that have appeared in the last 30 years belong to the chemical picture and are based on the free-energy minimization method. This

method uses approximate statistical mechanical models (for example the nonrelativistic electron gas, Debye-Hückel theory for ionic species, hard-core atoms to simulate pressure ionization via configurational terms, quantum mechanical models of atoms in perturbed fields, etc.). From these models a macroscopic free energy is constructed as a function of temperature T, volume V, and the concentrations $N_1, \ldots, N_m$ of the m components of the plasma. The free energy is minimized subject to the stoichiometric constraint. The solution of this minimum problem then gives both the equilibrium concentrations and, if inserted in the free energy and its derivatives, the equation of state and the thermodynamic quantities.

We note again that this procedure automatically guarantees thermodynamic consistency. As an example, when the Debye-Hückel correction (3.6) is taken into account, it affects both the pressure and the equilibrium concentration, i.e., the degrees of ionization. In contrast, the mere inclusion of the pressure correction would be inconsistent.

The starting point is Eq. (3.2), and the notion of individual particles (atoms, ions, molecules, and electrons) is introduced, despite the plasma environment. Formally, with the exception of the classical part (3.3), the species are treated as non-interacting, thus allowing a factorization of the total partition function, which in turns causes the free energy to be a sum of individual particle contribution. However, although the quantum-mechanical part of Eq. (3.2) formally looks non-interacting, various types of interactions can be introduced, as long as they are expressed as modifications of the individual particles. Such modifications can be given, e.g. by an expression of the destruction by the environment of the internal states of bound systems. Another possibility is to introduce an energy-level shift for certain (or all) bound states. Since plasma spectroscopy cannot constrain absolute energies but only differences, there is not much known about these plasma-polarization shifts (see Hummer and Mihalas 1988). Nevertheless, although spectroscopically only energy-level differences matter, in general the thermodynamic quantities depend on a global shift of all energy levels (see Jackson and Klein 1969). In other words, thermodynamically it is not the same if the ground-state energy is lifted or the continuum is lowered. Notice that such modifications of atomic states, occupation probabilities, or energy levels are clearly heuristic, analogous perhaps to the introduction e.g. of an effective mass in solid-state physics, which allows treating electron-electron interactions in a formally non-interacting model.

3.3.1 The simple Saha equation

Disregarding the even simpler polytropic relations for the equation of state, the simplest prescriptions available consist in mixtures of ideal gases with ionization (and molecular dissociation) reactions. Since interaction terms are absent, the free-energy-minimization method becomes very simple and one obtains the equation of state

$$p = \frac{k_B \rho T}{\mu m_u} , \tag{3.7}$$

with μ and m_u being the mean molecular mass and the atomic mass unit, respectively. The ionization equilibrium (and thus μ) is found by the minimum of the free energy; the resulting equation for this minimum is, in the language of astrophysicists, the Saha equation. We note that in this simple case there is no need to use the free-

energy-minimization method, but conceptually it is nice to view it as the trivial part of the more realistic models discussed below. For a simple hydrogen plasma (without molecules) the Saha equation is

$$\frac{N_{\rm H}}{N_{\rm H^+}N_{\rm e^-}} = \frac{\lambda^3}{V}\exp(-E_1/k_BT)Z^{\rm internal}\,, \tag{3.8a}$$

with

$$Z^{\rm internal} = \sum_i g_i \exp\left(-\frac{E_i - E_1}{k_BT}\right)\,. \tag{3.8b}$$

Here, $N_{\rm H}$, $N_{\rm H^+}$, and $N_{\rm e^-}$ are the numbers of hydrogen atoms, protons, and electrons in the volume V, respectively, and $\lambda \equiv h/\sqrt{2\pi m_e k_B T}$ is the thermal wavelength of electrons; also, E_i is the (negative) energy of the assumed internal states of hydrogen atoms and g_i is statistical weight of the states (which are labeled by the index i, with $i = 0$ denoting the ground state). The g_i do not contain the factor 2 due to the spin of the electrons, because it cancels in the ratio $N_{\rm H}\,/\,N_{\rm e^-}$. The divergence of the sum in Eq. (3.8b) has always plagued the statistical mechanics of partially ionized plasmas, but the simplest equations of state avoid the problem by including only the ground state. The Saha equation thus becomes

$$\frac{N_{\rm H}}{N_{\rm H^+}N_{\rm e^-}} = \frac{\lambda^3}{V}\exp(I/k_BT)\,, \tag{3.9}$$

where $I = -E_0$ is the (positive) ionization potential of hydrogen. More realistic internal partition functions with elaborate cut-off procedures have been developed e.g. for opacity calculations (Cox 1965; Huebner 1986). They allow calculations of ionization fractions and occupation numbers, at least at not too high densities. Nevertheless, the Saha equation suffers from its inability to describe pressure ionization. From physical arguments it is clear that atoms must be ionized at very high densities, but, unless the temperature gradient is sufficiently steep to keep the factor λ^3/V in Eq. (3.9) small, the Saha equation predicts just the contrary, i.e., an unphysical recombination of atoms. In the solar centre, where temperature is not high enough because of the subadiabatic temperature gradient beneath the convection zone, it predicts as much as 30 per cent of neutral hydrogen. [To understand this, note that the thermal wavelength λ is of the order of a Bohr radius for the temperature $T = I/k_B$ (about 1.6×10^5 K). Also note that the Boltzmann factor $\exp(I/k_BT)$ is essentially unity at high temperatures (i.e., $k_BT \gg I$).]

This Saha recombination is clearly at variance with elementary volume considerations, from which one concludes that at the densities of $150\,{\rm g\,cm^{-3}}$ of the solar centre there is no room for neutral hydrogen atoms, which have (in tightly packed configurations) densities of the order of $1\,{\rm g\,cm^{-3}}$. Since the simple equations of state considered here know nothing about the radius of the hydrogen atom, their predicted recombination is, in this approximation, a legitimate quantum-mechanical effect. In the absence of an effective interaction term between "extended" particles (i.e., all particles except electrons and nuclei), the recombination is caused by two quantum effects of the free electrons which work in the same direction. The first effect is only a consequence of the quantum nature of the electron gas (i.e., it does not depend on the statistics of the free electrons; note however that the nature of the *bound* states very much depends on the statistics of the electrons). The reason for this quantum recombination is that if the sum of cubes of the thermal wavelengths $N\lambda^3$ exceeds the

available total volume V, the electrons effectively become quantum correlated, which drastically reduces their entropy. The entropy maximum principle, on which Eq. (3.8) is based, responds by reducing the number of free electrons. A second quantum effect, this time based on the Fermi-Dirac statistics of the electrons, reinforces the recombination. The reason is that at higher densities the continuum states of the electrons become less accessible. This is due to a smaller density of electronic states per energy interval at higher densities (one should think of the problem of electrons in a box, and note how the discrete energy spectrum gets wider-spaced the smaller the box is). The rest is done by the Pauli principle: at high densities it causes a piling up to such high continuum energies that the system finally responds with favouring atomic recombination as the lesser evil.

Of course, both these recombinations do not occur in nature because there are "hard-core" interactions between extended particles that prevent them by forcing the so-called "pressure ionization". Pressure ionization can only be modelled by non-ideal equations of state that treat interactions between extended species and the surroundings (see Sect. 3.3.3).

3.3.2 The EFF and CEFF equations of state

Eggleton et al. (1973) developed a simple equation of state (EFF) that is formally consistent and includes an *ad hoc* pressure ionization device that works at least qualitatively correctly. The device is not based on a physical model (e.g. a description of an atom and its surrounding particles), but is imposed by forcing the anticipated result, i.e., full ionization at high densities. In addition, the EFF equation of state incorporates a correct treatment of the partially degenerate electrons according to Fermi-Dirac statistics. Bound systems (atoms and ions) are always assumed to be in their ground state; the ground-state energy is constant and equal to the free-particle value.

Despite the lack of a physical foundation of its pressure ionization device, the EFF equation of state is nonetheless useful because of its thermodynamic consistency. Compared to simple prescriptions, like those imposing full ionization above an empirically determined temperature (such procedures can still be found in some of the current programmes of stellar evolution), the EFF equation of state is better suited for stellar pulsation applications, and has, for example, been successfully employed in many solar models (e.g. Christensen-Dalsgaard 1982). In addition, the relative simplicity of the EFF formalism allows accurate numerical computation of higher-order thermodynamical derivatives in a way that can be put directly into the programmes of stellar evolution, without interpolation of pre-tabulated results. Furthermore, the manifestation of pressure ionization in stellar structure can be discussed with the help of the parameters that fix the actual location of the EFF pressure ionization zone. By varying these parameters one might get some indication about the sensitivity of stellar and solar models on the precise nature of pressure ionization, as suggested by Bahcall and Ulrich (1988).

On the negative side of the EFF equation of state, we mention its principal limitations, given by the absence of: 1) a physical mechanism for pressure ionization, 2) excited states in the bound systems, 3) a treatment of hydrogen molecules (important for low-mass stars; see e.g. Lebreton and Däppen 1988), and 4) the Coulomb-pressure correction. Another potential problem is the fact that at low temperatures and high

densities pseudo phase-transitions appear in the EFF equation of state, resulting in multivalued state functions (see Christensen-Dalsgaard 1978). This behaviour does not occur under solar conditions; however, it has been noted by VandenBerg (*private communication*) that it causes problems in computations of low-mass stars, where the density is substantially higher than in the Sun at given temperature. It should in principle be repaired with Maxwell constructions, analogous to that applied to the Van-der-Waals equation of state. We note that a similar behaviour, at roughly comparable conditions, has been noted by Ebeling (1990) for a more realistic treatment of pressure ionization. The more sophisticated equations of state discussed in the following have not yet been examined with respect to possible phase transitions (artificial or physical). However, if for a given model it cannot be rigorously proved that there are no multi-valued state functions, it is certainly wise to be on the alert for this possibility.

To overcome the lack of a Coulomb term in the EFF equation of state, the present authors have added a Coulomb configurational term in the Debye-Hückel approximation (3.6) (taken from the MHD equation of state, which is presented in Sect. 3.3.4). Such an upgrade of the EFF equation of state was motivated by the fact that adding a Coulomb term to the EFF equation of state makes a significant contribution towards a more realistic equation of state (see Sect. 3.5). Of course the remaining disadvantages of the EFF equation of state still point to the need of more complete formalisms (see below). However, the successful application of the CEFF equation of state to solar physics (Christensen-Dalsgaard 1991b; see also Sect. 4.3) makes it very well suited as a reference equation of state.

3.3.3 The confined-atom and static-screened Coulomb potential (SSCP)

In the confined-atom model, the Coulomb potential outside a sphere of radius R_i is replaced by an infinitely high potential wall (this is equivalent to a zero boundary condition of the wave function at R_i). The value of R_i is chosen as a function of the volume available for a given bound species. For $R_i < \infty$, all bound-state energies are lifted from their unperturbed values and the number of bound states becomes finite. With decreasing R_i, the higher states are gradually spilled over into the continuum. The confined-atom model thus provides an automatic cut-off for the otherwise divergent internal partition functions [e.g. in Eq. (3.8)]. However, the spilling-over causes jumps in the internal partition functions when the "external" parameters continuously vary; these jumps would lead to singularities in the thermodynamic derivatives. Appropriate smoothing of the internal partition function is therefore necessary. Such a smoothing can be done, for instance, with weighted sums (see Sect. 3.3.4).

While physically the confined-atom model is certainly not very realistic, it has some formal advantages. For instance, it can describe pressure ionization at cold temperature without the presence of initial or "seed" electrons. Such "starters" are often required in other approaches, such as the static-screened Coulomb potential (SSCP). The static-screened Coulomb potential is a Yukawa potential in which the Debye length λ_D [cf. Eq. (3.4)] serves as the screening radius. The problem with the SSCP is that the infinite-range Coulomb potential is only screened by ionized surroundings. However, at sufficiently cold temperatures, there are no such ionized surroundings, and they therefore have to be provided artificially, for instance by adding alkali-type "donor" metals. Without such starters, the free energy is always equal to

minus infinity for a completely unionized system. This provides a spurious solution, which makes the search for other (local) minima difficult, especially if they lie close to the spurious one. In contrast to this, the confined-atom model needs no charged background for pressure ionization (see Däppen 1980).

As mentioned in Sect. 3.3, formalisms based on the confined-atom or the SSCP models suffer from the ambiguity in choosing either a fixed ground-state energy for all parameters (λ_D or R_j), which effectively means a lowering of the continuum, or leaving the continuum fixed, which causes an increase of the ground-state energy (and thus the internal energy) of each species. Jackson and Klein (1969) discussed this ambiguity in the case of the SSCP and concluded, from consistency arguments correct to first order in the inverse Debye length, that it makes more sense to lower the continuum than lifting the ground-state energy. However, even then problems remain. First, the relative energy-level shifts predicted by the SSCP are by about one order of magnitude too large when compared with spectroscopic observations (Wiese et al. 1972; see also Hummer and Mihalas 1988). Secondly, a lowering of the continuum cannot be defined in the case of more than one species, because physically there can be only one continuum.

If the confined-atom model is realized with an added Coulomb configurational term and partially degenerate electrons (Fontaine et al. 1977; Däppen 1980), an equation of state results that is equipped with a very powerful pressure ionization mechanism, especially at cool and moderate temperatures. However, since atoms are only destroyed by extended particles, and not by charged particles, the ionization fraction predicted by the confined atom model is clearly too low in hot, strongly ionized plasmas.

On the other hand, as we have mentioned above (Sect. 3.3.1), the Saha recombination in hot dense regions is a legitimate quantum mechanical effect, subject to availability of excluded volume. A convincing model that predicts the precise amount of ionization above that minimum requirement has still to be found. The full ionization that results from the MHD equation of state is, in this sense, merely the other extreme, and it remains to be shown where, between these extreme cases, reality lies. Of course, in the solar centre, there is no room for neutral hydrogen, but a significant fraction of He^+ ions could easily survive, first because they occupy a factor of 8 less volume (estimated with the Bohr radius), and second because the number abundance of helium is still less than half that of hydrogen, despite the creation of helium by nuclear fusion. Detailed calculations with the confined-atom model predict a ratio of He^+ over He^{++} of about 0.30. Of course this is merely an upper bound. Other mechanisms are also at work to destroy the He^+ ions, and it is possible that helium is virtually fully ionized in the solar centre. For instance, the MHD equation of state (Sect. 3.3.4) predicts full ionization. Since there is so far no rigorous result (or convincing argument) that would *prove* such a complete ionization, it is certainly useful to have, in the form of the confined-atom model, an equation of state that predicts the maximum recombination allowed by extended volume considerations, especially, because there are indications that deep-core helioseismology could address this issue of 'residual' He^+ ions (see Sect. 4.4).

3.3.4 The MHD equation of state

In the chemical picture, perturbed atoms must be introduced on a more-or-less *ad-hoc* basis to avoid the familiar divergence of internal partition functions (see, for example,

Ebeling et al. 1976). In other words, the approximation of unperturbed atoms precludes the application of standard statistical mechanics, i.e., the attribution of a Boltzmann factor to each atomic state. The conventional remedy of the chemical picture against this is a modification of the atomic states, e.g. by cutting off the highly excited states depending on the density and temperature of the plasma. Such cut-offs, however, have in general dire consequences due to the discrete nature of the atomic spectrum, leading to jumps in the number of excited states and thus in the partition functions and in the free energy when the external parameters (temperature and density) are varied smoothly.

Mihalas et al. (Hummer and Mihalas 1988; Mihalas et al. 1988; Däppen et al. 1988) have developed a new treatment of the equation of state (hereafter MHD), which is part of the "Opacity Project" (see Seaton 1987). The MHD equation of state avoids the discontinuities in the free energy by introducing "soft" cut-offs in the form of occupational probabilities. These occupation probabilities have the same function as the "hard" cut-offs mentioned above. The occupational probabilities of a state simulate a result from quantum mechanics, denoting the fraction of atoms where the state can exist. Only then, these "available" states are populated according to statistical mechanics. It is clear that such an approach is largely intuitive. However, its advantage is that complicated plasmas can be modelled, with *detailed* internal partition functions for a large number of atomic, ionic, and molecular species. Also, full *thermodynamic* consistency is assured by analytical expressions of the free energy and its first- and second-order derivatives. This not only allows an efficient Newton-Raphson minimization, but, in addition, the ensuing thermodynamic quantities are of analytical precision and can therefore be differentiated once more, this time numerically. Reliable third-order thermodynamic quantities are thus calculated.

In the MHD occupation probabilities, perturbations by charged and neutral particles are taken into account. Correlations between the two effects are neglected (for lack of knowing how to describe them); thus the occupation probabilities due to charged and neutral perturbers are simply multiplied. Specifically, the perturbations are described by an occupation probability w_i for each energy level in the sum over internal states in Eq. (3.8b), which is generalized to the multicomponent plasma and renormalized so that the energies of the excited states are measured with respect to the ground state. No energy-level shifts whatsoever are assumed. This decision was due to the fundamental uncertainty in deciding otherwise, and is based on some theoretical and observational circumstantial evidence (see Sect. 3.3.3 and Hummer and Mihalas 1988). Furthermore, in the alternative physical picture (see Sect. 3.4), it turns out that there are no energy-level shifts.

The resulting *weighted* internal partition functions [see Eq. (3.8b)] Z_s^{internal} of species s are (with is labelling the state i of species s)

$$Z_s^{\text{internal}} = \sum_i w_{is} g_{is} \exp\left(-\frac{E_{is} - E_{1s}}{k_B T}\right) . \tag{3.10}$$

The coefficients w_{is} take into account charged and neutral surrounding particles. In physical terms, w_{is} gives the fraction of all particles of species s that can exist in state i with an electron bound to the atom or ion, and $1 - w_{is}$ gives the fraction of those that are so heavily perturbed by nearby neighbours that the state is effectively destroyed. Perturbations by neutral particles are based on an excluded-volume treatment and perturbations by charges are calculated from a fit to a quantum-mechanical Stark-ionization theory. Hummer and Mihalas's (1988) choice has been

$$\ln w_{is} = -\left(\frac{4\pi}{3V}\right)\left\{\sum_{\nu} N_{\nu}(r_{is}+r_{1\nu})^3 + 16\left[\frac{(Z_s+1)e^2}{\chi_{is}k_{is}^{1/2}}\right]^3 \sum_{\alpha\neq e} N_{\alpha}Z_{\alpha}^{3/2}\right\}. \quad (3.11)$$

Here, the index ν runs over neutral particles, the index α runs over charged ions (except electrons), r_{is} is the radius assigned to a particle in state i of species s, χ_{is} is the (positive) binding energy of such a particle, k_{is} is a quantum-mechanical correction, and Z_s is the net charge of a particle of species s. Note that $\ln w_{is} \propto -n^6$ for large principal quantum numbers n (of state i), and hence provides a density-dependent cut-off for Z_s^{internal}. A first comparison of these occupation probabilities with experiment has been made: Däppen et al. (1987) have used them to simulate the radiation from a precision plasma experiment (Wiese et al. 1972). Though the agreement is good, it serves only as a necessary condition (see Däppen et al. 1987), and other equations of state (realized both in the chemical and physical picture) have succeeded in equally good agreements (Seaton 1990; Iglesias and Rogers 1992).

Apart from formal thermodynamic consistency, the MHD equation of state also achieves some degree of statistical mechanical consistency (Hummer and Mihalas 1988). Statistical mechanical consistency refers to the more subtle requirement that each time a bound configuration (like an atom) is modified by its surroundings in the plasma, then the relevant force has to be described in the physical description of the surroundings as well. To be more specific, consider as an example the EFF equation of state: this is thermodynamically consistent, but not statistical mechanically consistent, because atoms are pressure ionized by an ad-hoc mechanism which does not have its counterpart in the free particles.

The MHD equation of state is a computational heavy-weight. Unless drastically simplified to a small number of atomic and ionic species, it has to be used in the form of tables. A tape with first results is already available (Mihalas et al. 1988). Furthermore, Lebreton and Däppen (1988) have developed programmes that can automatically create tables that are centered around the temperatures and densities of stellar interiors. These table-creating programmes can also handle the changes in chemical composition during the main-sequence evolution of stars. As we have mentioned above, the smoothness of the MHD formalism allows tabulation of third-order thermodynamic quantities. Furthermore, by tabulating the results from EFF – or, as is done in Sect. 4.1.3, CEFF – in the same way as those of MHD, and by comparing the models that use the interpolated EFF results with the models that call EFF directly (Christensen-Dalsgaard et al. 1988b; Lebreton and Däppen 1988), we can control the precision of the interpolation process and adjust the necessary fineness of the tables. Sect. 4.1.3 below presents the analogous test for the tables used in the present work.

Before leaving the MHD equation of state we add just one general remark. Though the MHD formalism was developed for stellar envelopes, there is no problem in applying it to interiors. Though one is leaving the domain for which MHD was originally conceived, the physical ingredients are, even at these high densities, quite the same as the ones conventionally used in models of stellar interiors. Only theories that treat higher-order correlations in plasmas seriously would distinctly go beyond the assumptions of MHD under these conditions. Such theories still await application in the context of stellar interiors, and in order to extend them to the low-density regime, special care will have to be given to overall consistency.

3.4 Equations of state in the physical picture

There is an impressive body of literature on the physical picture. Important sources of information with many references are the books by Ebeling et al. (1976), Kraeft et al. (1986), Ebeling et al. (1991). However, the majority of work on the physical picture was not dedicated to the problem of obtaining a high precision equation of state for stellar interiors. Such an attempt was made for the first time by a group at Livermore as part of an opacity project (Rogers 1986; Iglesias et al. 1987).

The Livermore group uses a many-body activity expansion of the grand canonical partition function (Rogers 1981). To explain the advantages of this approach for partially ionized plasmas it is instructive first to discuss the activity expansion for gaseous hydrogen. The interactions in this case are all short ranged and the pressure is determined from a self-consistent solution of the equations (Hill 1960)

$$\frac{p}{k_B T} = z + z^2 b_2 + z^3 b_3 + \dots \,, \tag{3.12}$$

$$\rho = \frac{z}{k_B T}\left(\frac{\partial p}{\partial z}\right) \,, \tag{3.13}$$

where $z = \lambda^{-3}\exp(\mu_i/k_B T)$ is the activity, λ the thermal (de Broglie) wavelength of electrons [see Eq. (3.8)], μ_i the chemical potential and T the temperature. The b_n are cluster coefficients such that b_2 includes all two particle states, b_3 includes all three particle states, etc. More specifically, the second cluster coefficient for hydrogen includes the formation of H_2 molecules as well as the scattering states of the H atoms. The states of the H–H system are of different type according to the configurations of the electrons. Molecules are always in the singlet state, with total electron spin $S = 0$, and the lowest symmetrical orbital wave function, the ${}^1\Sigma_g$ bonding orbital. In this configuration, the interaction between the H atoms is described by the attractive ${}^1\Sigma_g$ bonding potential. The scattering states of the H atoms are either singlet states, with sufficient kinetic energy of the H atoms so that they are in the continuum of the ${}^1\Sigma_g$ bonding potential. Or, they belong to the triplet states (total electron spin $S = 1$), for which even the lowest orbital (the ${}^3\Sigma_u$ antisymmetric orbital) leads to a repulsive ${}^3\Sigma_u$ antibonding potential, which, of course, has only scattering states of the H–H system. Or, they belong to excited electronic states (singlet and triplet), which are never bound, either.

As a consequence, the second cluster coefficient for hydrogen includes the formation of H_2 molecules, the scattering states in the ${}^1\Sigma_g$ potential, in the ${}^3\Sigma_u$ potential, and in the potentials of all excited electronic states. The third cluster coefficient includes H_3 bound states, $H - H_2$ and $H - H - H$ scattering states. Eq. (3.12) demonstrates that the equation of state for reacting gases can be obtained without an explicit knowledge of the occupation numbers of the internal states of the composite particles.

For low-density gases the bound-state contributions to the b_n can be important at low temperature while the scattering contributions are too small to matter. Strict application of Eq. (3.12) would contain a large amount of unimportant information which is very hard to calculate. Consequently it is necessary to reorganize Eq. (3.12) such that the bound-state terms from each b_n are treated as being of the same order as the ideal gas term, i.e., of order z. Terms of order z in the physical picture are roughly equivalent to what in the chemical picture is called the Saha equation. Similar reorganization of terms involving scattering from composite particles is also required. Assuming that H_2 molecules are the only bound complex to form, Eq. (3.12) becomes

$$\frac{p}{k_B T} = z_{\mathrm{H}} + z_{\mathrm{H}_2} + z_{\mathrm{H}}^2 b_2^s + 2 z_{\mathrm{H}} z_{\mathrm{H}_2} b_3^* + z_{\mathrm{H}_2}^2 b_4^* + \ldots \,, \tag{3.14}$$

and Eq. (3.13) is replaced by the conditions

$$\rho_{\mathrm{H}} = \frac{z_{\mathrm{H}}}{k_B T}\left(\frac{\partial p}{\partial z_{\mathrm{H}}}\right) \,, \quad \rho_{\mathrm{H}_2} = \frac{z_{\mathrm{H}_2}}{k_B T}\left(\frac{\partial p}{\partial z_{\mathrm{H}_2}}\right) \,, \tag{3.15}$$

where $z_{\mathrm{H}_2} = z_{\mathrm{H}}^2 b_2^b$ is the activity for molecules and the superscripts b and s refer to bound and scattering parts of b_2, b_3^* is the part of b_3 involving scattering of H from H_2, and b_4^* is the part of b_4 involving scattering of H_2 from H_2.

In the case of partially ionized plasmas very similar steps are required, except that now even Eq. (3.12) must involve at least two species (nuclei and electrons) to assure electrical neutrality. In addition, due to the long range of the Coulomb potential each of the b_n is composed of a number of divergent terms, some of which are fictitious and some of which are real.

An example of real divergence is afforded by the classical ring diagrams occurring in each b_n (Mayer 1950). They are individually divergent but the many-body correlations introduced by summing over the b_n yields the Debye-Hückel correction [see Eq. (3.6)]. This type of divergence occurs even for an electron gas in a neutralizing background for which there are no bound states. Although the original equations involved only even powers in the activity [see Eq. (3.14)], as a result of many-body Coulomb correlations, the Debye-Hückel term appears in the power of $z^{3/2}$ in the activity (also in density).

An important example of a fictitious divergence is that associated with the atomic partition function. This divergence is fictitious in the sense that the bound-state part of b_2 is divergent but the scattering state part, which is omitted in the Saha approach, has a compensating divergence. Consequently the total b_2 does not contain a divergence of this type (Ebeling et al. 1976; Rogers 1977). A major advantage of the physical picture is that it incorporates this compensation at the outset. A further advantage is that no assumptions about energy-level shifts have to be made (see Sect. 3.3.3); it follows from the formalism that there are none.

As a result, the Boltzmann sum appearing in the atomic (ionic) free energy is replaced with the so-called Planck-Larkin partition function (PLPF), given by (Ebeling et al. 1976; Kraeft et al. 1986)

$$\mathrm{PLPF} = \sum_{nl} (2l+1)\left[\exp\left(-\frac{E_{nl}}{k_B T}\right) - 1 + \frac{E_{nl}}{k_B T}\right] \,. \tag{3.16}$$

The PLPF is convergent without additional cut-off criteria as are required in the chemical picture. We stress, however, that despite its name the PLPF is not a partition function, but merely an auxiliary term in a virial coefficient (see, for example, Däppen et al. 1987).

The power of the activity expansion method, arising in the physical picture, lies in the fact it produces expressions for thermodynamic quantities that systematically take account of density corrections without the introduction of models or cut-off mechanisms.

An important feature of the PLPF is that it picks out the states that are highly occupied. In a perturbation sense it corresponds to that part of the occupation of the allowed states that is large enough to be treated as a new variable when the plasma reorganization equivalent to Eq. (3.14) is carried out. Some residual effects of the

discreteness of high-lying states appear in correction terms of order z^2 that are the next higher corrections beyond Debye-Hückel. This additional occupation of high-lying states is important for frequency-dependent opacities and must be added to the PLPF occupation numbers when opacities are calculated (Rogers 1986).

3.5 Comparison of results from the chemical and physical picture

So far there are no laboratory experiments that could distinguish between equations of state in the chemical and physical picture. One of the purposes of this article is to show that solar oscillations are precise enough to become an astrophysical test. However, at the moment, detailed and precise comparisons of theoretical results from both formalisms are probably the best way to learn about their strong and weak points. Also, from comparisons between totally independent formalisms, solar physicists will obtain an idea of the basic uncertainty in the equation of state.

In the following, we discuss what so far has been emerged from such comparisons. While earlier comparisons showed a striking agreement between the MHD and Livermore equation of state for conditions as found in the hydrogen-helium ionization zones of the Sun (Däppen et al. 1990; Däppen 1990), it turned out later that this agreement was nearly accidental. Of course, solar physicists were happy that two completely different formalisms delivered the same equation of state, but, by the same token, a first attempt to use the Sun as a test was also thwarted. Nevertheless, from these first comparisons the practically useful simple CEFF equation of state has resulted (see Sect. 3.3.2). Recently, these comparisons have been extended to higher densities, and also beyond the simple hydrogen-helium mixtures, by including a representative heavy element (see Däppen 1992). In the following, we briefly show and discuss the results of these comparisons. The equations of state participating in these comparisons are the EFF, CEFF and MHD equation of state all realized in the chemical picture, and the Livermore equation of state, realized in the physical picture.

3.5.1 Early low-density H-He comparisons

For convenience, a representative result from Däppen et al. (1990) is shown in Fig. 5, which compares MHD and Livermore with the simple EFF equation of state. The absolute curves in Fig. 5a are merely able to show the difference between MHD (or Livermore) and EFF results. The difference between the MHD and Livermore results is only visible in the magnified Fig. 5b, which shows the *relative* differences between MHD and EFF, and between Livermore and EFF values. This relative plot not only now allows to see the difference between MHD and Livermore results clearly, but also to realize their striking similarity.

By varying the parameters of the MHD equation of state (see Däppen 1990), the *physical reason* of this agreement was found to be that on the chosen isochore, all thermodynamical quantities are mainly dominated by the Coulomb correction. This correction overshadows the effect of the excited states (which are of course treated differently in the MHD and Livermore approach). However, note that there are two contributions due to the Coulomb term: one associated with the free energy [cf. Eq. (3.6)] of the Debye-Hückel term itself, the other with the Coulomb-term induced shift

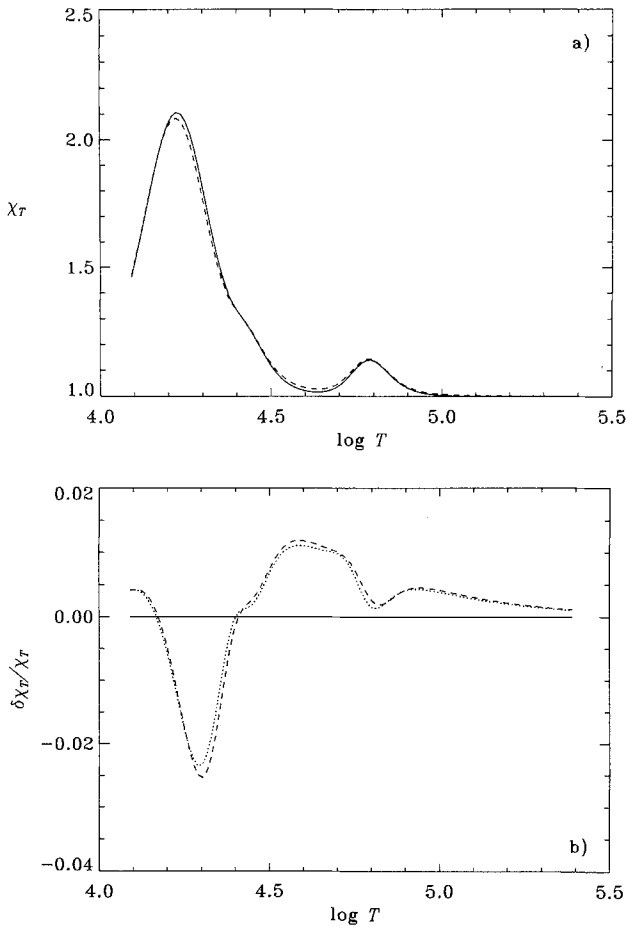

Fig. 5a,b. Comparison of the logarithmic pressure derivative $\chi_T = (\partial \ln p/\partial \ln T)_\rho$ on an isochore with $\rho = 10^{-5.5}\,\mathrm{g\,cm^{-3}}$. **a** Absolute values; the solid line represents EFF and the dashed line MHD. The chemical composition consists of hydrogen and helium only, with number abundances of 90 per cent H and 10 per cent He. The Livermore result would be indistinguishable from the MHD curve. Panel **b** magnifies the effect by showing the relative differences between Livermore and EFF values, i.e., $(\chi_T^{\mathrm{Livermore}} - \chi_T^{\mathrm{EFF}})/\chi_T^{\mathrm{EFF}}$ (dotted line) and between MHD and EFF values, i.e., $(\chi_T^{\mathrm{MHD}} - \chi_T^{\mathrm{EFF}})/\chi_T^{\mathrm{EFF}}$ (dashed line). The solid line indicates the zero level. Other thermodynamic quantities show essentially the same behaviour. (Adapted from Däppen et al. 1990)

in the ionization equilibrium which plays an important role in the deviation of the thermodynamical quantities from the unperturbed EFF result.

The resulting virtually perfect low-density agreement was by no means expected, and even when it turned out that it was essentially due to the Coulomb interaction (contained both in the MHD and Livermore equations of state), it is still somewhat mysterious. At the selected temperature and density, the number of excited states in the MHD formalism, when compared with the admittedly large Boltzmann weight of the ground state, would predict a sizeable shift in the ionization balance, at least of the same order of magnitude than that due to the Coulomb pressure. The implicit can-

cellation of the contribution of the partition functions in the thermodynamic quantities is therefore perhaps accidental, and it is currently being investigated.

3.5.2 Present comparisons

While the rather striking agreement shown above is important for solar physics, it also follows that the hydrogen-helium ionization zones of the Sun cannot be used as an observational test that could discriminate between the MHD and Livermore equations of state. In contrast, solar oscillations clearly distinguish between the MHD and EFF equation of state, as shown by Christensen-Dalsgaard et al. (1988b). The result is confirmed by the comparisons presented in Sect. 4.3 (although there, strictly speaking, the comparison is made between the EFF and CEFF equation of state). Looking for testable manifestations of the influence of internal partition functions, the comparison were extended to higher densities and, for the first time, beyond H-He mixtures.

Intermediate- and high-density H-He comparisons. Fig. 6 shows results analogous to those in Fig. 5 for an intermediate-density ($\rho = 0.1\,\mathrm{g\,cm^{-3}}$) and a higher-density ($\rho = 1.0\,\mathrm{g\,cm^{-3}}$) isochore. However, here Γ_1 is shown, and CEFF (see Sect. 3.3.2) has replaced EFF as the reference. There is good agreement for *solar conditions*, that is for temperatures such as found in the Sun at these densities. However, the Sun just marginally passes: for slightly less massive stars, the temperature is lower at the densities considered, and the discrepancy soon becomes very important indeed.

A first case involving a heavy element (oxygen). The first comparison involving a representative heavy element was made for a H, He, and O mixture. The density has been chosen as $\rho = 0.005\,\mathrm{g\,cm^{-3}}$, suggested from a study on the solar helium abundance (Kosovichev et al. 1992). Figure 7 shows the result for Γ_1. Here, the large MHD partition functions not only cause shifts in the ionization balance but also a propagation of these shifts into thermodynamic quantities. Despite their small relative number in the mixture, the heavy elements cause a distinct discrepancy, which appears to be within reach of helioseismology (Däppen 1992). To examine the MHD ionization fractions, a single case was examined ($T = 2.10\times10^5$ K, $\rho = 5.00\times10^{-3}\,\mathrm{g\,cm^{-3}}$), once with the full MHD equation of state, once with a "stripped-down" version of MHD, called MHD(S), which does not contain any excited states (but is otherwise identical). The resulting ionization fractions of O^{3+}, O^{4+}, O^{5+} were, respectively, 0.314, 0.248, 0.364 for the stripped-down MHD (without excited states), and 0.304, 0.476, 0.182 for the full MHD. (The result for the stripped-down very closely reflects the ground-state weights of the ions). Not unexpectedly in view of the Planck-Larkin partition function, the Livermore equation of state predicts ionization fractions close to those of the stripped-down MHD equation of state (Rogers, *private communication*).

This comparison for the first time establishes a clear case of disagreement between the MHD and Livermore results. Clearly, the origin of the discrepancy in the ionization degrees is due to the treatment of the excited states. Of course, only some 2 per cent of the matter in the Sun consist of elements heavier that H and He, and therefore the signature of the MHD-Livermore discrepancy on thermodynamic quantities (Fig. 7) is small (of the order of 10^{-3}). Nevertheless, as will be demonstrated in the next section, the resulting sound-speed differences are within reach of a helioseismological diagnosis.

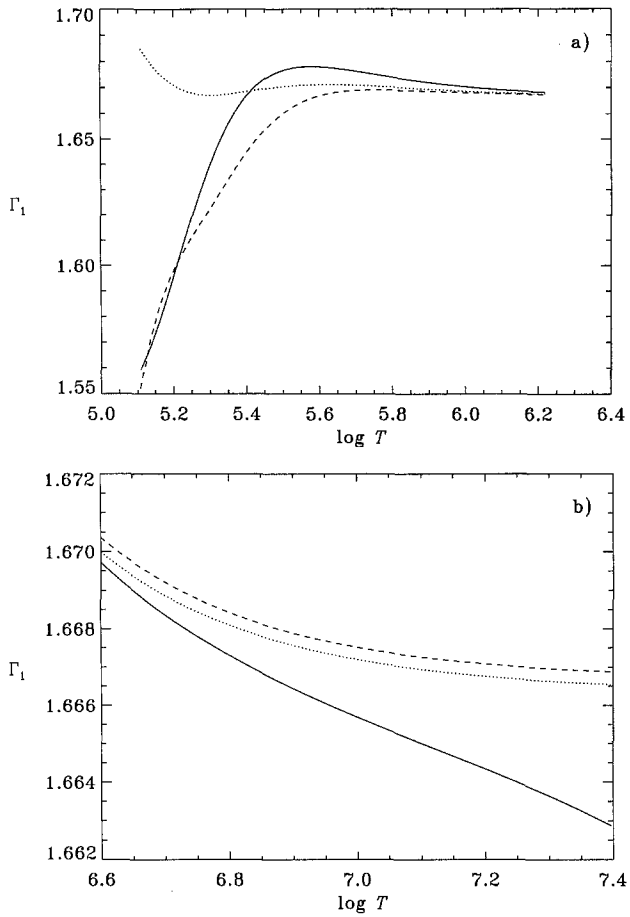

Fig. 6a,b. Adiabatic gradient Γ_1 for the mixture of Fig. 5. The solid line denotes the CEFF, the dashed the MHD, and the dotted the Livermore equation of state. In part **a**, density is $\rho = 0.1\,\mathrm{g\,cm^{-3}}$, in **b** $\rho = 10\,\mathrm{g\,cm^{-3}}$

4. The equation of state and the solar interior

In the previous sections we discussed aspects of solar structure and oscillations, and of the physical properties of the gas in the solar interior. Here we investigate the extent to which the treatment of the equation of state affects the properties of the models and their frequencies, and consider the prospects for using helioseismic observations to study the physics of the gas.

As discussed in Sect. 2.1.2, the convection zone is particularly suitable for such analysis, in that its properties do not depend directly on the opacity, except for a thin region very near the solar surface. The bulk of the convection zone is essentially adiabatically stratified; hence its structure and the frequencies of modes trapped within it are largely determined by the (constant) value of the specific entropy which defines the adiabat, by the chemical composition and by the equation of state. Therefore, in most of this section we concentrate on models of the outer part of the Sun. Such models can conveniently be computed as envelope models with the proper solar radius

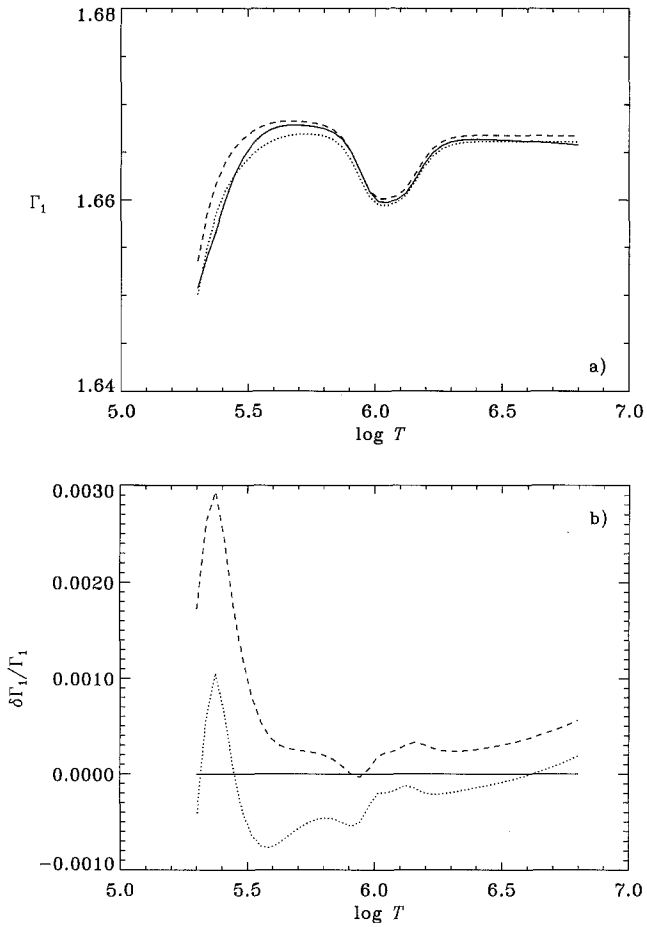

Fig. 7a,b. Comparison of Γ_1 for a mixture involving a representative heavy element. Density is $\rho = 5.00 \times 10^{-3}\,\mathrm{g\,cm^{-3}}$, and the chemical composition is a representative solar mixture of H, He, and O, with mass abundances of 0.7429, 0.2371, 0.0200, respectively. **a** absolute values; **b** relative differences $(\Gamma_1^{\mathrm{Livermore}} - \Gamma_1^{\mathrm{CEFF}})/\Gamma_1^{\mathrm{CEFF}}$ and $(\Gamma_1^{\mathrm{MHD}} - \Gamma_1^{\mathrm{CEFF}})/\Gamma_1^{\mathrm{CEFF}}$, with respect to the CEFF equation of state. The line styles are the same as in Fig. 6; in panel **b** the solid line therefore indicates the zero level

and luminosity, thus bypassing the complications of the nuclear energy generation and evolution of the Sun.

Effects of the equation of state in the solar core are potentially very interesting, although difficult to isolate. To study them evidently requires complete solar models; also, it follows from the discussion in Sect. 2.2.3 that amongst the five-minute oscillations only those of low degree probe the core. In Sect. 4.4 we briefly discuss possible departures from the conventional assumption of complete ionization in the core, motivated by a comparison between observed and computed properties of low-degree p modes.

4.1 Techniques for the analysis

4.1.1 Comparisons of equation of state, models and frequencies

The basic goal is to study the effects of using different equations of state. This is analyzed in several different steps. The simplest comparison is between various quantities, evaluated with different equations of state at the conditions corresponding to a given solar model; this is a natural extension of the results presented in Sect. 3, where differences between various quantities, evaluated at fixed temperature T on different isochores, were presented as functions of T. The direct analogue is to consider conditions at given density and temperature, defined by the structure of a specific model. In this way we can investigate the immediate result of modifying the physics of the equation of state. Here we consider differences between pressure and adiabatic exponent Γ_1. It should be recalled, however, that the hydrostatic structure of the model, and the frequencies of adiabatic oscillation, are given in terms of pressure and density (cf. Sect. 2.2.2); it might be noted also that in Eqs. (2.9) – (2.12) the changes to the model resulting from a change in physics were expressed naturally in terms of the intrinsic change $(\delta \ln \Gamma_1)^{(i)}$ in Γ_1 at fixed (ρ, p). This suggests that it is of interest to consider changes in the thermodynamic properties, particularly Γ_1, also at fixed (ρ, p). We note that the two types of differences are related through

$$\left(\frac{\delta\Gamma_1}{\Gamma_1}\right)_{(\rho,p)} = \left(\frac{\delta\Gamma_1}{\Gamma_1}\right)_{(\rho,T)} + \left(\frac{\partial \ln \Gamma_1}{\partial \ln T}\right)_\rho \left(\frac{\delta T}{T}\right)_{(\rho,p)} ; \tag{4.1}$$

here subscripts "(ρ, p)" and "(ρ, T)" denote differences at fixed (ρ, p) and (ρ, T). Also, it is obvious that there is the identity

$$\left(\frac{\delta p}{p}\right)_{(\rho,T)} = -\left(\frac{\partial \ln p}{\partial \ln T}\right)_\rho \left(\frac{\delta T}{T}\right)_{(\rho,p)} \tag{4.2}$$

between the change in pressure at fixed (ρ, T) and the change in temperature at fixed (ρ, p). To indicate the properties of these relations, Fig. 8 shows the quantities $(\partial \ln \Gamma_1/\partial \ln T)_\rho$ and $(\partial \ln p/\partial \ln T)_\rho$, for Model C1 (cf. Table 1 below), computed with the CEFF equation of state.

Of more direct relevance are the differences between the structure of two models that only differ in the assumed equation of state, and between the frequencies of such models. A convenient (although by no means unique) method of analyzing the model differences is to consider differences at fixed fractional radius. In particular, we note that they are related to the frequency differences through the asymptotic relations (2.37) and (2.38).

From an observational point of view, the most important quantities are the computed frequencies. For each of the models considered we have computed frequencies for extensive sets of p modes; since the analysis is based on envelope models, only modes of degree in excess of 20 were included. When considering frequency differences, one should take into account the fact that with increasing r_t the modes extend over a smaller fraction of the solar mass, and hence their frequencies are easier to perturb. As a result, frequency differences caused by perturbations near the solar surface generally increase in magnitude with increasing l, because of the resulting increase in r_t. Using a perturbation analysis of the exact oscillation equations for modifications to the model or the physics of the oscillations (Christensen-Dalsgaard

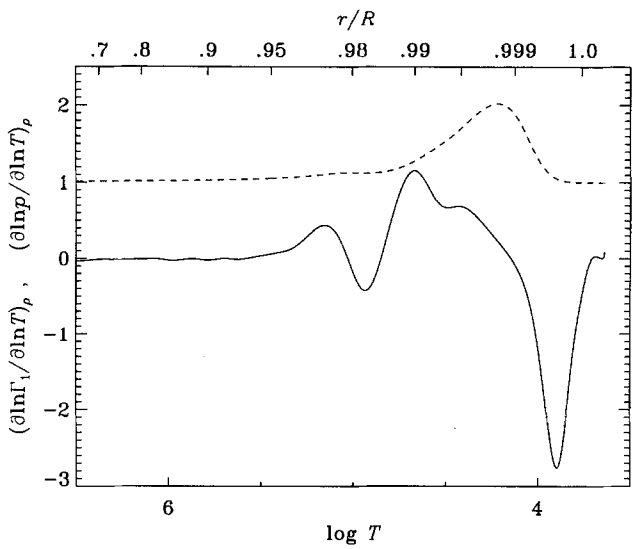

Fig. 8. Logarithmic derivatives of pressure p (·····) and adiabatic exponent Γ_1 (————) with respect to temperature T at fixed density ρ, for the CEFF equation of state. They have been evaluated at the conditions (ρ, T) defined by the envelope Model C1 (cf. Table 1 below). The lower abscissa shows $\log T$, the upper abscissa the fractional radius r/R in the model

1988a; Christensen-Dalsgaard and Berthomieu 1991), one can show that the principal l-dependent part of the frequency differences is inversely proportional to the mode inertia E_{nl} defined in Eq. (2.25). Since E_{nl} depends strongly on frequency, it is more convenient to replace it by the scale factor Q_{nl}, defined by

$$Q_{nl} = \frac{E_{nl}}{\bar{E}_{\rm ref}(\omega_{nl})} , \tag{4.3}$$

where $\bar{E}_{\rm ref}(\omega)$ is the value of E_{nl} at a reference degree $l = l_{\rm ref}$, interpolated to the frequency ω. Roughly speaking, the scaled frequency differences $Q_{nl}\delta\omega_{nl}$ measure the effect of that part of the modification which is confined to the region where the actual mode is trapped, on a mode of low degree $l_{\rm ref}$ with the same frequency. When considering complete models it is natural to take $l_{\rm ref} = 0$; in the present case, where most of the results are based on envelope models, we have used instead $l_{\rm ref} = 20$. This makes very little difference, however.

As argued in Sect. 2.2.3, the behaviour of the oscillations near the surface depends on frequency but not on l. Thus, if the modification is confined close to the surface its effect on the frequency, when corrected for the l-dependence of the mode inertia, is a function of frequency alone; so therefore is $Q_{nl}\delta\omega_{nl}$. The condition for this to be true is that the extent of the region over which the modification is significant is much smaller than the depth of penetration of the modes considered. It follows that if $Q_{nl}\delta\omega_{nl}$ *does* depend on l for a set of modes, the change in the model extends at least to the lower turning point of those modes. Furthermore, it was mentioned in Sect. 2.2.2 that with decreasing frequency the mode amplitude very near the surface, relative to the amplitude in the interior, decreases, and the mode inertia increases. As a result, low-frequency modes are relatively insensitive to modifications that are confined to the superficial layers of the model. It follows from this analysis that

the currently unavoidable errors near the surface of the model might be expected to introduce scaled frequency errors that are essentially independent of l and small at low frequency. Frequency errors that do not have these properties therefore indicate errors in the bulk of the model.

This behaviour of the frequency differences is also contained in the asymptotic expression (2.37). Indeed, the scaling S in that equation is closely related to Q_{nl} introduced in Eq. (4.3) (Christensen-Dalsgaard 1991b). Furthermore, Eq. (2.37) shows that asymptotically $S\delta\omega/\omega$ should be separable into a function of ω/L and a function of ω. It was shown by Christensen-Dalsgaard et al. (1989) how this separation could be accomplished by a least-squares fit of $S\delta\omega/\omega$ to an expression of this form, where H_1 and H_2 were represented as cubic splines. Here, roughly speaking, H_1 is determined by the sound-speed difference $\delta c/c$ in the interior of the Sun; as discussed in Sect. 2.3.2, H_1 may be inverted to obtained an estimate of $\delta c/c$. On the other hand, H_2 is predominantly determined by the region near the solar surface. Christensen-Dalsgaard and Pérez Hernández (1992) showed how $H_2(\omega)$ is related to the differences in sound speed and Γ_1 in the outer parts of the Sun: differences localized very near the surface give rise to a component of H_2 that varies slowly with ω, whereas differences at somewhat greater depth introduce an oscillatory variation with ω in H_2, the "frequency" of which increases with the depth of the difference. This is in fact a general property of frequency differences caused by sharply localized modifications to solar structure (Thompson 1988; Vorontsov 1988b; Gough 1990), and reflects the variation with frequency in the phase of the eigenfunction at the location of the modification. At the surface the behaviour of the eigenfunction changes slowly with frequency, whereas at greater depth a change in frequency causes the eigenfunction to "sweep through" the point where the model was changed, causing a rapid variation in the frequency change. In the case of the variation of H_2 with ω, Christensen-Dalsgaard and Pérez Hernández (1991) found several cases where the relatively sharp change in Γ_1 in the second helium ionization zone caused an oscillatory behaviour of $H_2(\omega)$. Similar variations in the Vorontsov phase function $\beta(\omega)$ (cf. Eq. [2.33]) were analyzed, for example, by Brodsky and Vorontsov (1988b, 1989) and Baturin and Mironova (1990). Vorontsov et al. (1992) showed how the phase could be separated in a quantitative fashion into components varying slowly and rapidly with frequency. This type of analysis provides a powerful diagnostic of the properties of the ionization zones of hydrogen and helium, of great interest both for the analysis of the equation of state and for attempts to determine the helium abundance of the solar convection zone.

Here we analyze frequency differences in terms of the asymptotic expressions in Eqs. (2.37) – (2.39). For the purpose of interpreting the results, it is convenient to write Eq. (2.39) as

$$\frac{S_{nl}}{S_0}\frac{\delta\omega_{nl}}{\omega_{nl}} \simeq S_0^{-1}\left[H_1\left(\frac{\omega_{nl}}{L}\right) + H_2(\omega_{nl})\right] . \tag{4.4}$$

Here

$$S_{nl} = \int_{r_t}^{R}\left(1 - \frac{L^2c^2}{r^2\omega_{nl}^2}\right)^{-1/2}\frac{dr}{c} \tag{4.5}$$

(for simplicity we neglect the small second term on the right-hand side of Eq. [2.38]); also

$$S_0 = \int_{r_0}^{R}\left(1 - \frac{c^2}{r^2w_0^2}\right)^{-1/2}\frac{dr}{c} , \tag{4.6}$$

where r_0 is the radius at the base of the envelope model, and $w_0 = c(r_0)/r_0$. The scaling of the frequency differences in Eq. (4.4) is closely analogous to the scaling introduced in Eq. (4.3); it is defined such that $(S_{nl}/S_0)\delta\omega_{nl}/\omega_{nl}$, and hence $S_0^{-1}H_1$ and $S_0^{-1}H_2$, correspond to relative frequency differences for the most deeply penetrating modes considered. It might be noted also that for complete solar models where $r_0 = 0$, $S_0 = \tau_0$ where

$$\tau_0 = \int_0^R \frac{dr}{c} \tag{4.7}$$

is the acoustical radius of the star.

The functions H_1 and H_2 were determined by means of the spline fit of Christensen-Dalsgaard et al. (1989), where details about the fitting method may be found. Briefly, the procedure is to approximate $H_1(\omega/L)$ and $H_2(\omega)$ by splines, the coefficients of which are determined through a least-squares fit to the scaled frequency differences. The knots of the splines in $w \equiv \omega/L$ are distributed uniformly in $\log w$ over the range considered, whereas the knots for the ω-splines are uniform in ω. We used 28 knots in w and 20 knots in ω. (As a technical point, we note that in the separation in Eq. [2.39] H_1 and H_2 are evidently only determined up to a constant term; hence in the following, when comparing H_2 for different cases, we are permitted to shift H_2 by a constant). The asymptotic separation may be questionable for modes penetrating beyond the lower boundary of the convection zone, where sharp features in the sound speed could introduce additional frequency dependence; furthermore, since the asymptotic description assumes that the properties of the modes are independent of l in the vicinity of the upper reflection point, it fails for modes trapped very near the surface. Hence, as argued by Christensen-Dalsgaard and Pérez Hernández (1991, 1992), H_2 is probably determined most accurately by modes trapped entirely in the convection zone, but of moderate degree. Here we compare H_2 determined for the full mode set with the result of using only those modes for which $20\,\mu\text{Hz} \leq \nu/L \leq 50\,\mu\text{Hz}$ (corresponding to the range $0.80R$ to $0.94R$ in turning point radius r_t).

4.1.2 The helium hump

It was mentioned in Sect. 2.1.2 that in the adiabatic part of the convection zone the quantity

$$\Theta \equiv \frac{1 - \Gamma_1 - \Gamma_{1,\rho}}{1 - \Gamma_{1,c^2}} \tag{4.8}$$

is closely related to the derivative of the sound speed, which can be estimated from helioseismic observations [cf. Eq. (2.7)]. Since Θ is sensitive to the helium abundance, it was proposed by Gough (1984a) and Däppen and Gough (1984) that the helium abundance Y_e of the solar convective envelope could be determined from analysis of Θ. It is evident that Θ depends also on the properties of the equation of state and hence has the potential of serving as a tool for investigating these properties. This requires that the effects of uncertainties in the equation of state and in the composition can be separated; that this may be possible, at least to a limited extent, follows from the fact that the composition can be assumed to be homogeneous throughout the convection zone, where the timescale of mixing is fast compared with any processes that might lead to composition differentiation.

This method for determining Y_e was developed further by Däppen and Gough (1986) who attempted to apply it to solar data by using the absolute asymptotic inversion technique described by Eq. (2.42); however, no definite results were obtained, largely due to observational errors. Däppen et al. (1988) used instead differential asymptotic inversion (cf. Eq. [2.43]); when tested on artificial data the method was found to be potentially useful, but noise in the observational data, and possibly the uncertainty in the equation of state, precluded a reliable determination of the solar Y_e.

Here we investigate the properties of Θ, particularly its sensitivity to the equation of state. The goal is partly to evaluate the extent to which uncertainties in the equation of state affect the determination of Y_e, partly to determine whether it is possible to study properties of the equation of state from measurements of Θ. It was argued in Sect. 2.3.3 that helioseismic inversion leads to estimates of ρ, p and Γ_1, if hydrostatic equilibrium is assumed. Provided that p is identified with the thermodynamic pressure (and hence that the effective pressure resulting from the turbulent convection is neglected) we may therefore regard pressure and density as being fixed seismically, independent of an equation of state. Hence to isolate the effects of the thermodynamic description it is natural to compare Θ, as evaluated with different equations of state, at fixed pressure and density. In addition, we consider the effects on Θ of changing the helium abundance.

4.1.3 Interpolation errors

Equations of state as complex as the MHD and Livermore formalisms cannot be called directly in a stellar structure calculation, but must be used through interpolation in previously computed tables of suitable thermodynamic quantities as functions of density, temperature and composition. This inevitably introduces errors in the computation, the magnitude of which depends on the interpolation procedure and on the mesh in the tables. Accurate comparisons of computations using different equations of state, and comparisons of the computed frequencies with observations, require that the effects of the interpolation errors be limited as far as possible.

The errors can be estimated by considering equations of state sufficiently simple that they can be called directly in the model computations, yet sufficiently realistic that the behaviour of the thermodynamic quantities approximates the behaviour in the tabulated equation of state. The procedure is to set up tables for the simplified equation of state, on precisely the same mesh in ρ, T and composition, and to compare the results of using interpolation in those tables with results obtained using direct call. Here we have used the CEFF equation of state, introduced in Sect. 3.3.2, for this purpose.

Figure 9 shows differences at given ρ and T, corresponding to the values in a solar envelope model, between p and Γ_1 obtained from interpolation and from direct call. In addition, the location of the points in T in the table is indicated. It is evident that the behaviour of the errors is closely related to those points, indicating that the errors are dominated by the interpolation in T. The largest errors are in Γ_1, particularly in the low-temperature region corresponding to the onset of hydrogen ionization where Γ_1 varies rapidly with T; this region does not have a substantial effect on the oscillation frequencies, however, and in any case it is affected by much larger uncertainties associated with nonadiabaticity and the treatment of convection. The second helium

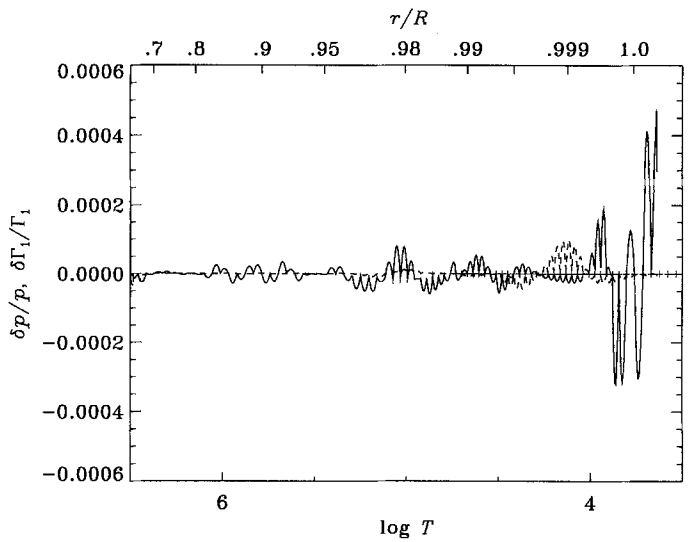

Fig. 9. Relative differences between values of pressure p (·····) and adiabatic exponent Γ_1 (————) evaluated from interpolation in tables and with direct call, in the sense (interpolation) – (direct call), for the CEFF equation of state. They have been computed at the conditions (ρ, T) defined by the envelope Model C1 (cf. Table 1 below). The lower abscissa shows $\log T$, the upper abscissa the fractional radius r/R in the model. The crosses mark the location of the temperature points in the tables

ionization zone, and ionization zones of carbon and oxygen, are also reflected in the error in Γ_1. Nevertheless, it is evident that with the present choice of mesh the errors resulting from interpolation have been reduced to a comparatively low level.

To indicate the effect of the interpolation errors on the computed frequencies, Fig. 10 shows differences, scaled asymptotically as in Eq. (4.4), between frequencies of a model computed with interpolation in CEFF tables and a model computed with direct call, the models having otherwise the same parameters. The comparatively large differences at $\nu/L \simeq 100\,\mu$Hz is caused by model differences that result from interpolation errors in the region affected by the EFF formulation for pressure ionization; in this region Γ_1 has a small sharp feature. However, in any case the relative errors are below 10^{-5} for essentially all the modes considered. Hence the effect of interpolation is below or comparable with the errors in the observed frequencies. Corresponding errors are found for H_1 and H_2 as obtained by fitting Eq. (2.39) to the frequency differences.

We finally note that the interpolation errors are determined by the distribution of mesh points and by higher derivatives of the quantities being interpolated. Hence to the extent that these higher derivatives are insensitive to the details of the formulation of the equation of state, the same is true of the interpolation errors. This suggests that errors arising from the interpolation would largely cancel in comparisons between different equations of state, obtained by interpolation on the same mesh. Therefore, when making comparisons between models computed with simple and complex equations of state, we base the models on tables even for the simple equations of state, essentially eliminating effects of interpolation error in the model and frequency differences.

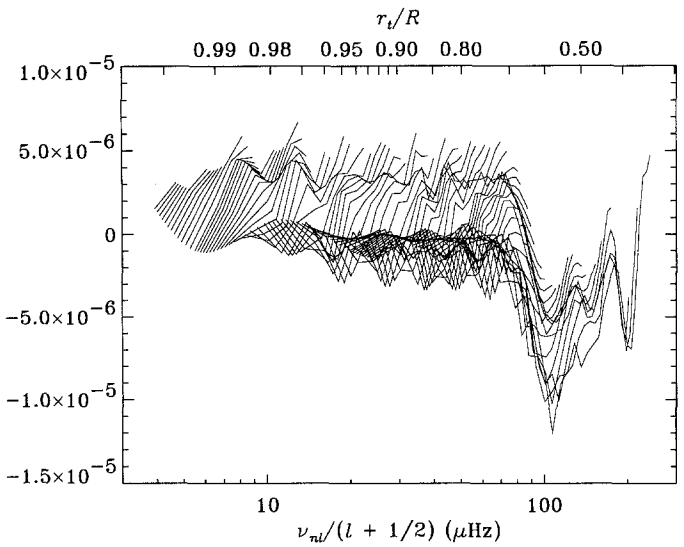

Fig. 10. Asymptotically scaled relative frequency differences (cf. Eq. [4.4]), illustrating the effect of interpolation errors. The differences are between frequencies of Model C1′ computed with interpolation in CEFF tables, and Model C1 computed with direct call to the CEFF routine (see Table 1), in the sense (Model C1′) – (Model C1). Points corresponding to the same value of the degree l have been connected. The lower abscissa gives $\nu_{nl}/(l + 1/2)$, where ν_{nl} is the cyclic frequency; the upper abscissa shows the corresponding fractional turning-point position r_t/R, which is related to $\nu_{nl}/(l + 1/2)$ through Eq. (2.29)

4.2 Effects of the equation of state in the solar convection zone

It was realized early in the development of helioseismology that the treatment of the equation of state might have a substantial effect on the computed oscillation frequencies. Berthomieu et al. (1980) and Lubow et al. (1980) computed solar envelope models with improvements in the equation of state and compared them with the observed frequencies of high-degree five-minute oscillations; this comparison, however, was also affected by uncertainties about the adiabat of the solar envelope. Effects of changing the equation of state, involving among other features electrostatic corrections, were studied by Ulrich (1982), Ulrich and Rhodes (1983), Shibahashi et al. (1983, 1984) and Noels et al. (1984), who considered also modes of low and moderate degree. More recently, Christensen-Dalsgaard et al. (1988b) compared models computed with the EFF and the MHD equation of state (for a somewhat simplified chemical composition); they found that the model with the MHD equation of state was in generally closer agreement with the whole range of observed solar oscillation frequencies. Stix and Skaley (1990) made an investigation of the effect on the oscillation frequencies of a simplified equation of state based on the SSCP model (see Sect. 3.3.3) and the classical Debye-Hückel Coulomb term (3.6). Electrostatic effects were also considered by Baturin (1991), who in particular studied the response of the Vorontsov phase $\beta(\omega)$. Christensen-Dalsgaard and Pérez Hernández (1991) considered the effect on the phase difference $H_2(\omega)$ of going from the EFF to the MHD equation of state. Pamyatnykh et al. (1991) varied a number of parameters in computations of solar envelope models, including the equation of state, analyzing the change in thermodynamic state and the response of the frequencies in terms of $\beta(\omega)$. Vorontsov et al. (1992) also considered the effects on the structure of the model and the oscillation

frequencies of electrostatic corrections, both in the simple form and including the τ cut-off for the size of atoms and ions (see Sect. 3.1); the frequency analysis utilized the asymptotic description in Eq. (2.30), furthermore separating the variation of the phase $\alpha(\omega)$ into a part varying slowly with frequency and associated with the extreme superficial layers and a part oscillating with frequency and predominantly related to the second helium ionization zone (see also Sect. 4.1.1). Baturin et al. (1992) made a similar study, but concentrating on the role of the assumed atomic size in pressure ionization.

To provide a homogeneous illustration of the effects of the physics, and of other parameters, on the structure of the solar envelope and its oscillation frequencies, we here consider a number of models computed specifically for this purpose. Since a major aim is to investigate the differential effect of introducing additional properties in, for example, the equation of state, it is natural to analyze the results in terms of the differential asymptotic expression (4.4), which was discussed in Sect. 4.1.1. Apart from the physics, in particular the equation of state, the models are characterized by the composition and by the value of the mixing-length parameter α_C. For most of the models we, somewhat arbitrarily, fix α_C by demanding that the model have the depth of convection zone of $0.287R$ which has been inferred helioseismically (Christensen-Dalsgaard et al. 1991). Except where otherwise noted the composition was characterized by $Y = 0.265$, $Z = 0.02$; the mixture of heavy elements consisted of C, N, O and Fe, with number densities relative to hydrogen of 4.17×10^{-4}, 0.87×10^{-4}, 6.92×10^{-4} and 1.72×10^{-4}, respectively. The consequences of modifying the helium abundance and the mixing length are briefly considered in Sect. 4.2.4.

Models have been computed with the EFF and CEFF equations of state, discussed in Sect. 3.3.2, as well as with the MHD formulation presented in Sect. 3.3.4. To investigate the effects of the details in the MHD formulation, we have considered both the full treatment [referred to in the following as MHD(F)] and the "stripped-down" version [cf. Sect. 3.5.3; in the following MHD(S)] where the effects of excited states of all elements other than hydrogen and helium are neglected. We consider models computed with two different sets of opacities: in most cases the Cox and Tabor (1976) tables (referred to as CT) were used; however, in the comparison with observed frequencies in Sect. 4.3 we also consider models computed with a set based on the Los Alamos Opacity Library [Huebner et al. 1977; details about how the tables were set up were given by Courtaud et al. (1990) and Turck-Chièze (1990)]; these tables are referred to as LAOL in the following.

A summary of the models considered is given in Table 1.

A notable feature is the difference between the CT and the LAOL opacities in the values of α_C required to obtain the specified depth of the convection zone. This is caused by the fact that the LAOL opacities are larger (by up to a factor two) at conditions corresponding to the solar atmosphere; as a result the atmospheric structure is different, and so therefore is the entropy jump, determined by α_C, required to reach the proper adiabat in the bulk of the convection zone.

4.2.1 Comparisons of the EFF and CEFF equations of state

The simple EFF equation of state has been used in a substantial number of calculations of solar and stellar structure. For this reason, it is of some interest to investigate in detail how it differs from more realistic formulations. Here we concentrate on the

Table 1. Summary of envelope models. The column marked EOS gives the equation of state, as defined in the text. "Opacity" indicates the opacity: CT denotes the Cox and Tabor (1976) tables and LAOL denotes tables derived from the Los Alamos Opacity Library. Y is the envelope helium abundance, d_b/R is the depth of the outer convection zone, in units of the solar radius, and α_C is the mixing-length parameter. In the column marked "Notes", (a) indicates that the equation of state was obtained through interpolation in tables

Model	EOS	Opacity	Y	d_b/R	α_C	Notes
E1	EFF	CT	0.265	0.2870	1.7297	
E2	EFF	LAOL	0.265	0.2870	2.7503	
C1	CEFF	CT	0.265	0.2870	1.7604	
C1'	CEFF	CT	0.265	0.2870	1.7591	(a)
C2	CEFF	CT	0.260	0.2870	1.7624	
C3	CEFF	CT	0.265	0.2904	1.8000	
C4	CEFF	LAOL	0.265	0.2870	2.8009	
MS1	MHD(S)	CT	0.265	0.2870	1.7528	(a)
M1	MHD(F)	CT	0.265	0.2870	1.7524	(a)
M2	MHD(F)	LAOL	0.265	0.2870	2.7877	(a)

effects of including the Coulomb terms, by comparing the EFF and CEFF formulations (cf. Sect. 3.3.2).

To illustrate the direct effect of the change in the equation of state, Fig. 11a shows Γ_1 evaluated with the EFF and the CEFF equations of state at the conditions (ρ, T) corresponding to Model C1 computed with the CEFF equation of state; Fig. 11b shows relative differences in p and Γ_1, in the sense (EFF) – (CEFF), at fixed (ρ, T). The behaviour of Γ_1 is dominated by the fact that it has "dips" for each ionization reaction: it decreases from the value of $5/3$ at no or complete ionization down to about 1.20 in the case of hydrogen ionization, and to about 1.55 in the case of the second ionization stage of helium (the effect of the first stage of helium ionization is mostly hidden in the high-temperature flank of the hydrogen dip).

To elucidate the consequences of including the Coulomb terms we recall (cf. Sect. 3.5.1) that there are two contributions due to the Coulomb term, one associated with the free energy [cf. Eq. (3.6)] of the Debye-Hückel term itself, the other with the Coulomb-term induced shift in the ionization equilibrium. The direct (negative) Coulomb pressure contribution, computed from the free-energy term of Eq. (3.6), gets as high as 10^{-1} (Baturin 1991; Shibahashi et al. 1983). This direct contribution basically causes the CEFF pressure to be smaller than that of EFF. However, the difference between the two is reduced by the Coulomb-term induced enhancement of the ionization equilibrium, which translates into a positive pressure contribution in CEFF, which offsets a part of the direct negative contribution. Changes in thermodynamic quantities such as Γ_1 are more difficult to trace. In the top part of the hydrogen ionization zone, where overall ionization is still low, the induced part has a more pronounced influence; however, as soon as a sizeable fraction of hydrogen is ionized, the direct part and the induced part become comparable.

The principal physical reason that causes the oscillatory behaviour of the relative differences in Γ_1 is the increased ionization fraction of hydrogen and helium due to the Coulomb interaction (see also Stix and Skaley 1990; Baturin 1991; Vorontsov et al. 1992): the higher ionization fractions shift the ionization zones of hydrogen and helium towards the surface; this in turn shifts upward the dips in Γ_1 which are associated with these ionization zones (cf. Fig. 11a), thus giving rise to the oscillatory

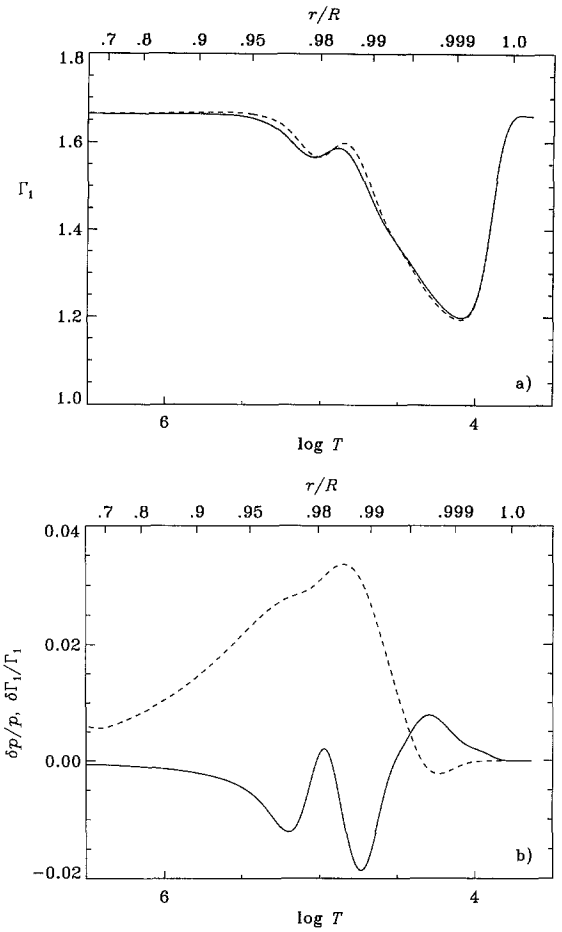

Fig. 11. a Adiabatic exponent Γ_1 evaluated with the EFF (————) and the CEFF (·····) equations of state. **b** Relative differences between values of pressure p (·····) and adiabatic exponent Γ_1 (————) evaluated with the EFF and the CEFF equations of state, in the sense (EFF) – (CEFF). They have been computed at the conditions (ρ, T) defined by the envelope Model C1 (cf. Table 1). The lower abscissa shows $\log T$, the upper abscissa the fractional radius r/R in the model

behaviour of $\delta\Gamma_1$. Pressure, on the other hand does not exhibit dips but rather steps for each ionization reaction; therefore, the principal effect of the Coulomb term is the different location of the steps, which explains the general behaviour of the relative pressure difference. It should be noticed that in the cases of little or of full ionization, the pressure difference appears to be rather small compared with the case of partial ionization. When the plasma is essentially neutral, in the uppermost part of the hydrogen ionization zone, the Coulomb pressure is small, though the the associated shift in the ionization balance already changes Γ_1 significantly. When the plasma is fully ionized, beneath the hydrogen and helium ionization zones, the Coulomb effect also becomes smaller. However, the reason is that the essentially adiabatic temperature gradient of the solar convection zone causes a steep increase of temperature, leading to a smaller Coulomb term [see Eqs. (3.4) and (3.6)]; for a more detailed discussion see Baturin 1991). Note that conversely in radiatively stratified regions (such as in

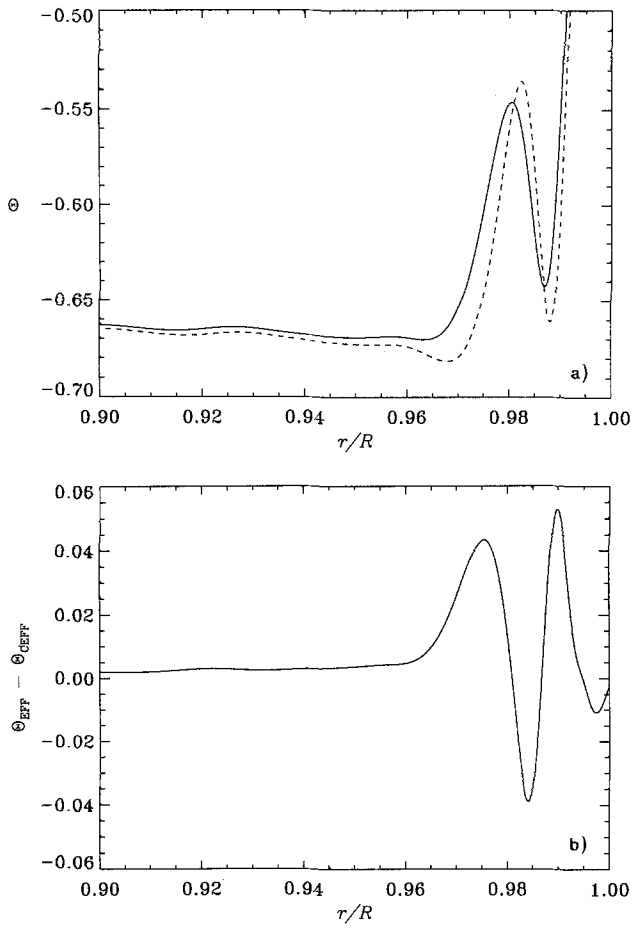

Fig. 12a,b. Properties of the function Θ (cf. Eq. [4.8]), evaluated at the conditions (ρ, p) defined by the envelope Model C1 (cf. Table 1). **a** Θ computed with the EFF (————) and the CEFF (·····) equations of state. **b** Difference between the two curves in **a**, in the sense (EFF) – (CEFF). The abscissa is fractional radius r/R

the inner part of the Sun), the Coulomb effect becomes more prominent with depth (Baturin 1991).

It was argued in Sect. 4.1.2 that the quantity Θ, defined by Eq. (4.8) provides a useful diagnostics for the composition and equation of state. As suggested there, Fig. 12 compares Θ evaluated with the EFF and the CEFF equations of state, at fixed (ρ, p) in Model C1. From panel (a) it is evident that the dominant effect of including the electrostatic corrections is indeed to shift the ionization zones, reflected in particular in the helium hump at $r \simeq 0.98R$, towards the surface. This behaviour is even more evident in the Θ difference shown in Fig. 12b.

Figure 13 shows differences at fixed r between a model computed with the EFF equation of state and a model computed with the CEFF equation of state. The behaviour of the differences can to some extent be understood in terms of Eqs. (2.9) – (2.13) (cf. Sect. 2.1.3; see also Christensen-Dalsgaard et al. 1988b). In particular, Eqs. (2.9) and (2.10) show that the change in sound speed is closely related to the

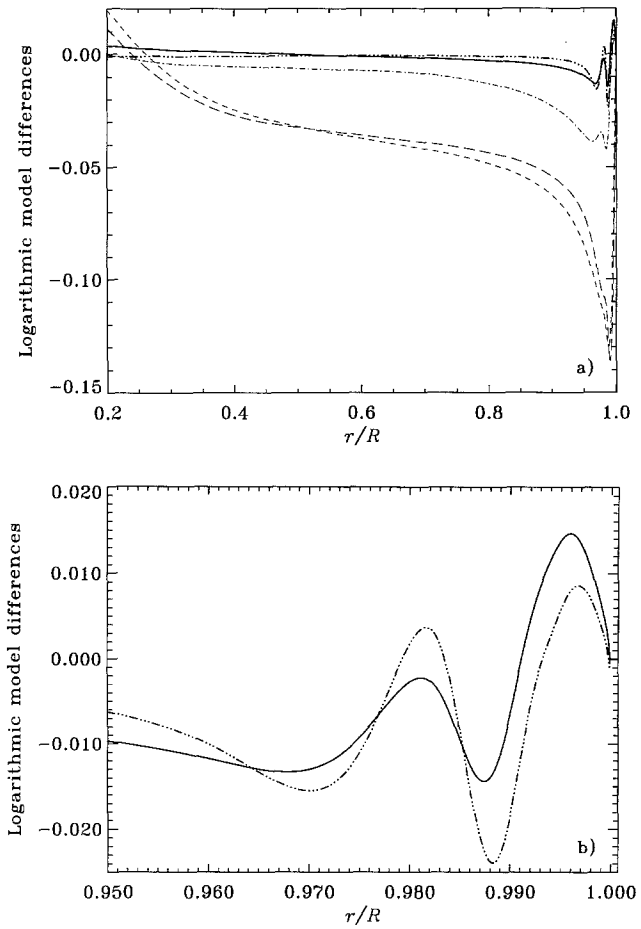

Fig. 13. a Logarithmic differences between Models E1 and C1 computed with the EFF and CEFF equations of state, respectively, in the sense (Model E1) – (Model C1). The quantities plotted are $\delta \ln p$ (----------); $\delta \ln \rho$ (--------); $\delta \ln T$ (—·—·—·—); $\delta \ln \Gamma_1$ (—···—···—···); and $\delta \ln c$ (————). The abscissa is fractional radius r/R. **b** $\delta \ln c$ and $\delta \ln \Gamma_1$ in the hydrogen and helium ionization zones

change in Γ_1 (in the present case the change in the superadiabatic gradient $\Gamma - \Gamma_1$ is small). However, as can be seen in Fig. 13b, the part due to structure changes $[\delta \ln(p/\rho) = \delta \ln c - \delta \ln \Gamma_1/2]$ is not always small. This shows that there are regions where the structure changes caused by changes in the equation of state can have a stronger influence on sound speed than pure thermodynamic changes (Baturin, *private communication*).

Furthermore, comparison of Figs. 11b and 13b suggests that in Eq. (2.12) the dominant term is the intrinsic change $(\delta \ln \Gamma_1)^{(i)}$, caused directly by the change in the equation of state. Indeed, it follows from Eqs. (4.1) and (4.2), the behaviour of $(\partial \ln \Gamma_1/\partial \ln T)_\rho$ and $(\partial \ln p/\partial \ln T)_\rho$ shown in Fig. 8, and the behaviour of $(\delta p/p)_{(\rho,T)}$ shown in Fig. 11b, that $(\delta \Gamma_1/\Gamma_1)_{(\rho,T)}$ which is shown in Fig. 11b and $(\delta \Gamma_1/\Gamma_1)_{(\rho,p)}$ which enters into Eq. (2.12) are quite similar. Hence there is a very direct link between the change in the physics, as expressed in $(\delta \ln \Gamma_1)^{(i)}$, and the change in the sound speed which in turn is reflected in the change in the frequencies.

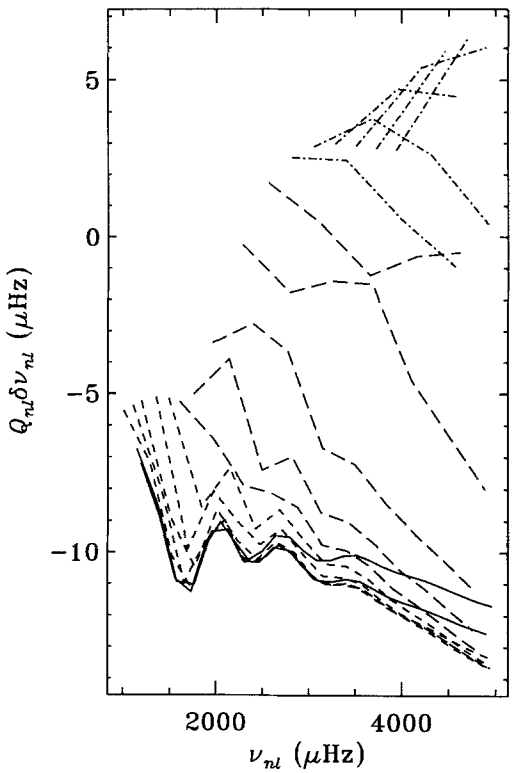

Fig. 14. Frequency differences, scaled by the inertia ratio Q_{nl} (cf. Eq. [4.3]), between Models E1 and C1 computed with the EFF and CEFF equations of state, respectively, in the sense (Model E1) – (Model C1). The abscissa is cyclic frequency ν_{nl}. The points have been connected with lines according to the value of the degree l: $l = 20, 30$: ————; $l = 40, 50, 60, 80, 100$: ·····; $l = 120, 150, 200, 300, 400$: – – – – – – –; and $l = 500, 600, 700, 800, 900, 1000$: —·—·—·—

The change in p follows, at least in a qualitative sense, the predictions of Eq. (2.13). Very near the surface there is a region where $\delta \ln(p/\rho)$ is positive, leading to a negative contribution to $\delta \ln p$; the extent of this region is approximately eight pressure scale heights, and hence the magnitude of the initial negative excursion of $\delta \ln p$ is roughly eight times as large as the average $\delta \ln(p/\rho)$. Below this region, $\delta \ln(p/\rho)$ is negative, and as a result $\delta \ln p$ decreases in magnitude with increasing depth.

Fig. 15. a Asymptotically scaled relative frequency differences (cf. Eq. [4.4]), between Models E1 and C1 computed with the EFF and CEFF equations of state, respectively, in the sense (Model E1) – (Model C1). Points corresponding to the same value of the degree l have been connected. The lower abscissa gives $\nu_{nl}/(l + 1/2)$, where ν_{nl} is the cyclic frequency; the upper abscissa shows the corresponding fractional turning-point position r_t/R, which is related to $\nu_{nl}/(l + 1/2)$ through Eq. (2.29).

Panels **b**–**f** show results of the asymptotic fit in Eq. (4.4). **b** Residual after subtraction of the fitted $H_2(\omega_{nl})$, for all modes in the set; the abscissas are as in panel **a**. **c** Residual after subtraction of the fitted $H_1(\omega_{nl}/L)$, for all modes in the set, plotted against cyclic frequency ν_{nl}. **d** Residual after subtraction of the fitted $H_1(\omega_{nl}/L)$, for modes with $20\,\mu\text{Hz} \leq \nu_{nl}/L \leq 50\,\mu\text{Hz}$. **e** The function $H_1(\omega/L)$ resulting from the fit, for the full mode set; abscissas as in panel **a**. **f** The function $H_2(\omega)$ resulting from the fit, against cyclic frequency ν. The solid curve shows the result of the fit to the full mode set, whereas the dashed curve is based on a fit to the modes with $20\,\mu\text{Hz} \leq \nu_{nl}/L \leq 50\,\mu\text{Hz}$

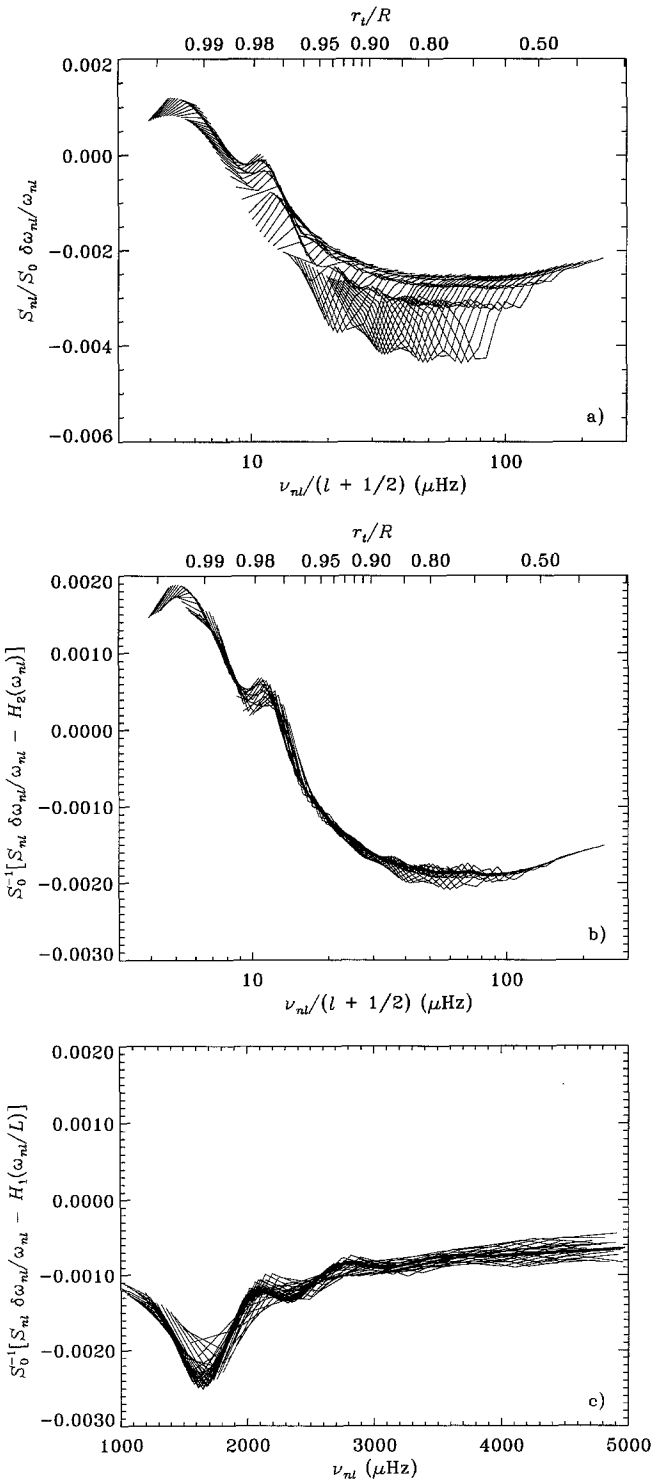
r_t/R
0.99 0.98 0.95 0.90 0.80 0.50
0.002
0.000
−0.002
−0.004
−0.006
$S_{nl}/S_0\ \delta\omega_{nl}/\omega_{nl}$
a)
10
100
$\nu_{nl}/(l + 1/2)$ (μHz)
r_t/R
0.99 0.98 0.95 0.90 0.80 0.50
0.0020
0.0010
0.0000
−0.0010
−0.0020
−0.0030
$S_0^{-1}[S_{nl}\ \delta\omega_{nl}/\omega_{nl} - H_2(\omega_{nl})]$
b)
10
100
$\nu_{nl}/(l + 1/2)$ (μHz)
0.0020
0.0010
0.0000
−0.0010
−0.0020
−0.0030
$S_0^{-1}[S_{nl}\ \delta\omega_{nl}/\omega_{nl} - H_1(\omega_{nl}/L)]$
c)
1000
2000
3000
4000
5000
ν_{nl} (μHz)

Fig. 15a–c

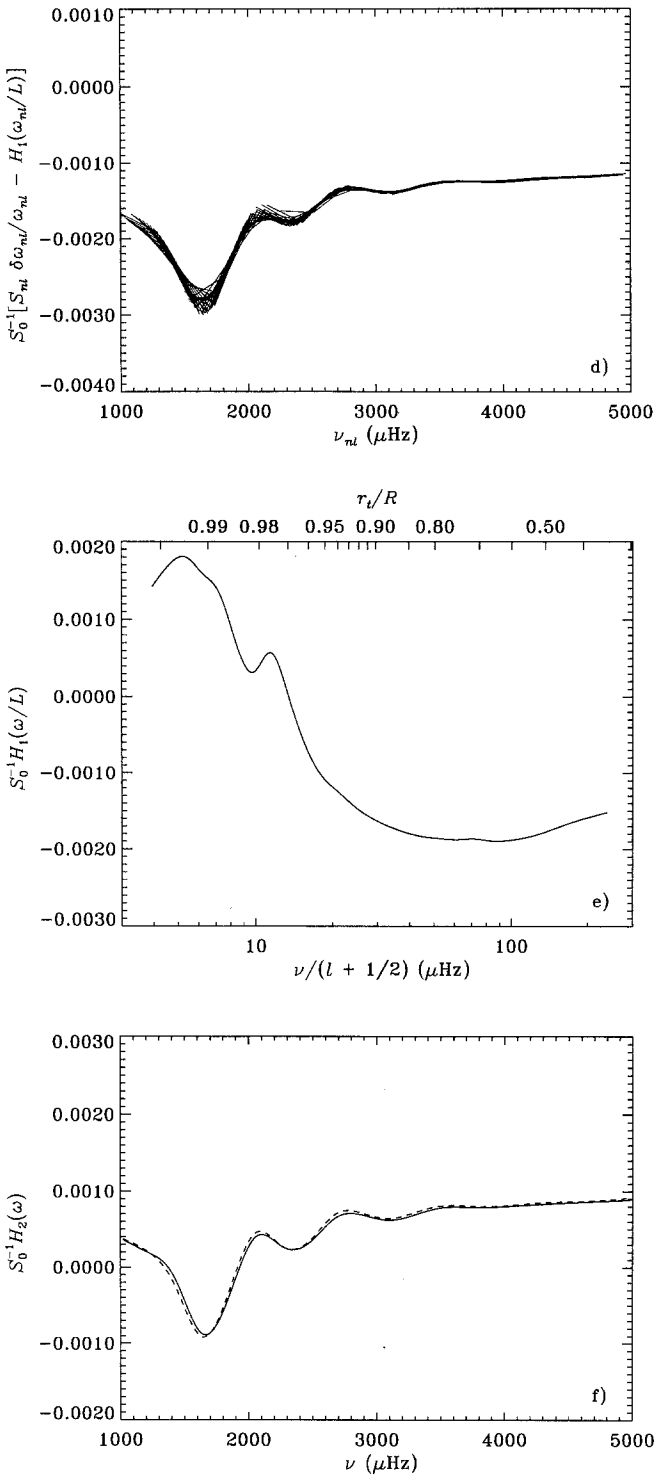
0.0010
0.0000
−0.0010
−0.0020
−0.0030
−0.0040
$S_0^{-1}[S_{nl}\,\delta\omega_{nl}/\omega_{nl} - H_1(\omega_{nl}/L)]$
d)
1000
2000
3000
4000
5000
ν_{nl} (μHz)
r_t/R
0.99 0.98 0.95 0.90 0.80 0.50
0.0020
0.0010
0.0000
−0.0010
−0.0020
−0.0030
$S_0^{-1}H_1(\omega/L)$
e)
10
100
$\nu/(l + 1/2)$ (μHz)
0.0030
0.0020
0.0010
0.0000
−0.0010
−0.0020
$S_0^{-1}H_2(\omega)$
f)
1000
2000
3000
4000
5000
ν (μHz)

Fig. 15d–f

The effects on the frequencies are shown in Fig. 14, in the form of frequency differences scaled by Q_{nl}. These differences can be understood qualitatively in terms of the sound-speed differences shown in Fig. 13, and the simple expression (2.40). Since the sound-speed difference is concentrated relatively near the surface, all modes of degree $l \lesssim 100$ sense the change in much the same manner, and hence for these modes $Q_{nl}\delta\nu_{nl}$ depends only on frequency. At higher degree the lower turning point of the modes moves into the region where $\delta \ln c$ is substantial; hence the magnitude of the negative contribution to $\delta\nu_{nl}$ decreases with increasing l, and $Q_{nl}\delta\nu_{nl}$ increases. Finally, for $l > 500$ the modes are trapped entirely in the thin region near the surface where $\delta \ln c$ is positive, and hence $Q_{nl}\delta\nu_{nl} > 0$.

These arguments show that there is a close connection between the frequency differences and the location of the turning point or, equivalently, ν/L (cf. Eq. [2.29]). Hence it is natural to plot frequency differences against ν/L. This has been done in Fig. 15a, using asymptotically scaled relative differences, in preparation for analyzing the differences in terms of the asymptotic separation in Eq. (4.4). Here it is evident that the overall behaviour of the differences is determined by location of the turning point, and reflects the variation in the sound speed. However, on top of this general trend there is apparent scatter where closer inspection reveals a pattern repeated in the individual curves, which each corresponds to a given value of l.

This behaviour is in accordance with the expected form of the frequency differences, and further motivates attempting a spline fit of the form (4.4), as discussed in Sect. 4.1.1. The results are presented in panels (b) – (f) of Fig. 15. Panel (b) shows that after subtraction of the fitted $H_2(\omega)$, the frequency differences are indeed largely a function of ω/L, as expected. Similarly, panel (c) shows that after subtraction of $H_1(\omega/L)$ the residual is largely a function of ω. The fits in panels (b) and (c) were based on the complete mode set; if instead only modes for which $20\,\mu\text{Hz} \leq \nu/L \leq 50\,\mu\text{Hz}$ are included, the scatter in the frequency-dependent residual is considerably reduced, as shown in panel (d). The fitted H_1 is shown in panel (e). Asymptotically, H_1 is related to the sound-speed difference by Eq. (2.37); this indicates that a sharp feature in $\delta c/c$ has a particularly significant effect for those modes which have turning point at or just below the location of the feature, as a result of the integrable singularity in the integrand defining H_1. In particular, one may identify the dip in H_1 at $\nu/L \simeq 10\,\mu\text{Hz}$ with the sharp dip in $\delta \ln c$ at $r \simeq 0.987R$ (cf. Fig. 13b), associated with the shift to greater depth of the merged hydrogen and first helium ionization zones in the EFF case. Finally, panel (f) shows the fitted H_2 both for the full and for the restricted mode set; it is evident that despite the considerably larger scatter for the full set, the resulting H_2 are very similar for the two sets. It was argued by Christensen-Dalsgaard and Pérez Hernández (1991) that the oscillatory behaviour in H_2, particularly at low frequency, is related to the sharp differences in Γ_1 near the second helium ionization zone (see also Sect. 4.1.1).

4.2.2 Comparison of MHD(S) and CEFF

To investigate the influence of the excited states of hydrogen and helium separately from that of the configurational Coulomb interaction, we here compare the stripped-down version of the MHD equation of state with the CEFF formulation. We recall that the stripped-down MHD(S) equation of state contains the full MHD treatment of all excited states of H, He and He^+, but uses only ground states for the heavier

atoms and their ions. The MHD(S) and CEFF equations of state therefore treat the heavy elements identically. Since, in addition, MHD(S) and CEFF have the same Coulomb term, the difference effectively shows the effect of the excited states of H, He, and He^+. It might be pointed out that there are some very small differences also in the treatment of the heavy elements: in the MHD equation of state the ground-state weight can be reduced by plasma effects, and this is not taken into account in CEFF; however, these differences are probably insignificant in the present comparison.

Figure 16 shows relative differences, in the sense MHD(S) – CEFF, in p and Γ_1 at fixed (ρ, T) corresponding to conditions in Model C1′; to minimize the effects of interpolation errors, the CEFF equation of state was used in the form of tables, on the same mesh in (ρ, T) as used for the MHD(S) values. A dominant feature is the large negative $\delta\Gamma_1$ at low temperature, corresponding to the atmosphere of the model; this is caused by the dissociation of the H_2 molecule which is taken into account in MHD(S) but not in CEFF. This region has little effect on the oscillation frequencies, however. Otherwise the dominant differences are again associated with the helium ionization zones.

The comparison of MHD(S) with CEFF reveals the influence of the excited states of hydrogen and helium (and to a small degree that of H_2 molecules). Simple estimates of the partition functions of hydrogen and helium (done in the MHD formalism) show that at first the influence of the excited states seems non-negligible compared with that of the ground state. The contribution of the excited states reaches more than 10 per cent of the internal partition function at some places in the ionization zones of hydrogen and helium. Christensen-Dalsgaard et al. (1988b) thought that this effect of excited states was responsible for the success the MHD equation of state had, especially with the high-degree modes, which probe the hydrogen and helium ionization zones.

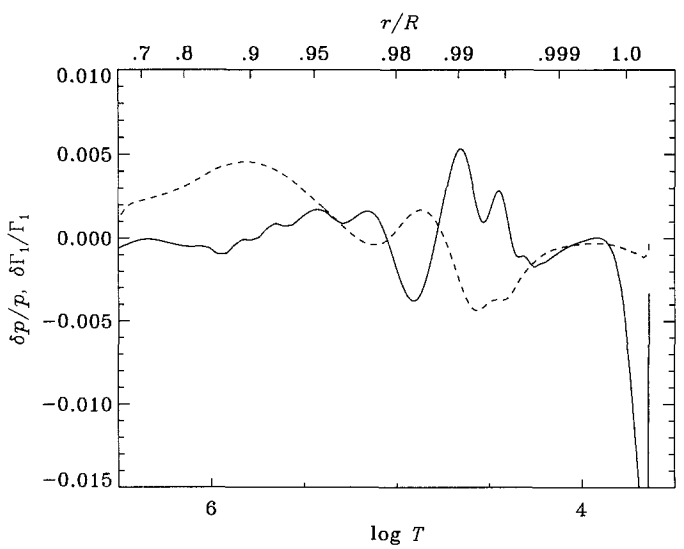

Fig. 16. Relative differences between values of pressure p (·····) and adiabatic exponent Γ_1 (————) evaluated with the stripped MHD [MHD(S)] and the CEFF equations of state, in the sense [MHD(S)] – (CEFF). The quantities were computed at the conditions (ρ, T) defined by the envelope Model C1′ (cf. Table 1). The lower abscissa shows $\log T$, the upper abscissa the fractional radius r/R in the model

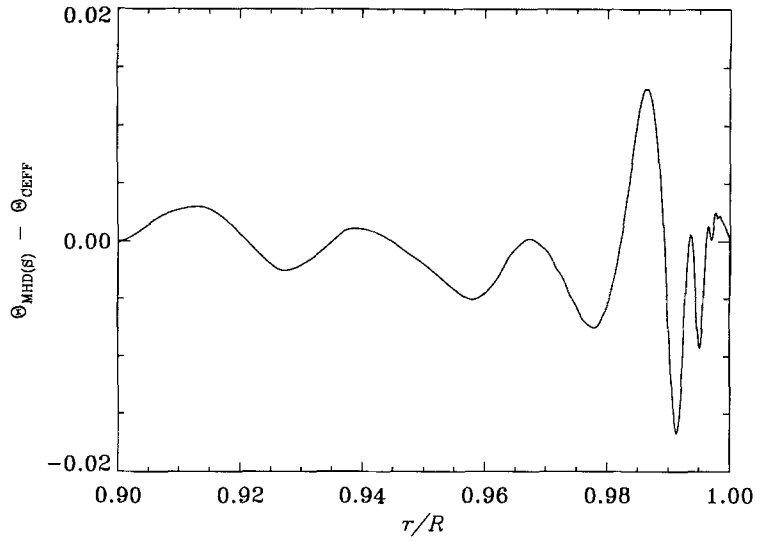

Fig. 17. Difference between the function Θ (cf. Eq. [4.8]), as evaluated with the stripped MHD [MHD(S)] and the CEFF equations of state, at the conditions (ρ, p) defined by the envelope Model C1′ (cf. Table 1). The difference is in the sense [MHD(S)] – (CEFF)

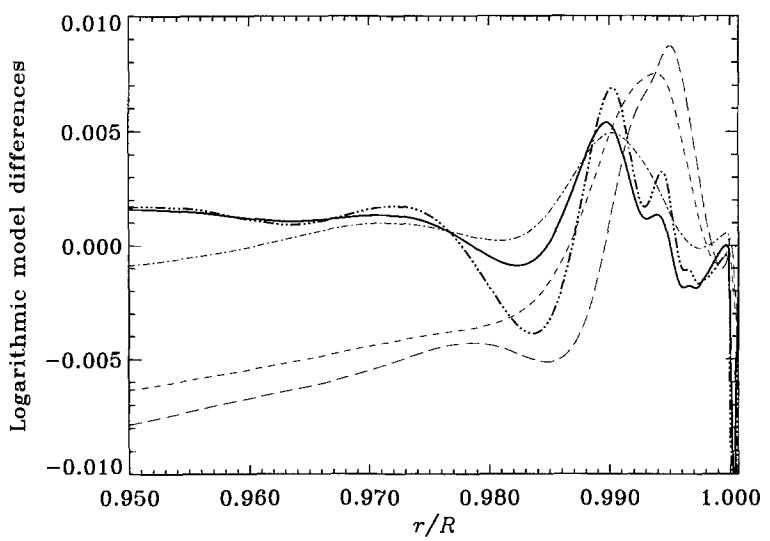

Fig. 18. Logarithmic differences between Models MS1 and C1′ computed with the MHD(S) and CEFF equations of state, respectively, in the sense (Model MS1) – (Model C1′). The quantities plotted are $\delta \ln p$ (- - - - - - - - - - -); $\delta \ln \rho$ (— — — — — —); $\delta \ln T$ (— · — · — · —); $\delta \ln \Gamma_1$ (— · · — · · — · · —); and $\delta \ln c$ (————————). The abscissa is fractional radius r/R

However, since the MHD equation of state simultaneously incorporates several different types of non-ideal corrections, it did not become immediately clear which particular correction was mainly contributing to this success. From a detailed comparison with the alternative non-ideal Livermore equation of state (see Sect. 3.4), it

turned out, rather surprisingly, that the net effect of the hydrogen and helium bound states on thermodynamic quantities was to a large degree eclipsed beneath the influence of the Coulomb term, which was thus recognized as the dominant non-ideal correction in the hydrogen and helium ionization zones.

As in Sect. 4.2.1 it is of interest to consider the effect of the change in equation of state on the helium hump, defined by the function Θ (see Fig. 12a, at $r \simeq 0.98R$). The difference in Θ at fixed (ρ, p) in Model C1′ as determined with MHD(S) and with CEFF is shown in Fig. 17. This rather substantial difference shows that unlike Γ_1 itself (see Fig. 16) the derivatives of Γ_1 (contained in Θ) clearly reveal the effect of the excited states of the bound systems, which is here principally He^+.

Differences between Models MS1 and C1′, computed with the MHD(S) and the CEFF equations of state using interpolation on the same mesh, are shown in Fig. 18. As in the case of EFF – CEFF, discussed in the previous section, the differences are predominantly concentrated in the hydrogen and helium ionization zones; in particular, the differences in c and Γ_1 are small in the deeper parts of the convection zone. Also, it should be noticed that $\delta\Gamma_1$ is quite similar to the difference at fixed thermodynamic conditions, shown in Fig. 16. This again indicates that the intrinsic change in Γ_1 dominates and that therefore the response of the envelope is directly related to the change in the properties of the equation of state.

Asymptotically scaled frequency differences, and the results of the separation in Eq. (4.4), are shown in Fig. 19. The behaviour of $H_1(\omega/L)$ can again be related to the sound-speed difference shown in Fig. 16; particularly prominent is the feature associated with the hump in $\delta c/c$ at $r \simeq 0.99R$. The dip and hump between $r = 0.98R$ and $r = 0.99R$ in the difference of Γ_1 are caused by a shift of the position of the second ionization zone of helium, where Γ_1 is lowered from about 5/3 to 1.55 (cf. Fig. 11a).

This shift is due to the sheer number of excited states of He^+ included in the internal partition functions of the MHD equation of state. As a result, the correction of the total statistical weight of the He^+ ion can be sizable, even though the weight of the ground state (with [negative] energy E_0) dominates that of a *single* excited state (with [negative] energy E_j) by a factor of $\exp[-(E_j - E_0)/kT]$. This modification of the internal partition function immediately translates into a change of the same order in the ionization degrees [see Eqs (3.8a) and (3.8b)]. The difference of Γ_1 between $r = 0.98R$ and $r = 0.99R$ precisely reflects this change of depth of the ionization zones. Also, the dominant oscillatory component in $H_2(\omega/L)$ reflects the rapid variation in δc and $\delta\Gamma_1$ in the vicinity of the helium ionization zones.

4.2.3 Comparison of MHD(S) and MHD(F)

As a final case, we consider differences between the full MHD treatment [MHD(F)] and the stripped-down version [MHD(S)]. In the stripped-down version MHD(S), only hydrogen and helium are treated with full internal partition functions, whereas the partition functions of heavier elements and their ions contain only ground states [having the same weight as in the full MHD(F)]. The motivation for a comparison of MHD(S) with MHD(F) is that it will show the effects of the treatment of the excited states of the heavy elements. As we have mentioned in Sect. 3.5.3b, it is precisely the influence of excited states of the heavy elements which reveals a distinct signature of the MHD formalism that could be tested by helioseismology. For hydrogen and

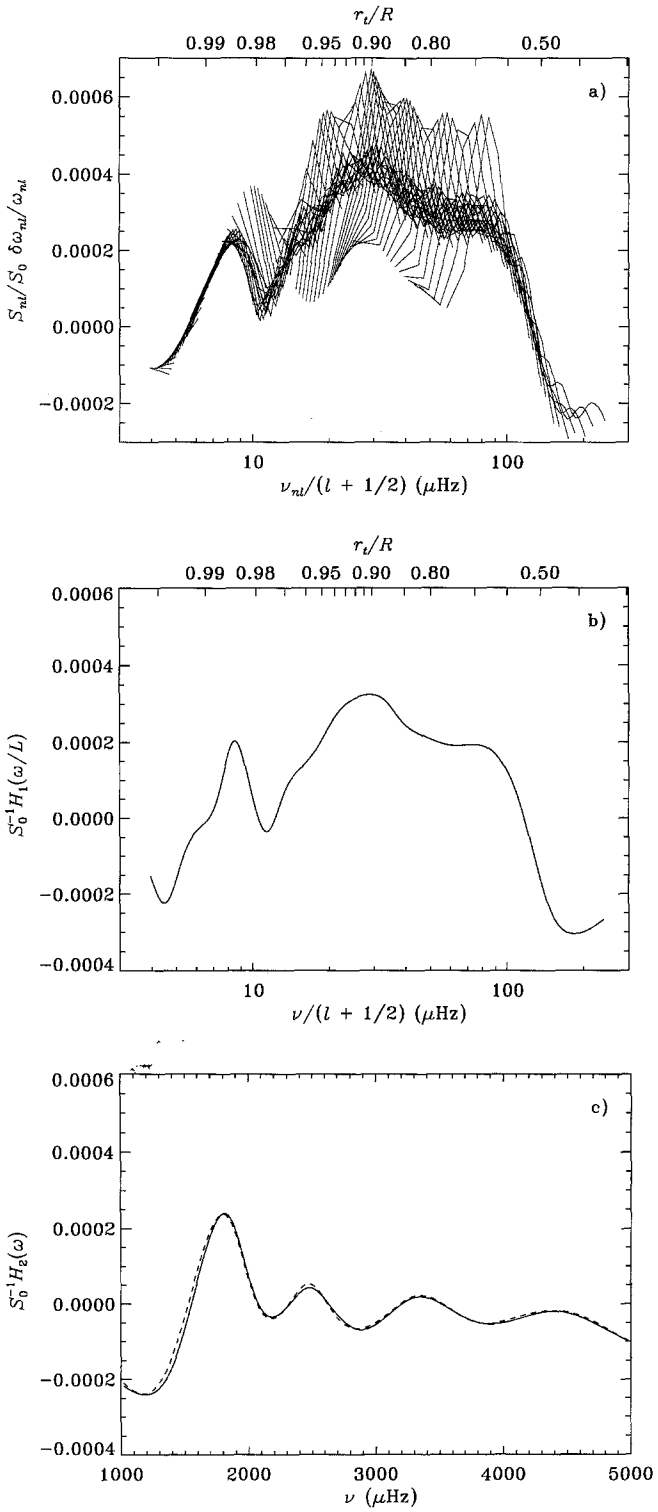
r_t/R
0.99 0.98 0.95 0.90 0.80 0.50
a)
$S_{nl}/S_0\ \delta\omega_{nl}/\omega_{nl}$
0.0006
0.0004
0.0002
0.0000
−0.0002
10
100
$\nu_{nl}/(l + 1/2)$ (μHz)
r_t/R
0.99 0.98 0.95 0.90 0.80 0.50
b)
$S_0^{-1}H_1(\omega/L)$
0.0006
0.0004
0.0002
0.0000
−0.0002
−0.0004
10
100
$\nu/(l + 1/2)$ (μHz)
c)
$S_0^{-1}H_2(\omega)$
0.0006
0.0004
0.0002
0.0000
−0.0002
−0.0004
1000
2000
3000
4000
5000
ν (μHz)

helium, the signature is hidden beneath the Coulomb correction, which is of course the fortunate circumstance that makes the CEFF equation of state useful.

Relative differences between p and Γ_1, in the sense MHD(F) – MHD(S), at fixed (ρ, T) in Model MS1, are shown in Fig. 20. Since MHD(S) and MHD(F) treat hydrogen and helium in the same way, the differences are relatively small in the hydrogen and helium ionization zones; this is unlike the cases considered previously. The dominant effects are associated with the ionization zones of heavier elements. This is reflected in the differences in Θ, shown in Fig. 21. Thus in this case we see potentially observable effects of what must be considered fine details of the physics of the solar plasma. We note that the modulation of Θ due to the ionization of heavy elements was discussed by Däppen and Gough (1984). Indeed, it might be recorded that already then Gough (*private communication*) believed in the possibility of a helioseismic probing of this effect.

Whether or not such effects can be observed in practice obviously depends on the extent to which they affect the structure of the Sun and hence its oscillation frequencies. Figure 22 shows differences between Models M1 and MS1, computed with MHD(F) and MHD(S), respectively. It is evident that the dominant effects are now associated with deeper-lying ionization zones, giving rise to a complex structure in the differences. Nonetheless, it is still the case that $\delta\Gamma_1$ between the models reflects the purely thermodynamical differences shown in Fig. 20, although to a lesser extent than for the cases considered in Sects. 4.2.1 and 4.2.2. The complicated variation of the model differences gives rise to a similarly complex behaviour of the corresponding frequency differences, shown in Fig. 23.

In fact, the asymptotic separation in Eq. (4.4) is less successful in this cases than for the differences between the EFF and CEFF, or the MHD(S) and CEFF, models. This is illustrated by the difference shown in Fig. 23c between $H_2(\omega)$ obtained from fits over the full and the restricted range in ν/L. This failure of asymptotics is no doubt caused by the comparatively sharp features in δc and $\delta\Gamma_1$, located at considerable depth. On the other hand, it is evident that the variation of $H_1(\omega/L)$ shown in Fig. 23b to some extent reflects $\delta c/c$.

It should be noted that the frequency differences obtained here, although certainly small, are nevertheless considerably larger than the errors in the currently most precisely determined observed frequencies. This offers considerable hope that, particularly with coming improvements in the observed data, it will be possible to investigate the properties of the equation of state to this level of detail. Libbrecht (1992) made an estimate of the limiting accuracy of solar p-mode frequency determinations; he found that with three years of continuous observations, a relative accuracy $\sigma(\nu_{nlm})/\nu_{nlm}$, for individual frequencies ν_{nlm}, of about 1.4×10^{-5} should be achievable. Assuming that the effects of departures from spherical symmetry are small, it should be possible

Fig. 19. a Asymptotically scaled relative frequency differences (cf. Eq. [4.4]), between Models MS1 and C1′ computed with the MHD(S) and CEFF equations of state, respectively, in the sense (Model MS1) – (Model C1′). Points corresponding to the same value of the degree l have been connected. The lower abscissa gives $\nu_{nl}/(l + 1/2)$, where ν_{nl} is the cyclic frequency; the upper abscissa shows the corresponding fractional turning-point position r_t/R, which is related to $\nu_{nl}/(l + 1/2)$ through Eq. (2.29). **b** The function $H_1(\omega/L)$ resulting from the asymptotic fit in Eq. (4.4) to the differences shown in panel **a**. **c** The function $H_2(\omega)$ resulting from the fit, shown against cyclic frequency ν. The solid curve shows the result of the fit to the full mode set, whereas the dashed curve is based on a fit to the modes with $20\,\mu\text{Hz} \leq \nu_{nl}/L \leq 50\,\mu\text{Hz}$

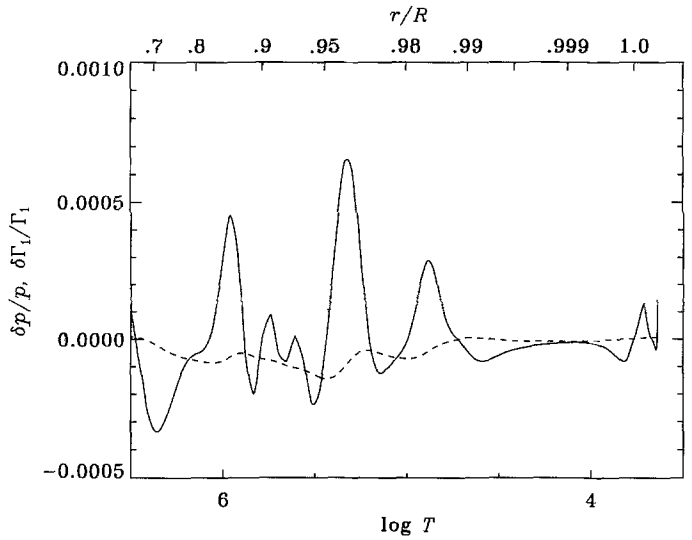

Fig. 20. Relative differences between values of pressure p (·····) and adiabatic exponent Γ_1 (————) evaluated with the full [MHD(F)] and the stripped [MHD(S)] version of the MHD equation of state, in the sense [MHD(F)] – [MHD(S)]. The quantities were computed at the conditions (ρ, T) defined by the envelope Model MS1 (cf. Table 1). The lower abscissa shows $\log T$, the upper abscissa the fractional radius r/R in the model

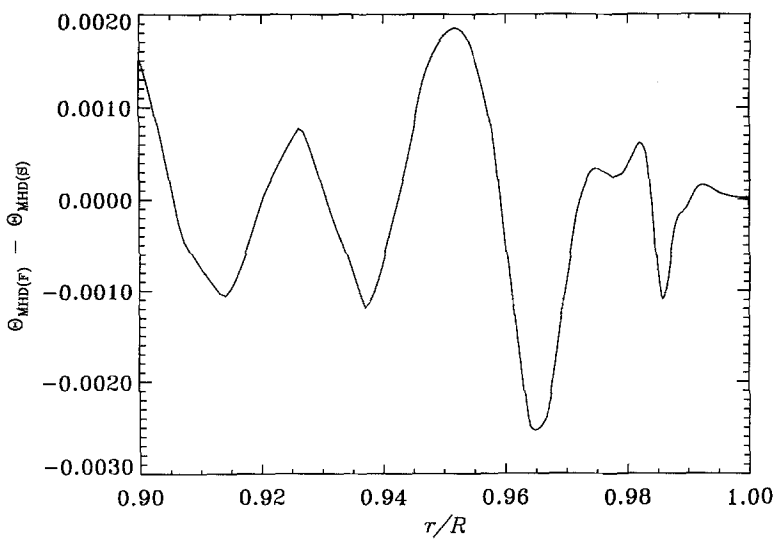

Fig. 21. Difference between the function Θ (cf. Eq. [4.8]), as evaluated with the full [MHD(F)] and the stripped [MHD(S)] versions of the MHD equation of state, at the conditions (ρ, p) defined by the envelope Model MS1 (cf. Table 1). The difference is in the sense [MHD(F)] – [MHD(S)]

to determine the m-averaged frequencies ν_{nl}, which reflect the spherically symmetric component of solar structure, with an error that is smaller by roughly a factor $\sqrt{2l+1}$. Hence relative errors in ν_{nl} of order 10^{-6} do not seem unrealistic. This appears to

be amply sufficient to study the equation of state at the level of detail exemplified by the difference between MHD(S) and MHD(F).

4.2.4 Other properties of the model

Although the main emphasis here is on the effects of the equation of state, it is of interest to consider also the sensitivity of the frequencies to other assumed properties of the model. It was argued in Sect. 2.1.2 that the structure of the convection zone is determined largely by the equation of state, the composition and the value of the specific entropy. In this subsection we illustrate the dependence of the envelope model and its frequencies on the helium abundance and on the value of the mixing-length parameter α_C which determines the specific entropy. There is an additional influence on the structure of the envelope of the assumed properties of the solar atmosphere; such effects are discussed briefly in Sect. 4.3, in connection with a comparison between the observed and the computed frequencies. It should be noted that, if the equation of state and the atmospheric structure are assumed to be fixed, any changes of the structure of the convective envelope and of the frequencies of modes trapped entirely within it can be obtained as linear combinations of the differences illustrated in this subsection, provided that the differences are sufficiently small that they can be linearized in the change in Y and α_C.

Figure 24 shows the changes resulting at fixed thermodynamic conditions, defined by the structure of Model C1, if Y is reduced by 0.005. In panel (a) relative differences in p and Γ_1 are shown, at fixed (ρ, T). It should be noticed that here, unlike the cases of changing the equation of state discussed in Sects. 4.2.1 – 4.2.3, there are substantial changes in p also outside the ionization zones; indeed, it follows from Eq. (3.7) that $(\delta p/p)_{(\rho,T)} \simeq -\delta\mu/\mu \simeq -0.76\delta Y$ in the region of full ionization; this is in approximate agreement with panel (a). From Eq. (4.1) and Fig. 8 one might now expect substantial differences between the changes in Γ_1 at fixed (ρ, T) and at fixed (ρ, p); this is confirmed by comparing panel (a) with panel (b) which shows differences in T and Γ_1 at fixed (ρ, p).

The effect of the decrease in Y on the function Θ defined in Eq. (4.8), evaluated at given (ρ, p) in Model C1, is illustrated in Fig. 25. It is evident that the dominant effect is associated with the second helium ionization zone. This graphically illustrates the sensitivity of Θ as a measure of the helium abundance.

Figure 26a shows how a decrease in the helium abundance by 0.005 affects the sound speed and Γ_1; as before, α_C was chosen such as to fix the depth of the convection zone to $0.287R$. Results are shown only for the outer parts of the convection zone; deeper in the convection zone the changes are considerably smaller. The largest effect on c is in the atmosphere and in the hydrogen and first helium ionization zones; however, there is also a substantial effect on c, and even more so on Γ_1, in the second helium ionization zone. It is interesting that even in this case the change in Γ_1 appears to be dominated by the intrinsic change, at fixed (ρ, p), shown in Fig. 24b; the only exception is the substantial peak in $(\delta\Gamma_1/\Gamma_1)_{(\rho,p)}$ at $\log T \simeq 4$, no doubt associated with the hydrogen ionization zone, which has no obvious counterpart in Fig. 26a.

The changes in the oscillation frequencies resulting from the model differences are illustrated in terms of the asymptotic separation (4.4) in Fig. 27; here H_1 was obtained from the full mode set, whereas for H_2 only those modes with $20\,\mu\text{Hz} \leq \nu/L \leq 50\,\mu\text{Hz}$ were used. Disregarding modes penetrating beyond the convection

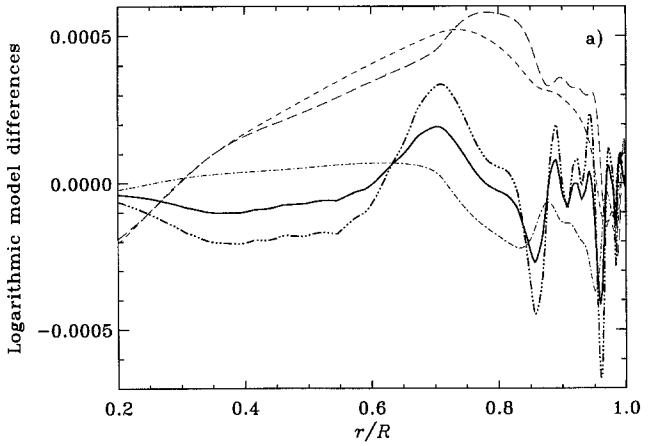
a)
0.0005
0.0000
−0.0005
Logarithmic model differences
0.2
0.4
0.6
0.8
1.0
r/R

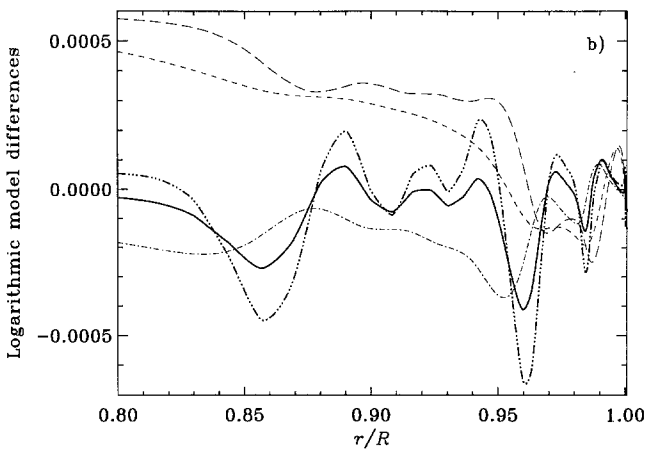
b)
0.0005
0.0000
−0.0005
Logarithmic model differences
0.80
0.85
0.90
0.95
1.00
r/R

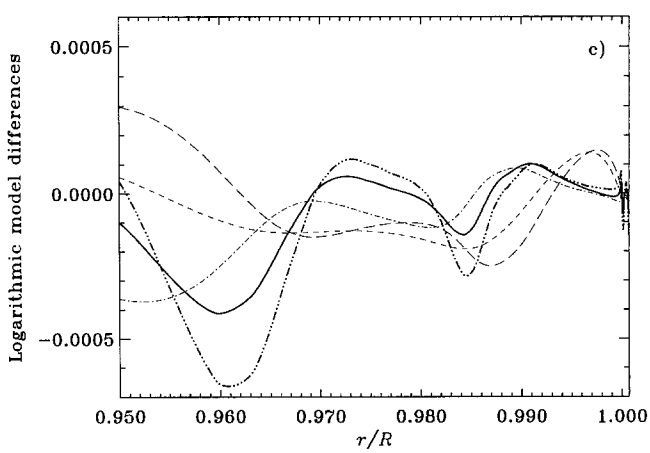
c)
0.0005
0.0000
−0.0005
Logarithmic model differences
0.950
0.960
0.970
0.980
0.990
1.000
r/R

zone, it is evident that the behaviour of H_1 is dominated by the change in c in the ionization zones, H_1 being essentially constant for modes whose lower turning point is deeper than the second helium ionization zone. H_2 is dominated by an oscillatory behaviour at frequencies below approximately $3000\,\mu$Hz. As shown by Christensen-Dalsgaard and Pérez Hernández (1988, 1991, 1992) this arises principally as a result of the relatively sharp change in Γ_1 in the second helium ionization zone.

Figure 26b shows effects of increasing α_C by 0.04, corresponding to an increase in the depth of the convection zone of about $0.003R$. The change in the thermodynamic state brought about by modifying the specific entropy changes c and Γ_1, although again predominantly in the ionization zones of hydrogen and helium; the changes are smaller in the remainder of the convection zone. In the radiative interior, the modification in c is substantially larger as a result of the increased depth of the convection zone; however, here we mainly concentrate on modes trapped within the convection zone. The changes in frequency are shown in Fig. 27, in terms of $H_1(\omega/L)$ and $H_2(\omega)$ determined as before. Again, $H_1(\omega/L)$ is dominated by the changes in the ionization zones for modes trapped in the convection zone; for modes penetrating beyond it H_1 increases rapidly with increasing penetration depth due to a sharp positive feature in δc just beneath the convection zone, resulting from the increase in its depth. The variation in H_1 associated with the ionization zones is superficially similar to, but different in detail from, the effect of changing the helium abundance. The same is true of $H_2(\omega)$. There is an oscillatory component arising from the sharp variation of Γ_1 in the second helium ionization zone, but unlike the case of modifying Y there is also a substantial slowly varying component; this may be caused by the somewhat more pronounced change in c in the hydrogen and first helium ionization zones. The details of the behaviour of H_2 can in principle be understood in terms of the behaviour of the kernels which relate H_2 to $\delta c/c$ and $\delta\Gamma_1/\Gamma_1$ (see Christensen-Dalsgaard and Pérez Hernández 1992); however, such an analysis is beyond the scope of this paper.

The results obtained here are of considerable interest in connection with attempts at helioseismic determination of the helium abundance in the solar convection zone. In particular, the helium hump method (cf. Sect. 4.1.2) is based on fitting to a grid of envelope models with varying Y and α_C the function W computed from the sound speed inferred from inversion of the observed frequencies. Hence it requires linear independence of the effects of modifications in Y and α_C on the changes in the relevant aspects of the oscillation frequencies. If the inversion is carried out by means of the differential asymptotic method in Eq. (2.43), this requirement translates into independence of the H_1 resulting from the two types of modification. Indeed it is clear from Fig. 27 that the behaviour of H_1 is somewhat different in the two cases, suggesting that a fit is possible. This was in fact found to be the case by Däppen et al. (1988) when testing the method on artificial data analyzed by means of asymptotic differential inversion, and assuming the equation of state to be known. Additional information about Y and α_C is contained in $H_2(\omega)$. From Fig. 27b it appears that

Fig. 22a–c. Logarithmic differences between Models M1 and MS1 computed with the MHD(F) and MHD(S) equations of state, respectively, in the sense (Model M1) – (Model MS1). The quantities plotted are $\delta \ln p$ (- - - - - - - - - - - -); $\delta \ln \rho$ (— — — — — —); $\delta \ln T$ (— · — · — · —); $\delta \ln \Gamma_1$ (— · · · — · · · — · · ·); and $\delta \ln c$ (————————). The abscissa is fractional radius r/R. **a** The complete envelope model; **b** behaviour in the outer layers of the model; **c** behaviour in the outmost layers of the model

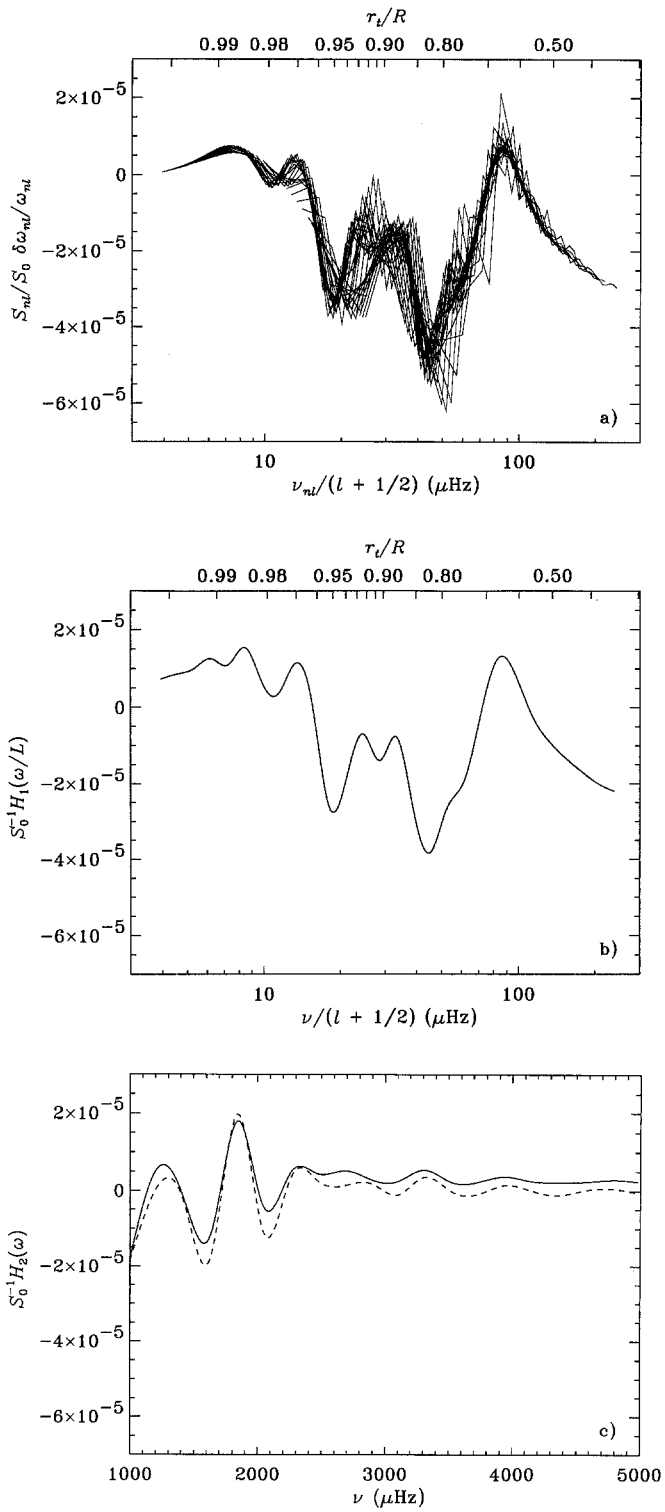
r_t/R
0.99 0.98 0.95 0.90 0.80 0.50
2×10^{-5}
0
-2×10^{-5}
-4×10^{-5}
-6×10^{-5}
$S_{nl}/S_0\ \delta\omega_{nl}/\omega_{nl}$
a)
10
100
$\nu_{nl}/(l + 1/2)$ (μHz)
r_t/R
0.99 0.98 0.95 0.90 0.80 0.50
2×10^{-5}
0
-2×10^{-5}
-4×10^{-5}
-6×10^{-5}
$S_0^{-1}H_1(\omega/L)$
b)
10
100
$\nu/(l + 1/2)$ (μHz)
2×10^{-5}
0
-2×10^{-5}
-4×10^{-5}
-6×10^{-5}
$S_0^{-1}H_2(\omega)$
c)
1000
2000
3000
4000
5000
ν (μHz)

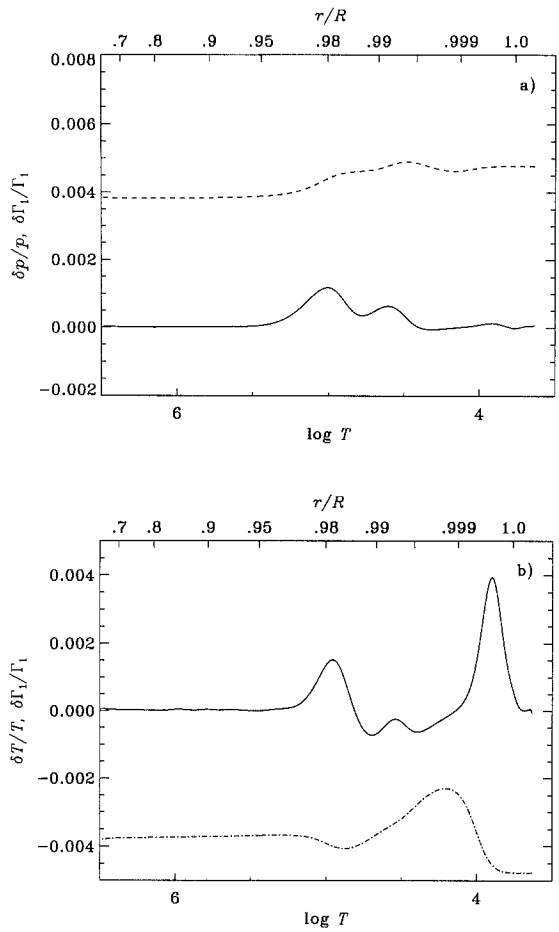

Fig. 24a,b. The effect on the thermodynamic state of a decrease $\delta Y = -0.005$ in the helium abundance, evaluated with the CEFF equation of state in Model C1. **a** Relative differences at fixed (ρ, T) in pressure p (------) and adiabatic exponent Γ_1 (————), in the sense (reduced helium) − (default case). **b** Corresponding relative differences at fixed (ρ, p) in temperature T (— · — · — · —) and Γ_1 (————). The lower abscissa shows $\log T$, the upper abscissa the fractional radius r/R in the model

the H_2 resulting from changing Y and α_C are rather more independent than is the case for H_1, particularly if modes with frequencies as low as 1000 μHz are included in the analysis. It must be kept in mind, however, that H_2 is only determined to

Fig. 23. a Asymptotically scaled relative frequency differences (cf. Eq. [4.4]), between Models M1 and MS1 computed with the MHD(F) and MHD(S) equations of state, respectively, in the sense (Model M1) − (Model MS1). Points corresponding to the same value of the degree l have been connected. The lower abscissa gives $\nu_{nl}/(l+1/2)$, where ν_{nl} is the cyclic frequency; the upper abscissa shows the corresponding fractional turning-point position r_t/R, which is related to $\nu_{nl}/(l+1/2)$ through Eq. (2.29). **b** The function $H_1(\omega/L)$ resulting from the asymptotic fit in Eq. (4.4) to the differences shown in panel **a**. **c** The function $H_2(\omega)$ resulting from the fit, shown against cyclic frequency ν. The solid curve shows the result of the fit to the full mode set, whereas the dashed curve is based on a fit to the modes with 20 μHz $\leq \nu_{nl}/L \leq$ 50 μHz

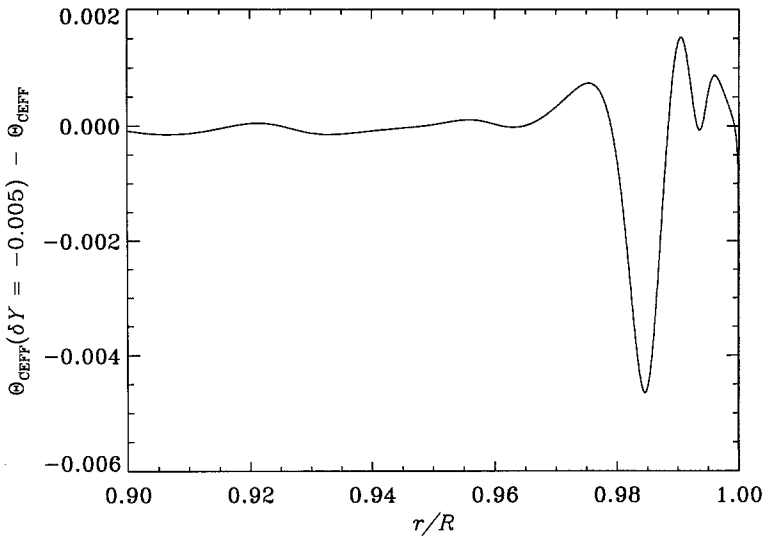

Fig. 25. Change in the function Θ (cf. Eq. [4.8]), resulting from a decrease $\delta Y = -0.005$ in the helium abundance, evaluated with the CEFF equation of state at the conditions (ρ, p) defined by the envelope Model C1 (cf. Table 1)

within a slowly varying function of frequency, associated with the uncertainties in the treatment of the superficial layers of the Sun (cf. Sect. 4.1.1).

The possibility of determining the solar envelope helium abundance from analysis of the behaviour of the Duvall phase $\alpha(\omega)$, the related Vorontsov phase function $\beta(\omega)$ or other similar properties of the oscillation frequencies has been considered in a number of investigations. Baturin and Mironova (1990) analyzed the effect on β of changes in the helium abundance. From a similar analysis of the observed frequencies, Vorontsov et al. (1991) inferred that $Y \simeq 0.25$. Christensen-Dalsgaard and Pérez Hernández (1991) attempted to estimate the solar envelope helium abundance from a fit of $H_2(\omega)$ obtained from differences between solar frequencies and those of a reference model, to the H_2 resulting from a change in Y, obtaining a value similar to that of Vorontsov et al. (1991). More generally, helioseismic determinations of Y can be carried out by means of inversion techniques which do not impose the asymptotic behaviour of the frequencies. Dziembowski et al. (1991) carried out a least-squares fit to differences between solar frequencies and those of a reference model of corrections to both the ratio p/ρ and the helium abundance, to obtain a solar $Y \simeq 0.23$. Däppen et al. (1991) performed an inversion by means of optimally localized averages (cf. Sect. 2.3.3) to obtain the difference between the solar Y and that of a reference model; their result, based on data similar to those used by Dziembowski et al., was $Y \simeq 0.27$. A detailed analysis of these inversion techniques, to evaluate their sensitivity to the various parameters entering the references model and the inversion methods, was carried out by Kosovichev et al. (1992).

A general problem with these determinations is that in all techniques Y is measured through its effect on Γ_1; hence the result is sensitive to details of the equation of state. Indeed, Kosovichev et al. (1992) found that the equation of state, and the assumed detailed composition of the heavy elements, was the major source of uncertainty in helioseismic determinations of Y. This is illustrated by a comparison of

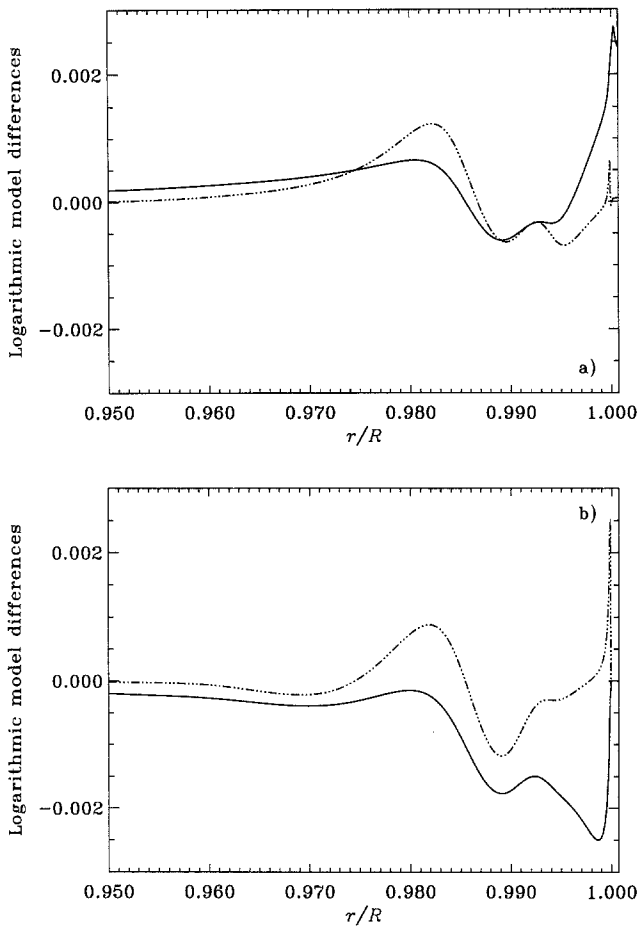

Fig. 26a,b. The effects on the structure of changing the helium abundance or the mixing-length parameter α_C. The quantities plotted are $\delta \ln \Gamma_1$ (—·····—·····—·····) and $\delta \ln c$ (————————). The abscissa is fractional radius r/R. **a** Differences between Model C2 with a helium abundance $Y = 0.260$ and the reference Model C1, with $Y = 0.265$, in the sense (Model C2) – (Model C1). **b** Differences between Model C3, with increased α_C, and Model C1, in the sense (Model C3) – (Model C1)

Fig. 27 with the results presented in Sects. 4.2.1 – 4.2.3. It is evident that the effects of a change of 0.005 in Y are far smaller than the H_1 and H_2 resulting from going from the EFF to the CEFF equation of state. Although this change presumably drastically overestimates the uncertainty in current equations of state, Fig. 19 shows that even the change from the CEFF equation of state to the MHD(S) formulation causes H_1 and H_2 of a somewhat greater magnitude than those resulting from the change in Y, although with a different detailed behaviour. On the other hand, the differences between MHD(F) and MHD(S) give rise to H_1 and H_2 that are smaller by approximately a factor four than the effect of a change of Y by 0.005, suggesting that this level of uncertainty in the equation of state would introduce errors of order 10^{-3} in the helioseismic determination of Y. This is roughly consistent with the results obtained by Kosovichev et al. (1992) [note that the equations of state here labelled MHD(S) and MHD(F) correspond to MHD3 and MHD5 of Kosovichev et al.].

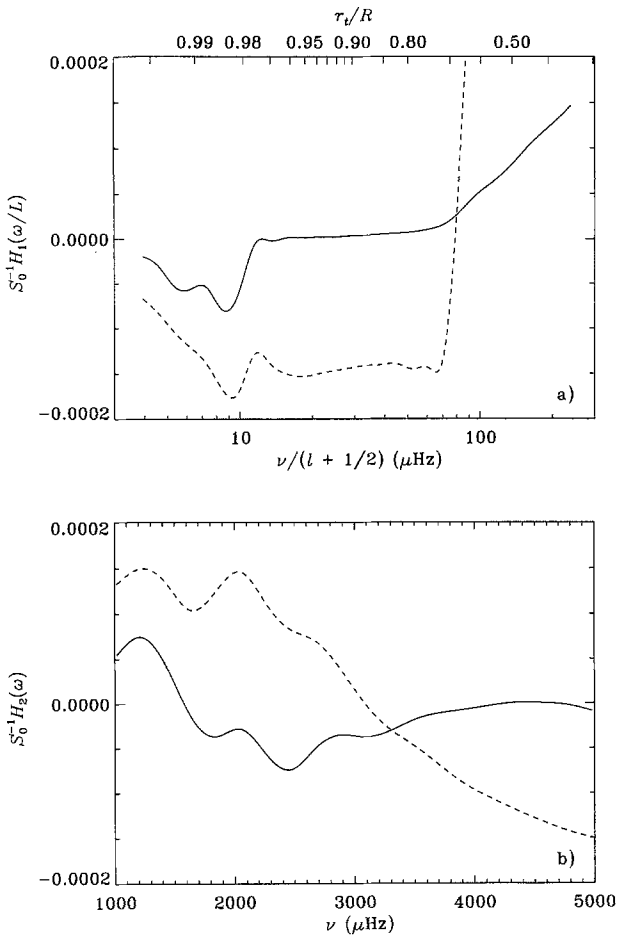

Fig. 27a,b. The effects on the frequencies of changing the helium abundance or the mixing-length parameter α_C, illustrated in terms of the functions H_1 and H_2 resulting from the asymptotic fit in Eq. (4.4). **a** $H_1(\omega/L)$ obtained from the frequency differences for reduced helium abundance ([Model C2] – [Model C1]) (————) and for increased mixing-length parameter ([Model C3] – [Model C1]) (·····). Here the full mode set was used. The lower abscissa gives $\nu_{nl}/(l + 1/2)$, where ν_{nl} is the cyclic frequency; the upper abscissa shows the corresponding fractional turning-point position r_t/R, which is related to $\nu_{nl}/(l + 1/2)$ through Eq. (2.29). **b** Corresponding functions $H_2(\omega)$, using the same line styles as in panel **a**, but based on a fit including only those modes with $20\,\mu\text{Hz} \leq \nu_{nl}/L \leq 50\,\mu\text{Hz}$

An important goal is evidently to assess the extent to which uncertainties in the equation of state can be separated from the uncertainty in the value of Y and the specific entropy, hence allowing the use of observed frequencies both to determine Y and to investigate the properties of the equation of state. This requires further careful investigation, however.

4.3 Comparison with observed frequencies

The central issue of this paper is evidently the extent to which the computed models match the observed frequencies, and the sensitivity of the match to the assumed properties of the equation of state. The simplest form of such an analysis is to make a direct comparison of the observed frequencies with frequencies computed under different assumptions. At a somewhat higher level of sophistication, one may attempt to construct combinations of the frequencies that are sensitive to specific aspects of the model or the physics; examples are the Vorontsov phase function $\beta(\omega)$ (cf. Eq. [2.33]), the functions H_1 and H_2 resulting from fitting the asymptotic expression (4.4) to frequency differences between the Sun and a reference model, or the frequency separations between low-degree modes discussed in Sect. 4.4. More complete information about solar structure can be obtained from performing detailed inverse analyses, as discussed in Sect. 2.3; however, it is not evident that the results will necessarily provide more information about the physics of the solar interior, in particular the equation of state, than do the simpler comparisons. As discussed in Sect. 2.3.1 one may eventually be able to carry out tertiary inversions aimed specifically at isolating properties of the physics; such analyses have apparently not been carried out so far for the equation of state, however.

Here we concentrate on the comparisons of frequencies and simple derived quantities, specifically H_1 and H_2 between observations and models. To illustrate the ability of the observations to distinguish between different formulations of the physics, we consider in some detail results for some of the models discussed in Sect. 4.2. Frequencies for these models are compared with observed frequencies from the compilation by Libbrecht et al. (1990). In addition, we provide a brief review of other, similar investigations.

An additional uncertainty in the comparisons is introduced by our incomplete knowledge about the properties of the solar surface layers. To indicate their possible effect on the analysis of the observations we consider models computed both with the CT and the LAOL opacities. For the present purpose the most significant difference between these tables is that the LAOL values are larger by approximately a factor two at conditions corresponding to the solar atmosphere. This introduces substantial differences in the superficial layers of the model, while having very minor effects in the interior of the solar convection zone (see Christensen-Dalsgaard [1990b] for a more detailed analysis). As before, the mixing-length parameter is fixed by requiring that the depth of the convection zone is $0.287R$.

Figure 28 shows frequency differences, scaled in the manner of Eq. (4.3), between the observations and models computed with the EFF and CEFF equations of state, and the CT and LAOL opacities. It is immediately obvious that there are considerable differences, depending on the physics used in the computations. In the models computed with the EFF equation of state there is a substantial variation with l in the frequency difference at given frequency; this reflects a dependence of the frequency differences on the location of the lower turning point, as a result of errors in the interior of the model. It is clear from panels (a) and (c) of the figure that this effect is much reduced if the CEFF equation of state is used. On the other hand, going from the CT to the LAOL opacities predominantly changes the frequency dependence of the frequency differences; they vary less with frequency, and are generally smaller, in the LAOL case.

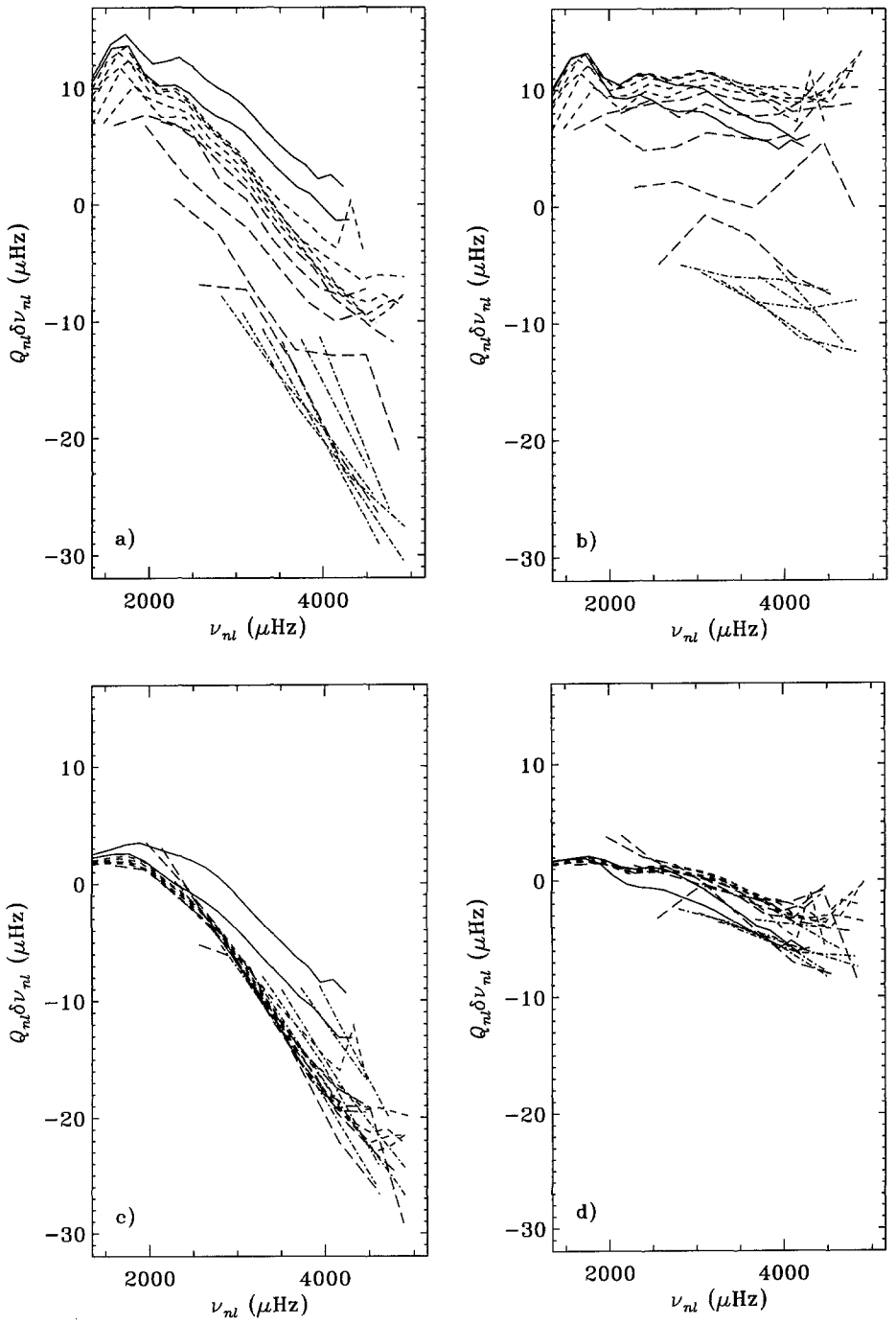
a)
b)
c)
d)
10
0
−10
−20
−30
2000
4000
$Q_{nl}\delta\nu_{nl}$ (μHz)
ν_{nl} (μHz)

These effects become clearer if the asymptotic separation in Eq. (4.4) is carried out. Since we are mainly interested in the qualitative behaviour of the result, we have for simplicity used a uniform weight in the least-squares fit implicit in the separation; a preferable procedure would have been to base the weight on the estimated error in each observed frequency. We first consider, in Fig. 29, the details of the analysis for the case of using the the EFF equation of state and the LAOL opacities. Figure 29a shows asymptotically scaled frequency differences, plotted against ν/L; already here the separate dependence on ν/L and ν is quite evident. After performing the spline fit over the entire mode set and subtracting $H_2(\omega)$ we obtain the residuals shown in Fig. 29b; although there remains some scatter, it is clear that we have succeeded in isolating what is predominantly a function of ν/L. Similarly, after subtraction of the fitted $H_1(\omega/L)$ we obtain a residual that is predominantly a function of ν, as illustrated Fig. 29c; here we restricted the fit to the modes in the interval $20\,\mu\text{Hz} \leq \nu/L \leq 50\,\mu\text{Hz}$, in accordance with the discussion in Sect. 4.1.1 (this mode set is used for the subsequent comparisons of H_2 as obtained for different reference models).

Figure 30 compares H_1 for the four different cases shown in Fig. 28. In addition, we include H_1 as obtained by using as reference models Models M1 and M2 computed with the full MHD equation of state [results computed with the stripped-down version MHD(S) would be indistinguishable on this scale]. It is evident that for modes trapped in the convection zone (with $r_t \gtrsim 0.71R$) the choice of opacity table has relatively little effect on H_1. This is in accordance with the fact that the opacity does not directly influence the structure of the bulk of the convection zone; as discussed below, the effect on the superficial layers of the Sun is absorbed into $H_2(\omega)$. Modes that penetrate more deeply sense the effects of the opacity differences in the radiative region beneath the convection zone. On the other hand, there is evidently a substantial effect on H_1 of the choice of equation of state. For the models computed with the EFF equation of state, H_1 varies considerably when the turning point is within the convection zone; this indicates, according to Eq. (2.37) that there are significant differences between the sound speed in the Sun and in the model. On the other hand, when models based on the CEFF equation of state are used, H_1 is essentially constant for the modes probing the convection zone; it follows from Eq. (2.43) that δc is small. Hence the CEFF equation of state achieves a better representation of the properties of the solar plasma than does the EFF formulation. The difference between the results using CEFF and those obtained with MHD(F) are substantially smaller, as expected. It is interesting that the CEFF models are apparently in better agreement with the solar data than are the models computed with MHD. Little significance can be attached to this result at present, however.

Fig. 28a–d. Frequency differences, scaled by the inertia ratio Q_{nl} (cf. Eq. [4.3]), between observed frequencies in the compilation by Libbrecht et al. (1990) and four sets of computed frequencies, in the sense (observation) – (theory). The abscissa is cyclic frequency ν_{nl}. The points have been connected with lines according to the value of the degree l: $l = 20, 30$: ——————; $l = 40, 50, 60, 80, 100$: ·····; $l = 120, 150, 200, 300, 400$: – – – – – – –; and $l = 500, 600, 700, 800, 900, 1000$: —·—·—·—. The models are distinguished by their equation of state and opacity, as described in Table 1. **a** Model E1 (EFF equation of state, CT opacity); **b** Model E2 (EFF equation of state, LAOL opacity); **c** Model C1 (CEFF equation of state, CT opacity); **d** Model C2 (CEFF equation of state, LAOL opacity)

A similar conclusion is reached from consideration of the $H_2(\omega)$ obtained from the fit, illustrated in Fig. 31. In the cases where the EFF equation of state was used there is a substantial oscillatory component of H_2; it follows from the results presented in Sect. 4.2 that such a component would result from rapidly varying differences between the Sun and a model, in the region of second He ionization. In contrast, for the models computed with the CEFF equation of state the H_2 are dominated by a slowly varying component, indicating again that the CEFF equation of state is the better. The results obtained with the MHD(F) models are similar to those obtained using CEFF, although they differ in detail. Both for CEFF and MHD(F) there remains a small rapidly varying component, although it appears to have opposite sign in the two cases. This could evidently be due to remaining errors in the equation of state. Alternatively, it may reflect a deviation of the assumed helium abundance of 0.265, or the specific entropy obtained from the assumed depth of the convection zone, from the actual values in the solar envelope. The effects of changing Y or α_C may be estimated from the curves shown in Fig. 27b. The oscillatory component in H_2 for the [MHD(F), LAOL] case in Fig. 31 can in fact be reduced considerably by subtracting three times the H_2 resulting from a change of Y by -0.005 (the solid curve in Fig. 27b). This suggests that the solar helium abundance is closer to 0.25; indeed, the estimate of $Y \simeq 0.25$ made by Christensen-Dalsgaard and Pérez Hernández (1991) was based on precisely this type of analysis. In contrast, it appears more difficult to suppress the oscillatory component in H_2 obtained with the (CEFF, LAOL) reference model by a simple change in Y; also, the oscillatory components apparently cannot be substantially reduced by changes in α_C. It is evident that these results can only be regarded as indicative; a proper analysis along these lines requires consideration of combinations of changes in Y and α_C, and a precise method for defining the oscillatory component of H_2 (Christensen-Dalsgaard and Pérez Hernández, in preparation); we recall also that Vorontsov et al. (1992) have introduced a procedure for isolating the rapidly varying component of the Duvall phase.

The behaviour of H_2 is evidently strongly affected by the choice of opacity tables. This effect arises solely from the modification of the structure of the atmosphere and outermost, significantly superadiabatic, part of the convection zone. As discussed in Sect. 4.1.1 the result of such a modification is a component of H_2 which varies slowly with frequency (see also Christensen-Dalsgaard and Pérez Hernández 1991; Vorontsov et al. 1992). This component is substantially larger for the models based on the CT opacity tables than for those using the LAOL tables, hence accounting for the larger frequency differences obtained in Fig. 28 for the CT models. Although this might suggest that the LAOL tables are to be preferred over the CT tables, such

Fig. 29a–c. Asymptotic analysis of the differences between the observed frequencies and the computed frequencies for Model E2 (EFF, LAOL), i.e., the case shown in Fig. 28b. **a** Asymptotically scaled relative frequency differences (cf. Eq. [4.4]). Points corresponding to the same value of the degree l have been connected. The lower abscissa gives $\nu_{nl}/(l + 1/2)$, where ν_{nl} is the cyclic frequency; the upper abscissa shows the corresponding fractional turning-point position r_t/R, which is related to $\nu_{nl}/(l + 1/2)$ through Eq. (2.29). **b** Residual after subtraction of the function $H_2(\omega_{nl})$ resulting from the asymptotic fit in Eq. (4.4), for all modes in the set; the abscissas are as in panel **a**. **c** Residual after subtraction of the fitted $H_1(\omega_{nl}/L)$, plotted against cyclic frequency ν_{nl}; the fit and the plot include only those modes with $20\,\mu\text{Hz} \leq \nu_{nl}/L \leq 50\,\mu\text{Hz}$

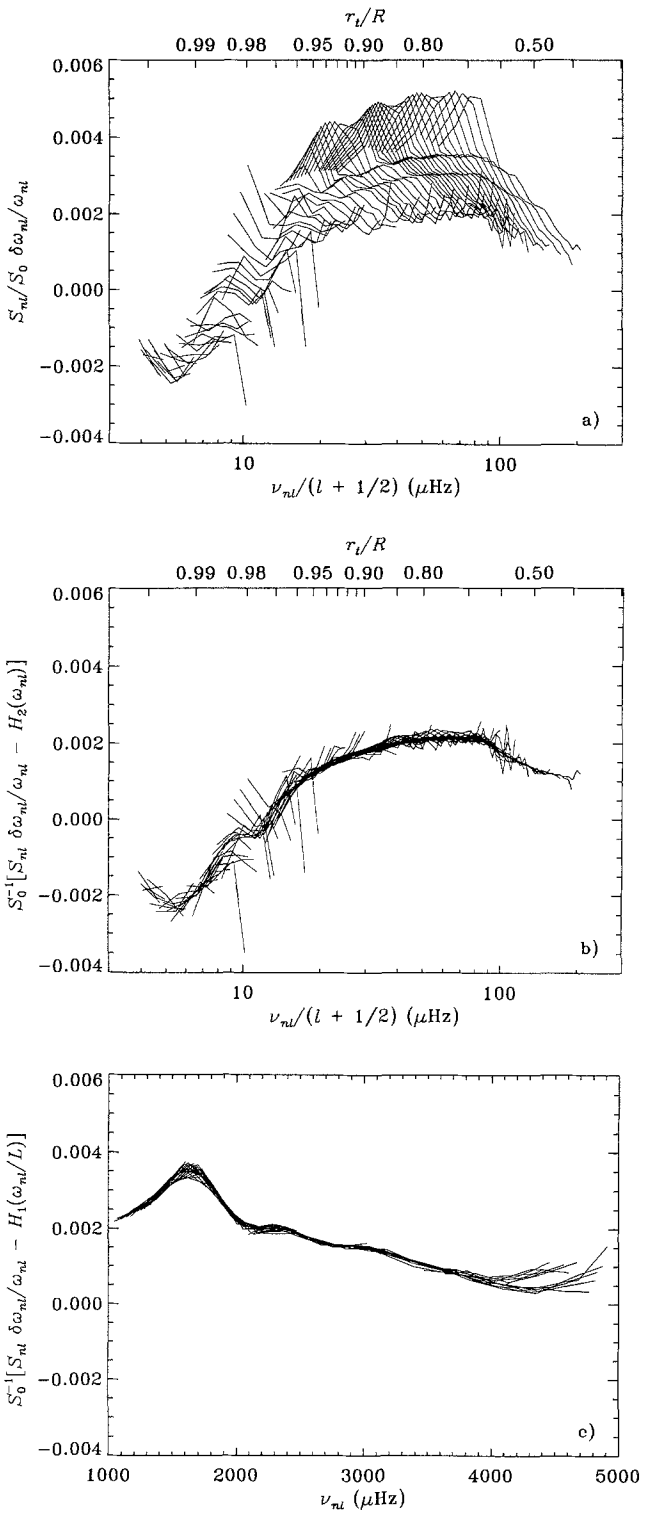
r_t/R
0.99 0.98 0.95 0.90 0.80 0.50
0.006
0.004
0.002
0.000
−0.002
−0.004
$S_{nl}/S_0\ \delta\omega_{nl}/\omega_{nl}$
a)
10
100
$\nu_{nl}/(l + 1/2)$ (μHz)
r_t/R
0.99 0.98 0.95 0.90 0.80 0.50
$S_0^{-1}[S_{nl}\ \delta\omega_{nl}/\omega_{nl} - H_2(\omega_{nl})]$
b)
10
100
$\nu_{nl}/(l + 1/2)$ (μHz)
$S_0^{-1}[S_{nl}\ \delta\omega_{nl}/\omega_{nl} - H_1(\omega_{nl}/L)]$
c)
1000
2000
3000
4000
5000
ν_{nl} (μHz)

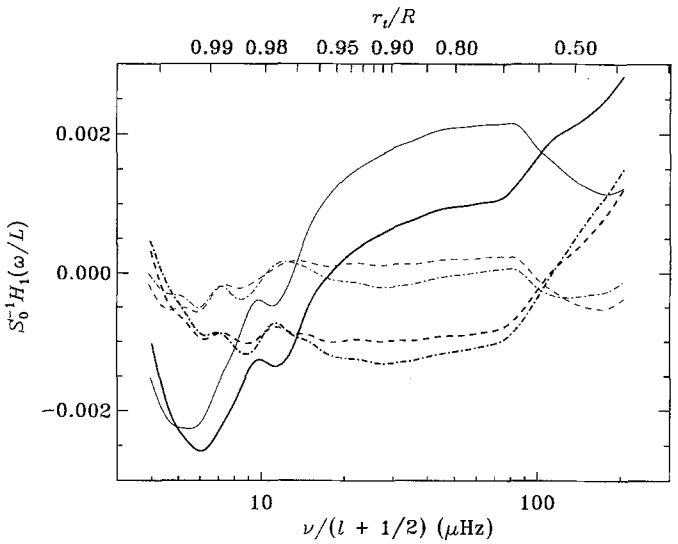

Fig. 30. The function $H_1(\omega/L)$ resulting from the asymptotic fit in Eq. (4.4) to differences between the observed frequencies of Libbrecht et al. (1990) and various sets of computed frequencies, in the sense (observation) – (theory). The full mode set was used. The lower abscissa gives $\nu_{nl}/(l + 1/2)$, where ν_{nl} is the cyclic frequency; the upper abscissa shows the corresponding fractional turning-point position r_t/R, which is related to $\nu_{nl}/(l + 1/2)$ through Eq. (2.29). The models are distinguished by the equation of state and opacity (see also Table 1), as indicated by the line style: Model E1 (EFF, CT) (————); Model E2 (EFF, LAOL) (————); Model C1 (CEFF, CT) (·····); Model C2 (CEFF, LAOL) (----------); Model M1 [MHD(F), CT] (—·—·—·—); Model M2 [MHD(F), LAOL] (— — — —)

a conclusion would be premature: the models that have been used were based on a highly simplified calculation of convection; in particular, it neglected the non-local nature of convective transport, and effects of turbulent stresses that may contribute substantially to hydrostatic balance just beneath the photosphere; and the frequency calculation assumed that the oscillations are adiabatic and neglected effects of the perturbation of the convective stresses. Since these effects are concentrated in the superficial layers of the Sun, they might be expected to contribute to the slowly varying component of H_2. Balmforth (1992b) found that inclusion of turbulent pressure and non-locality in the treatment of convection in the calculation of the equilibrium models caused frequency changes that would account for a substantial part of the H_2 obtained for the differences between the Sun and the model computed with the CT opacity tables; smaller effects, of the opposite sign, resulted from aspects of the physics of the oscillations which have been neglected here.

From the results presented so far it is evident that current observations can distinguish between models computed with the EFF and the CEFF equation of state, the latter being definitely preferred. It behoves us then to consider the extent to which finer details of the equation of state can be probed; as discussed in Sect. 4.2.4 it must be kept in mind also that the composition of the envelope, particularly the helium abundance, and the specific entropy are uncertain. No complete analysis of these questions can be attempted here; however, an indication can be obtained by comparing the magnitude of H_1 and H_2 obtained in Sects. 4.2.1 – 4.2.4 for various modifications of equation of state or parameters with the scatter in Figs. 29b and 29c. From the scatter one may estimate the uncertainty in the determination of H_1 and H_2 from comparing

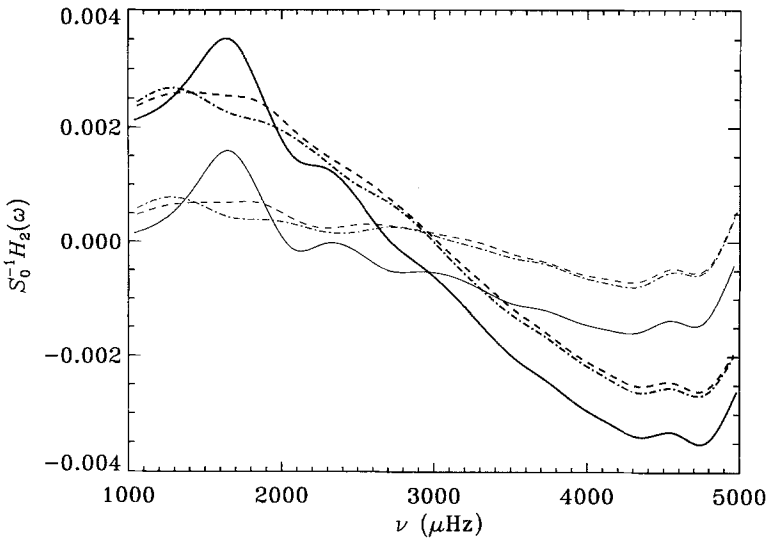

Fig. 31. The function $H_2(\omega)$ resulting from the asymptotic fit in Eq. (4.4) to differences between the observed frequencies of Libbrecht et al. (1990) and various sets of computed frequencies, in the sense (observation) − (theory). The fit used only those modes with $20\,\mu\text{Hz} \leq \nu_{nl}/L \leq 50\,\mu\text{Hz}$. The abscissa is cyclic frequency ν. The models and line styles are as described in the caption to Fig. 30

the observed frequencies with a reference model to be of order 10^{-4}. This is substantially smaller than the effect of going from the CEFF to the MHD(S) equation of state (cf. Fig. 19), offering some hope that properties of the equation of state can be probed at least to a somewhat finer level than the mere addition of the Coulomb terms. On the other hand, the transition from MHD(S) to MHD(F) causes frequency differences that are probably below what can be studied with present observations, at least by using the comparatively simple techniques employed here (see Fig. 23). It should be noted, however, that the asymptotic separation appears to be rather less successful for this pair of models than for the other cases considered, perhaps indicating that a more detailed analysis would have a greater chance of distinguishing between MHD(S) and MHD(F). Finally, we note that the change in helium abundance of 0.005 considered in Sect. 4.2.4 caused H_1 and H_2 that were slightly larger than the estimated uncertainty in the fit to the observations (cf. Fig. 27), indicating that if other properties of the Sun, including the equation of state, are assumed to be known Y can be determined from analysis of the oscillation frequencies to roughly this level of precision. This is not inconsistent with the estimates of Christensen-Dalsgaard and Pérez Hernández (1991), Vorontsov et al. (1991) and Kosovichev et al. (1992).

The principal conclusion of the present comparison is that the simple EFF equation of state is not consistent with the observed frequencies, whereas many aspects of the observations can be reproduced with an equation of state incorporating the features of CEFF or MHD. This was already noted by Christensen-Dalsgaard et al. (1988b) who used the MHD equation of state with a somewhat simplified chemical mixture. A similar conclusion was reached by Baturin et al. (1991) from analysis of the Vorontsov phase $\beta(\omega)$ (cf. Eq. [2.33]), when comparing with models computed with an equation of state including the Coulomb terms and a partition function with a number of excited states estimated from the confined-atom model (Däppen 1980). Pamyatnykh et al.

(1991) fitted the observed $\beta(\omega)$ to a grid of envelope models of varying composition and convective efficiency; they found that while a reasonable fit was possible when the MHD equation of state was used, this was not the case for models based on the simple Saha equation. Christensen-Dalsgaard and Pérez Hernández (1991) found that when a version of MHD was used $H_2(\omega)$ could be reduced essentially to a slowly varying part, presumably arising from errors in the superficial layers, by a proper choice of the helium abundance. Finally, a careful analysis of the Duvall phase, including an explicit separation into a rapidly and a slowly varying part, was made Vorontsov et al. (1992). As did the previous investigations they found that a simple equation of state, based on the Saha equation and ignoring electrostatic corrections was inconsistent with the observations. Interestingly enough they concluded that the simplest Debye-Hückel treatment of the collective Coulomb interaction, which ignores the τ correction for extended charged particles (see Sect. 3.1), provided the best fit to the data, but even then discrepancies remained; the discrepancies were slightly larger if instead the τ corrections were included, or if the full MHD equation of state was used. To assess the detailed significance of these results requires further work, however.

It might also be noted that Kim et al. (1991) investigated the effects of the choice of equation of state and opacity on the structure and oscillations of complete solar models. They only considered low-degree modes and, as a result, did not notice the improvement resulting from the use of the MHD equation of state; however they did point out the apparently improved agreement between observed and computed frequencies resulting from the increase in the atmospheric opacity.

Although somewhat outside the main topic of the present paper, it behoves us to remark that the investigation of the equation of state constitutes only a part of the use of the observed solar oscillation frequencies. Determinations of the solar helium abundance based on the observed frequencies were reviewed in Sect. 4.2.4. More generally, inverse analyses may be used to determine corrections to the solar models. The principles of such analyses were discussed in Sect. 2.3. The sound speed, or corrections to it, can be obtained from the asymptotic techniques discussed in Sect. 2.3.2 (see, for example, Christensen-Dalsgaard et al. 1985; Brodsky and Vorontsov 1987, 1988a; Kosovichev 1988; Shibahashi and Sekii 1988; Vorontsov 1988a, 1989; Sekii and Shibahashi 1989; Christensen-Dalsgaard et al. 1988c, 1991; Vorontsov and Shibahashi 1990, 1992). From numerical inversions (cf. Sect. 2.3.3) corrections can be obtained for two independent properties of solar structure, which may, for example, be chosen as sound speed and density, or density and the ratio $u = p/\rho$. A number of such inversions have been carried out (e.g. Gough and Kosovichev 1988, 1990; Dziembowski et al. 1990; Thompson 1991). In much of the Sun the results of these inversions are in broad agreement. It appears that in most of the convection zone the sound speed in typical models agrees with that of the Sun; this is in accordance with Eq. (2.38) which suggests that in much of the convection zone the sound speed is determined largely by the surface gravity of the Sun. Below the convection zone, however, the solar sound speed is generally higher than that of the models by 1 – 2 per cent, at least in the outer parts of the radiative region; this could be caused by fairly modest errors in the opacity tables used to construct the models. In fact, Dziembowski et al. (1992) recently performed an inversion relative to a reference model which employed new opacities from Iglesias and Rogers (1991); this caused a substantial reduction in the discrepancy between the model and the Sun. Dziembowski et al. (1992) also found evidence for inadequacies in the version of the MHD equation of state which was used for the model computation, in a region extending over much

of the convection zone. This, however, was largely due to the fact that the heavy elements were assumed to consist of only oxygen.

The results for the solar core are substantially more uncertain, largely due to the fact that only the low-degree modes penetrate into the core. Early results gave a slight indication that the sound speed, and hence quite likely the temperature, of the solar core might be substantially higher than in standard solar models; there were also indications that the central density was higher by perhaps as much as 20 per cent than in the models. This has not been confirmed by analysis of more recent data, however, although there remain interesting, and apparently significant, differences between the Sun and the models, the origin of which is currently not understood.

4.4 Effects in the core of the Sun

It follows from Fig. 4 that to obtain helioseismic information about the solar core, modes of low degree must be considered. Also, it is evident that the interpretation of the results must be based on complete solar models. As discussed in Sect. 2.2.3, a suitable quantity for probing the core is the frequency separation $\delta\nu_{nl} = \nu_{nl} - \nu_{n-1\,l+2}$. The asymptotic expression (2.36) suggests that $\delta\nu_{nl}$ is sensitive to conditions in the solar core while being less sensitive to the outer parts of the Sun. In particular, the uncertain aspects in the modelling of the the superficial layers of the Sun largely cancel in the difference defining $\delta\nu_{nl}$. It follows from Eq. (2.36) that asymptotically $\delta\nu_{nl} \propto 2l + 3$; this motivates considering instead the scaled quantity

$$d_{nl} \equiv \frac{3}{2l+3}\delta\nu_{nl} \,, \tag{4.9}$$

which is then expected to depend little on l. Equation (2.36) shows that d_{nl} decreases with ν roughly as ν^{-1}.

As an example, Fig. 32 shows d_{nl} in a standard solar model, for $l = 0, \ldots, 3$. It is evident that, as predicted by asymptotic theory, d_{nl} depends only rather weakly on l.

For comparisons between different models, or between computed and observed frequencies, it is convenient to parameterize the behaviour of d_{nl} in terms of a few parameters. Elsworth et al. (1990) proposed using a linear least-squares fit of the form

$$d_{nl} = \overline{d_l} + s_l(n - n_1) \,, \tag{4.10}$$

where n_1 is a suitable reference value of the order n. Here we consider the sensitivity of the coefficients in this fit to conditions in the core.

Christensen-Dalsgaard (1991a,b) made an extensive investigation of the effects of modifications of the physics, within the framework of standard solar models, on d_{nl}. The conclusion was that for models of fixed age d_{nl} varied relatively little, compared with the uncertainty in the observed values, over a wide range of opacity tables, nuclear energy generation parameters, and equations of state.

Table 2 shows a few representative values of the average scaled separations $\overline{d_0}$ and $\overline{d_1}$ arising from a least-squares fit of Eq. (4.10) to the computed frequencies, together with the corresponding observed values from Elsworth et al. (1990). Details about the computations were given by Christensen-Dalsgaard (1982, 1991a,b). The computations used the CT and LAOL opacity tables that have been used here (although for Model 6 Z was taken to be 0.0192); the version of the MHD equation of state was the same as used by Christensen-Dalsgaard et al. (1988b). In all cases, the models

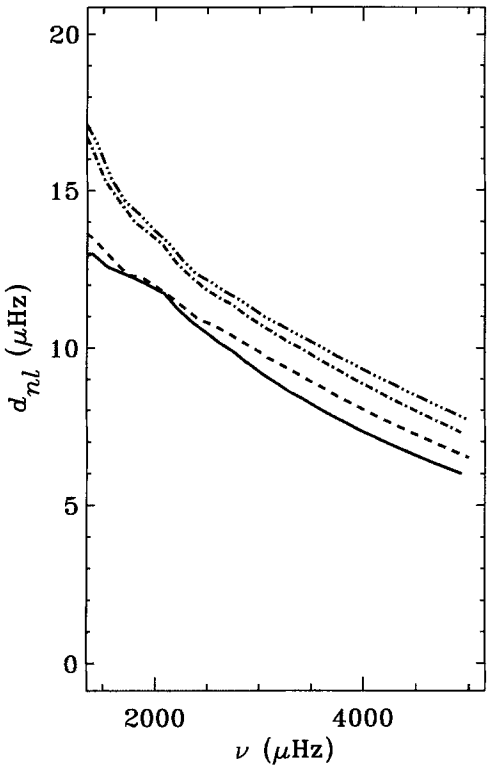

Fig. 32. Scaled frequency separations d_{nl} (cf. Eq. [4.9]) based on computed frequencies for a standard model of the present Sun. Each curve correspond to a value of the degree l, according to the following line styles: $l = 0$ (————); $l = 1$ (·····); $l = 2$ (—·—·—·—); $l = 3$ (—··—··—··)

were calibrated by adjusting the mixing-length parameter α_C and the initial helium abundance Y_0 to have the observed solar radius and luminosity at the age of the present Sun, which, unless otherwise noted, was assumed to be 4.75×10^9 years. The resulting values of Y_0 and α_C depend rather strongly on the opacity table. In the case of Y_0 this is due to the fact that the LAOL opacities are somewhat higher than those obtained from the CT tables in much of the radiative interior, requiring a higher value of Y_0 to achieve the correct luminosity. The increase in α_C for LAOL is caused by the substantially higher opacities in the solar atmosphere; a similar effect was noted in the calibration of the envelope models to obtain a fixed depth of the convection zone (cf. Sect. 4.2).

It is striking that for the standard models of age 4.75×10^9 years (i.e., Models 1 – 5) the computed values of $\overline{d_l}$ are higher than the observed values by an amount that is at least formally statistically significant, although only barely so. This is true despite the rather wide range in physics and initial composition. Although this discrepancy is marginal, it is nevertheless interesting to consider how it might be explained. It was pointed out by Christensen-Dalsgaard (1988a) and Gough and Novotny (1990) that the frequency separation is quite sensitive to the assumed age of the Sun. In fact, Model 6 in Table 2 shows that the computed $\overline{d_0}$ can be brought into agreement with the observations by increasing the age of the model to 5.05×10^9 years, although a small discrepancy remains for $\overline{d_1}$. Such an age of the Sun is probably inconsistent

Table 2. Results for complete solar models. All models have been calibrated to have solar radius and luminosity. The first column gives an identification number. The columns labelled "EOS" and "Opacity" identifies the equation of state and opacity tables, as defined in the text. Y_0 and α_C are the initial helium abundance and mixing length parameter required to calibrate the model, and T_c is the central temperature. The columns labelled "$\overline{d_0}$" and "$\overline{d_1}$" give the results of linear least-squares fits to frequency separations d_{nl}, for $l = 0$ and 1. The fit was of the form given in Eq. (4.10) and included modes with n in the range 15 – 27, and taking $n_1 = 21$. The bottom row gives the results of a corresponding fit by Elsworth et al. (1990) to observed frequency separations; $\overline{d_0}$ and $\overline{d_1}$ were obtained with a standard error of 0.06 μHz.

Model No.	EOS	Opacity	Y_0	α_C	T_c (10^6 K)	$\overline{d_0}$ (μHz)	$\overline{d_1}$ (μHz)
1	EFF	CT	0.2496	1.6425	15.052	9.233	9.688
2	EFF	LAOL	0.2806	2.5167	15.685	9.250	9.681
3	CEFF	CT	0.2404	1.6840	15.009	9.249	9.685
4	MHD	CT	0.2393	1.6896	15.001	9.303	9.724
5	MHD	LAOL	0.2706	2.5752	15.624	9.304	9.714
6[a]	EFF	LAOL	0.2747	2.5598	15.703	9.010	9.496
7[b]	EFF	LAOL	0.2863	2.3546	15.131	12.434	12.202
8[c]	EFF	LAOL	0.2650	2.7200	14.313	7.331	8.575
Obs.						9.00	9.36

[a] assuming the age of the present Sun to be 5.05×10^9 years (rather than the default value of 4.75×10^9 years);
[b] hydrogen profile obtained by scaling from the partially mixed model (with "turbulent Reynolds number" $Re^* = 100$) of Schatzman et al. (1981);
[c] model with core opacity reduced to match observed neutrino flux (see Christensen-Dalsgaard 1992b)

with inferred ages of meteorites and general ideas about the formation of the Sun and the solar system (Guenther 1989). However, the example illustrates the sensitivity of d_{nl} to changes in the mean molecular weight μ_c in the centre of the Sun, brought about in this case by a change in the central helium abundance Y_c.

Other effects may modify the mean molecular weight. Proffitt and Michaud (1991) found that settling of helium in the solar core may increase Y_c by about 0.015, i.e., by an amount similar to the increase arising in Model 6 in Table 2. From the point of view of the present paper it is more relevant to note that μ_c would also be increased relative to standard models if helium were not completely ionized in the solar core. Indeed, it is easy to see that if roughly 10 per cent of helium were in the singly ionized state, the effect on μ_c would be the same as that arising from an increase of Y_c by 0.015. Such a degree of recombination of helium probably cannot be excluded (cf. Sect. 3.3.3).

It should be noted that other modifications may have a more substantial effect on the frequency separation. This is particularly true of modifications that have been proposed to account for the discrepancy between the predicted and the observed flux of neutrinos from the Sun (for an overview of this so-called *solar neutrino problem*, see, for example, Bahcall 1989). Partial mixing of the core, which reduces the computed neutrino flux, also leads to a substantial increase of d_{nl} (Schatzman et al. 1981; Cox and Kidman 1984; Provost 1984; Christensen-Dalsgaard 1986; see Model 7 in Table 2). The effect is the opposite of the changes induced by, for example, increasing the age, since mixing reduces Y_c and hence the mean molecular weight in the core. On the other hand, if it is assumed that a part of the energy transport in the solar core takes place through the motion of the so-called WIMPs, d_{nl} is decreased (Faulkner et al. 1986; Däppen et al. 1986; Cox et al. 1990). The effect can be simulated by

reducing the opacity in a region localized to the core (Christensen-Dalsgaard 1992b); this is illustrated by Model 8 in Table 2, where the opacity reduction has been chosen such as to reduce the neutrino flux of the model to the observed value. In all the cases that have been considered modifications of a magnitude sufficient to account for the observed neutrino flux lead to values of d_{nl} that are totally incompatible with the observed frequencies (see, for example, Elsworth et al. 1990; Cox et al. 1990; Christensen-Dalsgaard 1992b). On the other hand, a small contribution to the energy transport from WIMPs, or a small localized reduction in the opacity in the core, could in principle explain the discrepancy between the computed d_{nl} and the observations of Elsworth et al. (1990).

Finally, it must be pointed out that the observational situation is not yet entirely settled: a recent analysis by Toutain and Fröhlich (1992) of observations made by the IPHIR instrument on the Soviet PHOBOS Mars mission gave separations that were closer to the computed values for standard models than those obtained by Elsworth et al. (1990).

It is evident that the present data can in no way be used to constrain the degree of ionization of matter in the solar core. However, the results discussed here indicate the potential sensitivity of such measurements to the thermodynamic state of the core, provided that improved observations become available and that effects of other possible uncertainties in the structure of the core can be limited.

5. Discussion and conclusion

It was stressed in Sects. 2 and 4 that the solar convection zone is especially suited for a study of the equation of state: its structure is nearly adiabatic (except very close to the surface) and thus virtually independent of opacity; furthermore, because of the rapid mixing the composition of the convection zone is homogeneous. The equation of state is, of course, equally important in other regions of the Sun; but there it is more difficult to disentangle its helioseismic signature from other factors, principally the opacity and spatial variations in the helium abundance. For this reason, most of the efforts towards helioseismic probing of the equation of state (including those reported here) have concentrated on effects in the convection zone.

It was suggested in a number of early papers (Berthomieu et al. 1980; Lubow et al. 1980; Ulrich 1982; Ulrich and Rhodes 1983; Shibahashi et al. 1983, 1984; Noels et al. 1984) that improvements in the equation of state can indeed reduce discrepancies between theory and observations. More recently, Christensen-Dalsgaard et al. (1988b) showed that the MHD (Mihalas, Hummer and Däppen) equation of state significantly reduced these discrepancies for a large range of oscillation modes. The MHD equation of state was especially successful with the high-degree modes which probe the hydrogen and helium ionization zones. Compared with the prediction of the simple Saha equation [in the form of the EFF (Eggleton, Faulkner and Flannery) equation of state], MHD pushes upward the hydrogen and helium ionization zones, and the resulting change in Γ_1 and sound speed explains the better agreement. However, since the MHD equation of state simultaneously incorporates several different types of non-ideal corrections, it did not become immediately clear which one of these corrections was mainly contributing to this success. Christensen-Dalsgaard et al. (1988b) thought that the specific MHD treatment of bound states of hydrogen and helium was responsible. However, from a detailed comparison with the alternative non-ideal

Livermore equation of state (see Sect. 3.4), it turned out, rather surprisingly, that the net effect of the hydrogen and helium bound states on thermodynamic quantities was to a large degree eclipsed beneath the influence of the Coulomb term, which was thus recognized as the dominant non-ideal correction in the hydrogen and helium ionization zones. This discovery suggested an upgrade of the simple EFF equation of state through the inclusion of the Coulomb interaction term. The resulting CEFF equation of state became a very useful and welcome tool for solar physics; at the same time, however, it became also clear that a helioseismic test of the important issue of models in the chemical picture versus models in the physical picture would be more difficult than first thought. The terms chemical and physical picture classify the two basic approaches with which partially ionized plasmas are treated (see Sect. 3.1) We recall that in the chemical picture, bound configurations (atoms, ions and molecules) are introduced and treated as new and independent species. Plasma interactions are dealt with through modifications of atomic states, i.e., the quantum mechanical problem is solved before statistical mechanics is applied. In the physical picture, only fundamental particles (nuclei and electrons) are explicitly introduced. The question of bound states is dealt with implicitly, through the Hamiltonian describing the interaction between the fundamental particles, and the problems of quantum mechanics and statistical mechanics are tackled simultaneously.

For reasons not yet fully understood it seems that the signature of internal partition functions, such as employed in models based on the chemical picture (e.g. in the MHD equation of state), is much less visible in the thermodynamic quantities than a naive estimation of the shift in the ionization equilibrium would predict. It is likely that, in the chemical picture, there are cancellations in the derivatives of the free energy. Notice that these cancellation have nothing to do with those appearing in the physical picture (see Sect. 3.4) which lead to the Planck-Larkin partition function. The cancellations of the chemical picture seem to be greatest for the ionization zone of hydrogen and somewhat less for those of helium. However, for the heavier elements it appeared that, still in the chemical picture, the internal partition functions finally entail the consequences for the thermodynamic quantities that are intuitively expected. The heavy elements could thus become the ideal testing ground for the effects of bound states in partially ionized plasmas. Unfortunately, the small abundance of heavy elements in the Sun will make a diagnosis difficult and stretch the power of helioseismology to its limits. On the other hand, this small sensitivity of the models to the precise formulation of the equation of state has obvious advantages when the models are needed for purposes other than testing the detailed thermodynamics. For instance, the seismological helium-abundance determination (Kosovichev et al. 1992) will benefit from all circumstance that reduce the uncertainty in the equation of state.

In Sect. 4 we have discussed in detail the connection between changes in the equation of state and various quantities related to solar models and oscillation frequencies. Ordering the effects by decreasing importance, we have examined, on a first level, the greatest change, encountered when going from the EFF to the CEFF equation of state. This comparison allows to isolate the influence of the Coulomb term. We emphasize that there are different practical realizations of the Coulomb term: the CEFF and MHD equations of state include the so-called τ cut-off as adopted by Graboske et al. (1969) (see Sect. 3.1). Different forms of the Coulomb term, with and without the τ cut-off, were recently compared by Vorontsov et al. (1992). On a second level, we have examined the substantially smaller transition from the CEFF equation of state to a "stripped-down" version of the MHD equation of state MHD(S), which is

identical to the full version for hydrogen and helium, but which contains only the ground-state contribution in the internal partition functions of all heavier elements and their ions. Thus the difference between the CEFF and MHD(S) equations of state reveals the influence of the bound states of hydrogen and helium (in the chemical picture). Finally, on an already sophisticated third level, we have examined the consequences when going from the stripped MHD(S) to the full MHD(F) formalism. As we have explained in Sect. 3.5.3b, it is precisely this small difference that carries the greatest diagnostic potential for a helioseismic answer to the fundamental test of the two classes of models, based either on the chemical or physical picture.

What has emerged from these comparisons? On the first level, the EFF-CEFF comparison, we have found that the observations definitively prefer the CEFF equation of state. We have been able to draw this conclusion despite some uncertainties related to finer things, such as the helium abundance or the specific entropy of the adiabat. On the next level, the CEFF-MHD(S) comparison, no such clear conclusion can be made, but the consequences for helioseismic analysis appear to be well within reach of present observational data. There are some hints that CEFF might be the better equation of state (see Sect. 4.3 and Vorontsov et al. 1992), but they are not conclusive. If further progress is made at this level, a helioseismic diagnosis of the appropriateness of one or the other treatment of bound states will become possible. The reason for this is that the Livermore equation of state, which is realized in the physical picture, mainly differs from MHD in its treatment of bound states. This is correct at least at the rather low densities of the hydrogen and helium ionization zones. The comparisons discussed in Sect. 3.5.2 have confirmed the intuitive expectation that the net effect of the physical picture with a Planck-Larkin partition function (3.16) is about the same as the analogous effect obtained in a simplified chemical-picture formalism, where the bound-state partition functions only contain their ground-state contribution. (However, at higher densities, the Livermore equation of state incorporates higher-order Coulomb terms in contrast to MHD, which never goes beyond the Debye-Hückel treatment.) If it turns out that observations can really distinguish between the CEFF and MHD(S) equation of state, i.e., between the different treatments of the hydrogen and helium bound states, then the difference between the Livermore and CEFF equation of state will also become accessible. Finally, on the third and finest level, the difference between the MHD(S) and MHD(F) equations of state seems to be small for present observational data.

These considerations provide an indication of the degree of detail to which the thermodynamic state of the solar interior can be probed at present. However, it should be noted that the observational basis for helioseismology is expected to expand greatly in the coming years, as a result of new facilities which are being established. These include ground-based networks of stations for whole-disk observations of low-degree modes (Aindow et al. 1988; Fossat 1991), and the GONG network to observe oscillations of degrees up to around 250 (see, for example, Harvey et al. 1987). Even higher resolution, and with that even better data on the important ionization regions near the solar surface, will be provided by the SOI-MDI instrument (Scherrer et al. 1991) on the satellite SOHO. Given the frequency accuracy expected from such measurements, it should be feasible to distinguish between, for example, MHD(S) and MHD(F). A further expansion of our ability to investigate details of the thermodynamic state will result from analysis of solar-like oscillations in other stars, where conditions differ from those found in the Sun. In particular, we note the possibility of probing conditions at higher density and lower temperature in main-sequence stars

of mass below that of the Sun. Oscillations of such stars may be within reach from the satellite PRISMA (see Lemaire et al. 1991) which is currently being considered by the European Space Agency ESA.

The previous comparisons were concentrating on equation-of-state effects in the solar convection zone. Beneath the convection zone there are of course further interesting effects, but their diagnosis becomes more difficult, because in that part of the Sun opacity also affects the stratification. Opacity and equation of state can be disentangled only under the tentative assumption that the equation of state is better known than opacity. Iteratively, a helioseismic diagnosis of the opacity could become possible. There is already a precedent for such a procedure. It has been realized for some time that for the layers below the convection zone, an opacity some 10 – 20 per cent above the LAOL values would remove important disagreements between theoretical and observed oscillation frequencies (Christensen-Dalsgaard et al. 1985; Korzennik and Ulrich 1989; Cox et al. 1989). Two independent efforts to recalculate stellar opacities have recently been made, one by the international so-called "Opacity Project" (Seaton 1987; in the following OP), and the other by a group at Livermore (Iglesias et al. 1987; in the following OPAL). In fact, the improved atomic and plasma physics of both projects has led to the desired increase. As mentioned above, Dziembowski et al. (1992) applied the most recent OPAL results to a solar model and verified the correctness of the earlier conjecture. This result will certainly be confirmed by the OP results as well, because selected comparisons (Yan 1992; Seaton 1992) have shown general good agreement between the results from the two projects. The remaining discrepancies (of the order of one magnitude less than the change with respect to the LAOL values) were supposed to be related to the role of the equation of state in the opacity calculations (Iglesias 1992). Indeed, OP uses the MHD equation of state based on the chemical picture (3.3.4), and OPAL the Livermore equation of state based on the physical picture (3.4). The fact that helioseismology predicted the direction of opacity improvement clearly demonstrates its potential to put constraints on the opacity. If it turns out that the "ultimate" uncertainty in the opacity is due to the equation of state and its underlying basic conceptual issue, opacity constraints will serve as further tests of the equation of state.

A final area of interest, also outside the solar convection zone and therefore less straightforward to probe, is the possibility of partial recombination of He^+ ions in the solar centre (see Sect. 3.3.3); this would affect the sound speed and hence the oscillation frequencies to an extent that may be observable. As was emphasized in Sect. 4.4, the solar centre is evidently a difficult region to probe; with helioseismic data alone, it is impossible to determine the ionization degree. Currently there are substantial uncertainties related to the opacity in the core, as well as to modifications in the chemical composition caused by helium settling or weak mixing. Such uncertainties must be reduced, or eliminated, before we can unambiguously investigate the ionization properties in the core. However, given the importance of the solar neutrino problem, a great deal of attention is given to these problems; hence it is not unlikely that helioseismology will be able to address also this rather exotic issue in the equation of state.

Acknowledgements. We are grateful to the Institute for Theoretical Physics, and to D.O. Gough and J. Toomre as organizers of the helioseismology program held there, for the opportunities provided for concentrated work on the issues addressed here. We thank V.A. Baturin, G. Chabrier, W. Ebeling, A. Förster, D O. Gough, D. Hummer, C.A. Iglesias, Y. Lebreton, D. Mihalas, R. More, F.J. Rogers, S. Turck-Chièze,

R.K. Ulrich, and S. Vorontsov for fruitful discussions. This research was supported in part by the National Science Foundation under Grant No. PHY89-04035, supplemented by funds from the National Aeronautics and Space Administration, and by the Danish Natural Science Research Council and the Danish Space Board.

References

Aindow, A., Elsworth, Y.P., Isaak, G.R., McLeod, C.P., New, R., van der Raay, H.B.: 1988, *Seismology of the Sun & Sun-like Stars*, eds Domingo, V., Rolfe, E.J., ESA SP-286, pp. 157–160

Bahcall, J.N.: 1989, *Neutrino astrophysics*, Cambridge University Press, Cambridge

Bahcall, J.N., Ulrich, R.K.: 1988, *Rev. Mod. Phys.* 60, 297–372

Balmforth, N.J.: 1992a, *Mon. Not. R. astr. Soc.* 255, 603–631

Balmforth, N.J.: 1992b, *Mon. Not. R. astr. Soc.* 255, 632–638

Balmforth, N.J.: 1992c, *Mon. Not. R. astr. Soc.* 255, 639–649

Balmforth, N.J., Gough, D.O.: 1988, in *Seismology of the Sun & Sun-like Stars*, eds Domingo, V., Rolfe, E.J., ESA SP-286, Noordwijk, The Netherlands, pp. 47–52

Balmforth, N.J., Gough, D.O.: 1990, *Solar Phys.* 128, 161–193

Baturin, V.A.: 1991, *Pis'ma Astron. Zh.* 17, 67–74 (English translation: *Sov. Astron. Lett.* 17, 30–33)

Baturin, V.A., Mironova, I.V.: 1990, *Pis'ma Astron. Zh.* 16, 253–259 (English translation: *Sov. Astron. Lett.* 16, 108–111)

Baturin, V.A., Däppen, W., Gough, D.O., Vorontsov, S.V.: 1992, *Mon. Not. R. astr. Soc.*, submitted

Baturin, V.A., Kononovich, E.V., Mironova, I.V.: 1991, *Solar Phys.* 133, 141–147

Berthomieu, G., Cooper, A.J., Gough, D.O., Osaki, Y., Provost, J., Rocca, A.: 1980, in Lecture Notes in Physics, Vol. 125: Nonradial and Nonlinear Stellar Pulsation, eds Hill, H.A., Dziembowski, W., Springer, Berlin Heidelberg New York, pp. 307–312

Brodsky, M.A., Levshin, A.: 1979, *Geophys. J.R. astr. Soc.* 58, 631–654

Brodsky, M.A., Vorontsov, S.V.: 1987, *Pis'ma Astron. Zh.* 13, 438–443 (English translation: *Sov. Astron. Lett.* 13, 179–181)

Brodsky, M.A., Vorontsov, S.V.: 1988a, in *Proc. IAU Symposium No 123: Advances in Helio- and Asteroseismology*, eds Christensen-Dalsgaard, J., Frandsen, S., Reidel, Dordrecht, pp. 137–140

Brodsky, M.A., Vorontsov, S.V.: 1988b, in *Seismology of the Sun & Sun-like Stars*, eds Domingo, V., Rolfe, E.J., ESA SP-286, Noordwijk, The Netherlands, pp. 487–491

Brodsky, M.A., Vorontsov, S.V.: 1989, *Pis'ma Astron. Zh.* 15, 61–69 (English translation: *Sov. Astron. Lett.* 15, 27–30)

Brookes, J.R., Isaak, G.R., van der Raay, H.B.: 1976, *Nature* 259, 92–95

Brown, T.M.: 1988, in *Proc. IAU Symposium No 123: Advances in Helio- and Asteroseismology*, eds Christensen-Dalsgaard, J., Frandsen, S., D. Reidel Publ. Co., Dordrecht, pp. 453–465

Brown, T.M., Christensen-Dalsgaard, J., Dziembowski, W.A., Goode, P., Gough, D.O., Morrow, C.A.: 1989, *Astrophys. J.* 343, 526–546

Christensen-Dalsgaard, J.: 1978, *PhD Dissertation*, University of Cambridge

Christensen-Dalsgaard, J.: 1982, *Mon. Not. R. astr. Soc.* 199, 735–761,

Christensen-Dalsgaard, J.: 1986, in *Seismology of the Sun and the distant Stars*, ed. Gough, D.O., Reidel, Dordrecht, pp. 23–53

Christensen-Dalsgaard, J.: 1988a, in *Seismology of the Sun & Sun-like Stars*, eds Domingo, V., Rolfe, E.J., ESA SP-286, Noordwijk, The Netherlands, pp. 431–450

Christensen-Dalsgaard, J.: 1988b, in *Multimode Stellar Pulsations*, eds Kovacs, G., Szabados, L., Szeidl, B.; Kultura Press and Konkoly Observatory, Budapest, pp. 153–180

Christensen-Dalsgaard, J.: 1990a, in *Reviews in Modern Astronomy,*, Vol. 3: Accretion and Winds (Proc. Spring Meeting of the Deutsche Astronomische Gesellschaft, Berlin, 1990), ed. Klare, G., Springer, Berlin Heidelberg New York, pp. 313–349

Christensen-Dalsgaard, J.: 1990b, in *Proc. IAU Colloquium No 121: Inside the Sun*, eds Berthomieu G., Cribier M., Kluwer, Dordrecht, pp. 305–326

Christensen-Dalsgaard, J.: 1991a, *Geophys. Astrophys. Fluid Dynamics* 62, 123–152

Christensen-Dalsgaard, J.: 1991b, *Challenges to Theories of the Structure of Moderate-mass Stars*, in Lecture Notes in Physics Vol. 388: eds Gough, D.O., Toomre, J., Springer, Berlin Heidelberg New York, pp. 11–36
Christensen-Dalsgaard, J.: 1992a, in *The Sun: A Laboratory for Astrophysics* (Proc. NATO ASI, Crieff, Scotland, June 1991), eds Schmelz, J.T., Brown, J .C., Kluwer, Dordrecht, pp. 29–80
Christensen-Dalsgaard, J.: 1992b, *Astrophys. J.* 385, 354–362
Christensen-Dalsgaard, J., Berthomieu, G.: 1991, in *Solar Interior and Atmosphere*, eds Cox, A.N., Livingston, W.C., Matthews, M., Space Science Series, University of Arizona Press, Tucson, pp. 401–478
Christensen-Dalsgaard, J., Frandsen, S.: 1983, *Solar Phys.* 82, 165–204
Christensen-Dalsgaard, J., Gough, D.O.: 1982, *Mon. Not. R. astr. Soc.* 198, 141–171
Christensen-Dalsgaard, J., Gough, D.O.: 1984, in *Solar Seismology from Space*, eds Ulrich, R.K., Harvey, J., Rhodes, E.J., Toomre, J., NASA, JPL Publ. 84-84, pp. 79–93
Christensen-Dalsgaard, J., Pérez Hernández, F.: 1988, in *Seismology of the Sun & Sun-like Stars*, eds Domingo, V., Rolfe, E.J., ESA SP-286, Noordwijk, The Netherlands, pp. 499–503
Christensen-Dalsgaard, J., Pérez Hernández, F.: 1991, *Challenges to Theories of the Structure of Moderate-mass Stars*, in Lecture Notes in Physics Vol. 388: eds Gough, D.O., Toomre, J., Springer, Berlin Heidelberg New York, pp. 43–50
Christensen-Dalsgaard, J., Pérez Hernández, F.: 1992, *Mon. Not. R. astr. Soc.* 257, 62–88
Christensen-Dalsgaard, J., Däppen, W., Lebreton, Y.: 1988b, *Nature* 336, 634–638
Christensen-Dalsgaard, J., Duvall, T.L., Gough, D.O., Harvey, J.W., Rhodes, E.J.: 1985, *Nature* 315, 378–382
Christensen-Dalsgaard, J., Gough, D.O., Pérez Hernández, F.: 1988a, *Mon. Not. R. astr. Soc.* 235, 875–880
Christensen-Dalsgaard, J., Gough, D.O., Thompson, M.J.: 1988c, in *Seismology of the Sun & Sun-like Stars*, eds Domingo, V., Rolfe, E.J., ESA SP-286, Noordwijk, The Netherlands, pp. 493–497
Christensen-Dalsgaard, J., Gough, D.O., Thompson, M.J.: 1989, *Mon. Not. R. astr. Soc.* 238, 481–502
Christensen-Dalsgaard, J., Gough, D.O., Thompson, M.J.: 1991, *Astrophys. J.* 378, 413–437
Christensen-Dalsgaard, J., Gough, D.O., Toomre, J.: 1985, *Science* 229, 923–931
Christensen-Dalsgaard, J., Schou, J., Thompson, M.J.: 1990, *Mon. Not. R. astr. Soc.* 242, 353–369
Clayton, D.D.: 1968, *Principles of Stellar Evolution and Nucleosynthesis*, McGraw-Hill, New York
Cooper, A.J.: 1981, *PhD Dissertation*, University of Cambridge
Courtaud, D., Damamme, G., Genot, E., Vuillemin, M., Turck-Chièze, S.: 1990, *Solar Phys.* 128, 49–60
Cowling, T.G.: 1941, *Mon. Not. R. astr. Soc.* 101, 367–375
Cox, A.N.: 1965, in *Stars and Stellar Systems Vol. 8: Stellar Structure*, eds Aller, L.H., McLaughlin, D.B., Univ. of Chicago Press, Chicago, pp. 195–267
Cox, A.N., Kidman, R.B.: 1984, in *Theoretical Problems in Stellar Stability and Oscillations*, Institut d'Astrophysique, Liège, pp. 259–263
Cox, A.N., Tabor, J.E.: 1976, *Astrophys. J. Suppl.* 31, 271–312
Cox, A.N., Guzik, J.A., Kidman, R.B.: 1989, *Astrophys. J.* 342, 1187–1206
Cox, A.N., Guzik, J.A., Raby, S.: 1990, *Astrophys. J.* 353, 698–711
Cox, J.P.: 1980, *Theory of Stellar Pulsation*, Princeton University Press
Craig, I.J.D., Brown, J.C.: 1986, *Inverse Problems in Astronomy: a Guide to Inversion Strategies for Remotely Sensed Data*, Adam Hilger, Bristol
Däppen, W.: 1980, *Astron. Astrophys.* 91, 212–220
Däppen, W.: 1983, *Astron. Astrophys.* 124, 11–22
Däppen, W.: 1990, *Progress of Seismology of the Sun and Stars*, in Lecture Notes in Physics, Vol. 367: eds Osaki, Y., Shibahashi, H., Springer, Berlin Heidelberg New York, pp. 33–40
Däppen, W.: 1992, in *Astrophysical Opacities*, eds Mendoza, C., Zeippen, C. (*Revista Mexicana de Astronomía y Astrofísica*) 141–149
Däppen, W., Gough, D.O.: 1984, in *Theoretical Problems in Stellar Stability and Oscillations*, Institut d'Astrophysique, Liège, pp. 264–269
Däppen, W., Gough, D.O.: 1986, in *Seismology of the Sun and the distant Stars*, ed. Gough, D.O., Reidel, Dordrecht, pp. 275–280
Däppen, W., Anderson, L.S., Mihalas, D.: 1987, *Astrophys. J.* 319, 195–206
Däppen, W., Gilliland, R.L., Christensen-Dalsgaard, J.: 1986, *Nature* 321, 229–231
Däppen, W., Gough, D.O., Thompson, M.J.: 1988, in *Seismology of the Sun & Sun-like Stars*, eds Domingo, V., Rolfe, E.J., ESA SP-286, Noordwijk, The Netherlands, pp. 505–510

Däppen, W., Gough, D.O., Kosovichev, A.G., Thompson, M.J.: 1991, in Lecture Notes in Physics Vol. 388: Challenges to Theories of the Structure of Moderate-mass Stars, eds Gough, D.O., Toomre, J., Springer, Berlin Heidelberg New York, pp. 111–120
Däppen, W., Keady, J., Rogers, F.: 1991, in *Solar Interior and Atmosphere*, eds Cox, A.N., Livingston, W.C., Matthews, M., Space Science Series, University of Arizona Press, Tucson, pp. 112–139
Däppen, W., Lebreton, Y., Rogers, F.: 1990, *Solar Physics* 128, 35–47
Däppen, W., Mihalas, D., Hummer, D.G., Mihalas, B.W.: 1988, *Astrophys. J.* 332, 261–270
Deepak, A.: 1977, *Inversion Methods in Atmospheric Remote Sounding*, Academic Press, New York
Deubner, F.-L., Gough, D.O.: 1984, *Ann. Rev. Astron. Astrophys.* 22, 593–619
Duvall, T.L.: 1982, *Nature* 300, 242–243
Duvall, T.L., Dziembowski, W.A., Goode, P.R., Gough, D.O., Harvey, J.W., Leibacher, J.W.: 1984, *Nature* 310, 22–25
Duvall, T.L., Harvey, J.W., Jefferies, S.M., Pomerantz, M.A.: 1991, *Astrophys. J.* 373, 308–316
Dziembowski, W.A., Pamyatnykh, A.A., Sienkiewicz, R.: 1990, *Mon. Not. R. astr. Soc.* 244, 542–550
Dziembowski, W.A., Pamyatnykh, A.A., Sienkiewicz, R.: 1991, *Mon. Not. R. astr. Soc.* 249, 602–605
Dziembowski, W.A., Pamyatnykh, A.A., Sienkiewicz, R.: 1992, *Acta Astron.* 42, 5–15
Ebeling, W.: 1990, in *Proc. IAU Colloquium No 121: Inside the Sun*, eds Berthomieu G., Cribier M., Kluwer, Dordrecht, pp. 43–58
Ebeling, W., Förster, A., Fortov, V.E., Gryaznov, V.K., Polishchuk, A.Ya.: 1991, *Thermodynamic Properties of Hot Dense Plasmas*, Teubner, Stuttgart
Ebeling, W., Kraeft, W.D., Kremp, D.: 1976, *Theory of Bound States and Ionization Equilibrium in Plasmas and Solids*, Akademie Verlag, Berlin
Ebeling, W., Kraeft, W.D., Kremp, D., Röpke, G.: 1985, *Astrophys. J.* 290, 24–27
Eggleton, P.P., Faulkner, J., Flannery, B.P.: 1973, *Astron. Astrophys.* 23, 325–330
Eliezer, S., Ghatak, A., Hora, H.: 1986, *An introduction to equations of state: theory and applications*, Cambridge University Press
Elsworth, Y.P., Jefferies, S.M., McLeod, C.P., New, R., Pallé, P.L., van der Raay, H.B., Régulo, C., Roca Cortés, T., 1989, *Astrophys. J.* 338, 557–562
Elsworth, Y., Howe, R., Isaak, G.R., McLeod, C.P., New, R.: 1990, *Nature* 347, 536–539
Elsworth, Y., Howe, R., Isaak, G.R., McLeod, C.P., New, R.: 1991, *Mon. Not. R. astr. Soc.* 251, 7p–9p
Faulkner, J., Gough, D.O., Vahia, M.N.: 1986, *Nature* 321, 226–229
Fontaine, G., Graboske, H.C., Van Horn, H.M.: 1977, *Astrophys. J. Suppl.* 35, 293–358
Fossat, E.: 1991, *Solar Phys.* 133, 1–12
Fossat, E., Grec, G., Gavryusev, V., Gavryuseva, E.: 1988, in *Seismology of the Sun & Sun-like Stars*, eds Domingo, V., Rolfe, E.J., ESA SP-286, Noordwijk, The Netherlands, pp. 393–397
Fröhlich, C.: 1988, in *Proc. IAU Symposium No 123: Advances in Helio- and Asteroseismology*, eds Christensen-Dalsgaard, J., Frandsen, S., Reidel, Dordrecht, pp. 83–86
Fröhlich, C., Delache, Ph.: 1984a, *Mem. Soc. astr. Ital.* 55, 99–105
Fröhlich, C., Delache, Ph.: 1984b, in *Solar Seismology from Space*, eds Ulrich, R.K., Harvey, J., Rhodes, E.J., Toomre, J., NASA, JPL Publ. 84-84, pp. 183–193
Gabriel, M.: 1989, *Astron. Astrophys.* 226, 278–283
Garcia, C., Pallé, P.L., Roca Cortés, T.: 1988, in *Seismology of the Sun & Sun-like Stars*, eds Domingo, V., Rolfe, E.J., ESA SP-286, Noordwijk, The Netherlands, pp. 353–357
Gell-Mann, M.: 1957, *Phys. Rev.* 106, 369–372
Gell-Mann, M., Brueckner, K.A.: 1957, *Phys. Rev.* 106, 364–368
Goldreich, P., Keeley, D.A.: 1977, *Astrophys. J.* 211, 934–942
Gough, D.O.: 1984a, *Mem. Soc. Astron. Ital.* 55, 13–35
Gough, D.O.: 1984b, *Phil. Trans. R. Soc. London, Ser. A* 313, 27–38
Gough, D.O.: 1985, *Solar Phys.* 100, 65–99
Gough, D.O.: 1986a, in *Hydrodynamic and Magnetohydrodynamic Problems in the Sun and Stars*, ed. Osaki, Y., University of Tokyo Press, pp. 117–143
Gough, D.O.: 1986b, in *Seismology of the Sun and the distant Stars*, ed. Gough, D.O., Reidel, Dordrecht, pp. 125–140
Gough, D.O.: 1990, *Progress of Seismology of the Sun and Stars*, in Lecture Notes in Physics Vol. 367: eds Osaki, Y., Shibahashi, H., Springer, Berlin Heidelberg New York, pp. 283–318
Gough, D.O.: 1992, in *Astrophysical Fluid Dynamics*, eds Zahn, J.-P., Zinn-Justin, J., North-Holland, Amsterdam

Gough, D.O., Kosovichev, A.G.: 1988, in *Seismology of the Sun & Sun-like Stars*, eds Domingo, V., Rolfe, E.J., ESA SP-286, Noordwijk, The Netherlands, pp. 195–201
Gough, D.O., Kosovichev, A.G.: 1990, in *Proc. IAU Colloquium No 121: Inside the Sun*, eds Berthomieu G., Cribier M., Kluwer, Dordrecht, pp. 327–340
Gough, D.O., Novotny, E.: 1990, *Solar Phys.* 128, 143–160
Gough, D.O., Thompson, M.J.: 1991, in *Solar Interior and Atmosphere*, eds Cox, A.N., Livingston, W.C., Matthews, M., Space Science Series, University of Arizona Press, pp. 519–561
Gough, D.O., Toomre, J.: 1991, *Ann. Rev. Astron. Astrophys.* 29, 627–685
Gough, D.O., Weiss, N.O.: 1976, *Mon. Not. R. astr. Soc.* 176, 589–607
Graboske, H.C., Harwood, D.J., Rogers, F.J.: 1969, *Phys. Rev.* A186, 210
Guenther, D.B.: 1989, *Astrophys. J.* 339, 1156–1159
Harvey, J.: 1988, in *Seismology of the Sun & Sun-like Stars*, eds Domingo, V., Rolfe, E.J., ESA SP-286, Noordwijk, The Netherlands, pp. 55–66
Harvey, J.W., Kennedy, J.R., Leibacher, J.W.: 1987, *Sky and Telescope* 74, 470–476
Hill, H.A., Caudell, T.P.: 1985, *Astrophys. J.* 299, 517–525
Hill, T.L.: 1960, *Statistical Thermodynamics*, Addison-Wesley, Reading Mass., Chapt. 15
Huang, K.: 1963, *Statistical Mechanics*, John Wiley, New York, Chapt. 14
Huebner, W.F.: 1986, in *Physics of the Sun, Vol. I*, eds Sturrock, P.A., Holzer, T.E., Mihalas, D., Ulrich, R.K., Reidel, Dordrecht, pp. 33–75
Huebner, W.F., Merts, A.L., Magee, N.H., Argo, M.F.: 1977, *Astrophysical Opacity Library*, Los Alamos Scientific Laboratory Report LA-6760-M
Hummer, D.G., Mihalas, D.: 1988, *Astrophys. J.* 331, 794–814
Ichimaru, S.: 1982, *Rev. Mod. Phys.* 54, 1017–1059
Iglesias, C.A., Rogers, F.J.: 1992, in *Astrophysical Opacities*, eds Mendoza, C., Zeippen, C. (*Revista Mexicana de Astronomía y Astrofísica*) 161–170
Iglesias, C.A., Rogers, F.J.: 1991, *Astrophys. J.* 371, 408–417
Iglesias, C.A., Rogers, F.J., Wilson, B.G.: 1987, *Astrophys. J.* 322, L45–48
Jackson, J.L., Klein, L.S.: 1969, *Phys. Rev.* 177, 352–358
Jeans, J.H.: 1929, *Astronomy and cosmogeny*, Cambridge University Press, Cambridge (1961: Dover Publications, New York)
Jefferies, S.M., Duvall, T.L., Harvey, J.W., Osaki, Y., Pomerantz, M.A.: 1991, *Astrophys. J.* 377, 330–336
Kemble, E.C.: 1937, *The fundamental principles of quantum mechanics*, McGraw-Hill, New York
Kidman, R.B., Cox, A.N.: 1984, in *Solar Seismology from Space*, eds Ulrich, R.K., Harvey, J., Rhodes, E.J., Toomre, J., NASA, JPL Publ. 84-84, pp. 335–343
Kim, Y.-C., Demarque, P., Guenther, D.B.: 1991, *Astrophys. J.* 378, 407–412
Korzennik, S.G., Ulrich, R.K.: 1989, *Astrophys.J.* 339, 1144–1155
Kosovichev, A.G.: 1988, in *Seismology of the Sun & Sun-like Stars*, eds Domingo, V., Rolfe, E.J., ESA SP-286, Noordwijk, The Netherlands, pp. 533–537
Kosovichev, A.G., Christensen-Dalsgaard, J., Däppen, W., Dziembowski, W.A., Gough, D.O., & Thompson, M.J.: 1992, *Mon. Not. R. astr. Soc.*, in the press
Kraeft W.D., Kremp D., Ebeling W., Röpke G.: 1986, *Quantum Statistics of Charged Particle Systems*, Plenum, New York
Krasnikov Yu.G.: 1977, *Zh. Eksper. teoret. Fiz.* 73, 516 (English translation: *Soviet Phys. - JETP* 46, 270–274; author's name misspelt as "Karsnikov")
Lebreton, Y., Däppen, W.: 1988, in *Seismology of the Sun & Sun-like Stars*, eds Domingo, V., Rolfe, E.J., ESA SP-286, Noordwijk, The Netherlands, pp. 661–664
Lebreton, Y., Berthomieu, G., Provost, J., Schatzman, E.: 1988, *Astron. Astrophys.* 200, L5–L8
Ledoux, P., Walraven, T.: 1958, *Handbuch der Physik*, Vol. 51, Chapter IV, Springer, Berlin Heidelberg New York
Lemaire, P., Appourchaux, T., Catala, C., Catalano, S., Frandsen, S., Jones, A., Weiss, W.: 1991, *Adv. Space. Res.* Vol. 11 No. 4, 141–145
Libbrecht, K.G.: 1988a, *Space Sci. Rev.* 47, 275–301
Libbrecht, K.G.: 1988b, in *Seismology of the Sun & Sun-like Stars*, eds Domingo, V., Rolfe, E.J., ESA SP-286, Noordwijk, The Netherlands, pp. 3–10
Libbrecht, K.G.: 1988c, *Astrophys. J.* 334, 510–516
Libbrecht, K.G.: 1992, *Astrophys. J.* 387, 712–714
Libbrecht, K.G., Woodard, M.F.: 1991, *Science* 253, 152–157

Libbrecht, K.G., Popp, B.D., Kaufman, J.M., Penn, M.J.: 1986, *Nature* 323, 235–238
Libbrecht, K.G., Woodard, M.F., Kaufman, J.M.: 1990, *Astrophys. J. Suppl.* 74, 1129–1149
Lubow, S.H., Rhodes, E.J., Ulrich, R.K.: 1980, in Lecture Notes in Physics, Vol. 125: Nonradial and Nonlinear Stellar Pulsation, eds Hill, H.A., Dziembowski, W., Springer, Berlin Heidelberg New York, pp. 300–306
Marchenkov, K.I., Vorontsov, S.V.: 1990, *Pis'ma Astron. Zh.* 16, 444–451 (English translation: *Sov. Astron. Lett.* 16, 189–192)
Marchenkov, K.I., Vorontsov, S.V.: 1991, *Solar Phys.* 133, 149–154
Mayer, J.E.: 1950, *J. Chem. Phys.* 18, 1426–1436
Mihalas, D., Däppen W., Hummer, D.G.: 1988, *Astrophys. J.* 331, 815–825
Noels, A., Scuflaire, R., Gabriel, M.: 1984, *Astron. Astrophys.* 130, 389–396
Pamyatnykh, A.A., Vorontsov, S.V., Däppen, W.: 1991, *Astron. Astrophys.* 248, 263–269
Parker, R.L.: 1977, *Ann. Rev. Earth Planet. Sci.* 5, 35–64
Proffitt, C.R., Michaud, G.: 1991, *Astrophys. J.* 380, 238–250
Provost, J.: 1984, in *Proc. IAU Symposium No 105: Observational Tests of the Stellar Evolution Theory*, eds Maeder, A., Renzini, A., Reidel, Dordrecht, pp. 47–65
Reichl, L.E.: 1980, *A Modern Course in Statistical Physics*, University of Texas Press, Austin
Rogers, F.J.: 1977, *Phys. Lett.* 61A, 358–360
Rogers, F.J.: 1981, *Phys. Rev.* A24, 1531–1543
Rogers, F.J.: 1986, *Astrophys. J.* 310, 723–728
Rouse, C.A.: 1983, *Astrophys. J.* 272, 377–379
Sawada, K.: 1957, *Phys. Rev.* 106, 372–383
Schatzman, E., Maeder, A., Angrand, F., Glowinski, R.: 1981, *Astron. Astrophys.* 96, 1–16
Scherrer, P.H., Wilcox, J.M.: 1983, *Solar Phys.* 82, 37–42
Scherrer, P.H., Hoeksema, J.T., Bush, R.I.: 1991, *Adv. Space Res.* vol. 11, No. 4, 113–122
Seaton, M.: 1987, *J. Phys. B: Atom. Molec. Phys.* 20, 6363–6378
Seaton, M.: 1990, *J. Phys. B: Atom. Molec. Phys.* 23, 3255–3296
Seaton, M.J.: 1992, in *Astrophysical Opacities*, eds Mendoza, C., Zeippen, C. (*Revista Mexicana de Astronomía y Astrofísica*) 180
Sekii, T., Shibahashi, H.: 1989, *Publ. Astron. Soc. Japan* 41, 311–331
Severny, A.B., Kotov, V.A., Tsap, T.T.: 1976, *Nature* 259, 87–89
Shibahashi H.: 1988, in *Proc. IAU Symposium No 123: Advances in Helio- and Asteroseismology*, eds Christensen-Dalsgaard, J., Frandsen, S., Reidel, Dordrecht, The Netherlands, pp. 133–136
Shibahashi, H., Sekii, T.: 1988, in *Seismology of the Sun & Sun-like Stars*, eds Domingo, V., Rolfe, E.J., ESA SP-286, Noordwijk, The Netherlands, pp. 471–480
Shibahashi, H., Noels, A., Gabriel, M.: 1983, *Astron. Astrophys.* 123, 283–288
Shibahashi, H., Noels, A., Gabriel, M.: 1984, *Mem. Soc. Astron. Ital.* 55, 163–168
Stix, M., Skaley, D.: 1990, *Astron. Astrophys.* 232, 234–238
Tanaka, S., Mitake, S., Ichimaru, S.: 1985, *Phys. Rev.* A32, 1896–1902
Tarantola, A.: 1987, *Inverse Problem Theory*, Elsevier, Amsterdam
Tassoul, M.: 1980, *Astrophys. J. Suppl.* 43, 469–490
Tassoul, M.: 1990, *Astrophys. J.* 358, 313–327
Thompson, M.J.: 1988, in *Seismology of the Sun & Sun-like Stars*, eds Domingo, V., Rolfe, E.J., ESA SP-286, Noordwijk, The Netherlands, pp. 321–324
Thompson, M.J.: 1991, in Lecture Notes in Physics Vol. 388: Challenges to Theories of the Structure of Moderate-mass Stars, eds Gough, D.O., Toomre, J., Springer, Berlin, pp. 61–80
Toutain, T., Fröhlich, C.: 1992, *Astron. Astrophys.* 257, 287–297
Turck-Chièze, S.: 1990, in *Rencontres de Moriond 1990: New and Exotic Phenomena*, eds Fackler, O., Tran Thanh Vân, J., Edition Frontieres, Gif sur Yvette, France, pp. 571–580
Turck-Chièze, S., Cahen, S., Cassé, M., Doom, C.: 1988, *Astrophys. J.* 335, 415–424
Ulrich, R.K.: 1982, *Astrophys. J.* 258, 404–413
Ulrich, R.K., Rhodes, E.J.: 1983, *Astrophys. J.* 265, 551–563
Unno, W., Osaki, Y., Ando, H., Shibahashi, H.: 1989, *Nonradial Oscillations of Stars, 2nd Edition*, University of Tokyo Press, Tokyo
Vandakurov, Yu.V.: 1967, *Astron. Zh.* 44, 786–797 (English translation: *Soviet Astronomy AJ* 11, 630–638)
Vernazza, J.E., Avrett, E.H., Loeser, R.: 1981, *Astrophys. J. Suppl.* 45, 635–725

Vorontsov, S.V.: 1988a, in *Seismology of the Sun & Sun-like Stars*, eds Domingo, V., Rolfe, E.J., ESA SP-286, Noordwijk, The Netherlands, pp. 475–480
Vorontsov, S.V.: 1988b, in *Proc. IAU Symposium No 123: Advances in Helio- and Asteroseismology*, eds Christensen-Dalsgaard, J., Frandsen, S., Reidel, Dordrecht, pp. 151–154
Vorontsov, S.V.: 1989, *Pis'ma Astron. Zh.* 15, 48–60 (English translation: *Sov. Astron. Lett.* 15, 21–26)
Vorontsov, S.V., Shibahashi, H.: 1990, in Lecture Notes in Physics Vol. 367: *Progress of Seismology of the Sun and Stars*, eds Osaki, Y., Shibahashi, H., Springer, Berlin, pp. 326–328
Vorontsov, S.V., Shibahashi, H.: 1992, *Publ. Astron. Soc. Japan* 43, 739–753
Vorontsov, S.V., Zharkov, V.N.: 1989, *Sov. Sci. Rev. E. Astrophys. Space Phys.* 7, 1–103
Vorontsov, S.V., Baturin, V.A., Pamyatnykh, A.A.: 1991, *Nature* 349, 49–51
Vorontsov, S.V., Baturin, V.A., Pamyatnykh, A.A.: 1992, *Mon. Not. R. astr. Soc.* 257, 32–46
Wiese, W.L., Kelleher, D.E., Paquette, D.R.: 1972, *Phys. Rev.* A6, 1132–1153
Woodard, M., Hudson, H.S.: 1983, *Nature* 305, 589–593
Yan, Yu: 1992, in *Astrophysical Opacities*, eds Mendoza, C., Zeippen, C. (*Revista Mexicana de Astronomía y Astrofísica*) 171–179
van der Raay, H.B.: 1988, in *Seismology of the Sun & Sun-like Stars*, eds Domingo, V., Rolfe, E.J., ESA SP-286, Noordwijk, The Netherlands, pp. 339–351

This article was processed by the author
using the Springer-Verlag TEX AAR macro package 1991.